Paper 61

Synthesis, Characterization and Molecular Docking of Condensed Molecules of Halogen Derivatives of Some Naturally Occurring Quinones and Phenylene Diamines

Rajendra T. Jagtap[1] and Sanjay. D. Gaikwad[2]
[1]Pimpri Chinchwad College of Engineering, Nigdi
[2] BJS college of Arts, Science and Commerce, Wagholi

Abstract

Naphthoquinones are natural pigments and widely distributed in nature and having interesting co-ordination, analytical and biological activities. Lawsone (2-hydroxy,1-4 naphthoquinone), its halogen derivatives and their synthetic polymeric molecules with phenylene diamine, have propitious potential for treatment of many diseases because of their ant seborrheic, anticancer, antituberculosis, antifungal, antibacterial and uninflammatory effects. The present communication deals with synthesis of condensed polymeric molecules of -*chloro* lawsone with para phenylene diamine and their characterization using IR, H^1 NMR. These molecules are subjected for molecular docking or modeling technique is used to predict how a protein (enzyme) interacts with small molecules (ligands). It allows prediction of molecular interactions that hold together a protein and a ligand in the bound state.

Keywords: Lawsone, Chlorolawsone, Condensed Molecules, Phenylene Diamine, Molecular Docking

Introduction

Lawsone (2-hydroxy,1-4 naphthoquinone) is naturally occurring pigment extracted from Henna plant (Lawsonia inermis). As already reported in literature, Lawsone shows antiseptic, antipyretic and astringent properties [1]

The synthesis and characterization of lawsone derivatives is carried out. All chemicals used were of A.R. grade. Solvents used were purified by methods given in literature. Ligands are purified by column chromatography using silica gel (100-200 mesh). Ligands like chlorolawsone were synthesizes on laboratory scale following literature reported procedures. Lawsone (2-hydroxy-1,4-naphthoquinone), dichlone (2,3-dichloro-1,4-naphthalenedione) and 2-methyl-1,4-naphthalenedione were obtained from Merks laboratory. All compounds were characterized by their identical TLC behavior with the standard and authentic samples. Melting points were obtained with paraffin oil bath. The elemental analysis for the percentage of hydrogen and carbon were performed in the micro analytical laboratory using a Hosli C,H micro analysis instrument.

Experimental

Chloro derivative of lawsone, namely 3-chlorolawsone were synthesized from dichlone and lawsone.

Synthesis of chlorolawsone [2,3]: In a 100 ml beaker, a slurry of 1 gm of dichlone solution was prepared using 20 ml methyl alcohol. Then 4M aqueous solution of potassium hydroxide solution was added drop by drop with constant stirring. The entire mass was warmed on a water bath at 60^{o}C until a red crystalline paste was formed. After about 1 hour of heating, a solution of hydrochloric acid (6M) was added dropwise to the above paste with constant stirring. This acidification converted the red paste in to bright yellow precipitate of 3-chlorolawsone (Figure 1). The precipitate was filtered under suction and washed repeatedly with cold distilled water and dried in vacuum over fused calcium chloride. The crude product was purified by column chromatography using chloroform as an eluent.

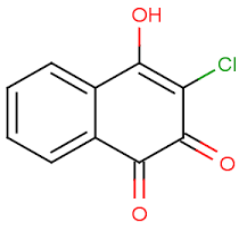

Figure 1. Chlorolawsone

Synthesis of Condensed molecules of chloro lawsone and phenylene diamine [4]

1) 0.001 mole (0.20865 gm) of chloro lawsone was dissolved in 20 ml pure ethanol and a solution of 0.001 mole (0.10810 gm) ortho phenylene diamine in 10 ml ethanol is added dropwise with constant stirring at room temperature. An intense brownish precipitate was obtained, after evaporation of all solvent content. The precipitate was washed with distilled water and dried under vacuum. It is then purified by column chromatography using chloroform solvent. Its purity was checked by TLC using mixture of 20 ml ethyl acetate and 80 ml n-hexane, where a single spot was obtained.

2) 0.001 mole (0.20865 gm) of chloro lawsone was dissolved in 20 ml pure ethanol and a solution of 0.001 mole (0.10810 gm) meta phenylene diamine in 10 ml ethanol is added dropwise with constant stirring at room temperature. A brown blackish precipitate was obtained, after evaporation of all solvent content. This precipitate was washed with distilled water and dried under vacuum. It is then purified by column chromatography using chloroform solvent. The purity was checked by TLC using mixture of 20 ml ethyl acetate and 80 ml n-hexane, where a single spot was obtained.

3) 0.001 mole (0.20865 gm) of chloro lawsone was dissolved in 20 ml pure ethanol and a solution of 0.001 mole (0.10810 gm) para phenylene diamine in 10 ml ethanol is added dropwise with constant stirring at room temperature. A brownish precipitate was obtained after evaporation of all solvent content. The precipitate was washed with distilled water and dried under vacuum. It is then purified by column chromatography using chloroform solvent. Its purity was checked by TLC using mixture of 20 ml ethyl acetate and 80 ml n-hexane, where a single spot was obtained.

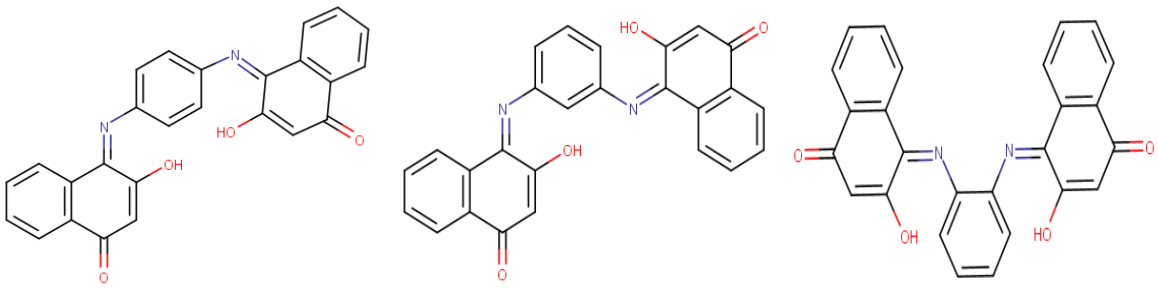

A B C

Figure 2. Condensed molecules

A is condensed molecule of chlorolawsone and o-phenylene diamine

B is condensed molecule of chlorolawsone and m-phenylene diamine

C is condensed molecule of chlorolawsone and p-phenylene diamine

UV Spectral Study

Table 1. Significant UV absorptions

Compound	Π – Π* transition		n – Π* transition
	BET	QET	
Clorolawsone	299	334	457
A	299	--	490

B	290	353	457540
C	---	--	--

Visible spectrum of 2-hydroxy,1-4 naphthoquinone in DMSO is recorded and studied. In this spectrum, prime transitions are observed in 296,339,415 and 448 wavelengths. The best commonly transitions are n to pi star and pi to pi star. Here because of conjugation, absorption shifted to longer wavelength and also pi to pi star transitions are more intense than n to pi star transitions.[5] The electronic spectra of the lawsone and condensed molecules are done in ethyl alcohol. The spectra has intense band at 230 – 245 nm and at 345 – 460 nm are due to Π – Π* transition. The first band is due to benzenoied electron transfer, while the second band is due to quinonoied electron transfer. The band at low intensity is observed in the spectra of lawsone is due to n – Π* transition. The new broad band with low intensity is observed at 500 – 600 nm in the spectra of the polymer, it may be due to increase in the chromophoric length of the polymers. In case of B the absorption is less than C, it is due to less planarity of the polymer.[6]

IR Spectral Study

In the IR spectra of the parent compound lawsone the frequency observed at 3300 cm^{-1}, it is attributed to ʊ(O-H). It is shifted to higher frequency by ~ 30 to 75 cm^{-1}, it is due to polymerization and are in conjugation. This peak is also broadened and its high intensity get reduced and it is merged in broad peak of N-H. The ʊ(C=O) stretching frequency is assign for the carbonyl group present in lawsone at 1 and 4th position. [7].This peak is not observed in the spectra of all polymers. The broad peak is observed at 3421 cm-1 is assign to ʊ(N-H) vibrations. It is not observed in lawsone. The broadness and shifting to higher frequency may be due to polymerization and in conjugation. The sharp band observed at 1629 cm-1 in all polymer spectra, it is attributed for ʊ(C=N) stretching frequency. Similarly the another stretching frequency at ~ 1135 cm-1 in all the polymers is observed, it is assign for the ʊ(C-N). IR studies showed that 3170 (stretching O-H which overlaps the C-H vibrations), 1681 and 1640 (stretching C=O, such splitting is due to presence of internal hydrogen bonding), 1578 and 1592 (C=C vibrational bands of naphthalene ring) and 1214 (stretching for C-O)[8]

Table 2, Significant peaks in Infrared Spectra (all frequencies are in cm^{-1})

Assignment	Lawsone	A	B	C

N-H	---	3421	3421	
C=O	1680	---	---	
C=N	---	1629	1630	1632
C-N	---	1135	1138	1139
O-H	3300	3360	3375	3367
Aromatic Stretching.	1617	1617	1617, 1560	1594, 1503

H1 NMR (FT-250 MHZ, DMSO-d6) showed d:7.78-8.01(m,4H of aromatic ring) and 6.17(s.1H).

Methodology , Results and Discussion [13]

Selection of particular Ligands from oxonaphthalenone derivatives

The important derivatives from synthesized compounds were used in the present investigation for the computational prediction of potential drugs from it by the process of molecular docking against Psoriasis. The important derivatives from synthesized compounds were used in the present investigation for the computational prediction of potential drugs from it by the process of molecular docking against Psoriasis.

Biological Activity Prediction

Due to the impossibility of performing a study of the biological activity of a large number of compounds in a short period, it was decided to conduct a preliminary assessment of the potential biological activity of compounds (RJ1, RJ2, & RJ3) using PASS-online modeling [22]. The PASS software product, which predicts more than 300 pharmacological effects and biochemical mechanisms on the basis of the structural formula of a substance, may be efficiently used to find new targets (mechanisms) for some ligands and, conversely, to reveal new ligands for some biological targets. The mean accuracy of prediction with PASS is about 86% in LOO cross-validation. The tool uses the descriptors to predict the activity of a substance.

The prediction of the biological activity spectrum of oxonaphthalenone derivatives RJ1, RJ2, RJ3 revealed that compounds are determined as promising TNF-α inhibitors. This indicates that all the

three compounds may show good activity against Psoriasis as TNF alpha is main target for psoriasis treatment.

The 3D SDF structures of the processed three oxonaphthalenone derivatives RJ1, RJ2, RJ3 were given as an input for PASS server. The PASS server provides all the possible activities of the given oxonaphthalenone derivatives as promising TNF-α inhibitors. PASS can be effectively applied to predict biological potential of compounds and to analyze large chemical databases. PASS predicted search results show all the available information on the pharmacological and toxicological activity of all the three compounds analysed. Similar observation in accordance with the present study using PASS server was already reported by many researchers. Pa and Pi are the estimates of probability to be active and inactive respectively from the biological activity spectrum. Their values vary from zero to one. Each active compound possesses a number of biological activities. Its specificity of action is always relative and is defined by the peculiarities of object, dose, route, etc. Biological activity spectrum of compound can be predicted on the basis of structure-activity relationships found by the analysis of the known data from the training set. Based on the analysis of large training set consisting of tens of thousands of the known biologically active compounds, computer program PASS provides the means to evaluate any new compound in huge chemical-pharmacological space. On the basis of this study it can be reveals that all the three compounds may show good activity against Psoriasis as TNF alpha is main target for psoriasis treatment.

Molecular Docking Studies

Target Protein Retrieval and Preparation

On the basis of literature survey we found that TNF-aplha is major target to study anti-psoriatic study. Therefore fasta sequence of TNF-aplha for homo sapience was retrieved from National centre for biotechnology information server and done Basic Local Alignment Search for regions of similarity between biological sequences available on Protein Data Bank. Then Three-dimensional X-Ray crystallographic structure of TNF-alpha (PDB id: 2AZ5) was obtained from PDB databank which was validated using various parameters like resolution, Mutation and Ramachandran plot. Details are given in table 3.

Table 3. Comparison between standard values and retrieved protein for validation of protein

Parameters	**Details**	**Standards**
Protein Id and	2AZ5	-

method of experiment	X-RAY Diffraction	X-RAY Diffraction
Mutation	No	No
Resolution	2.10 A^0	Near about 2.00 A^0
Ramchandran Plot **(**by PROCHECK server) Residues in favoured + Allowed regions		 >88 %

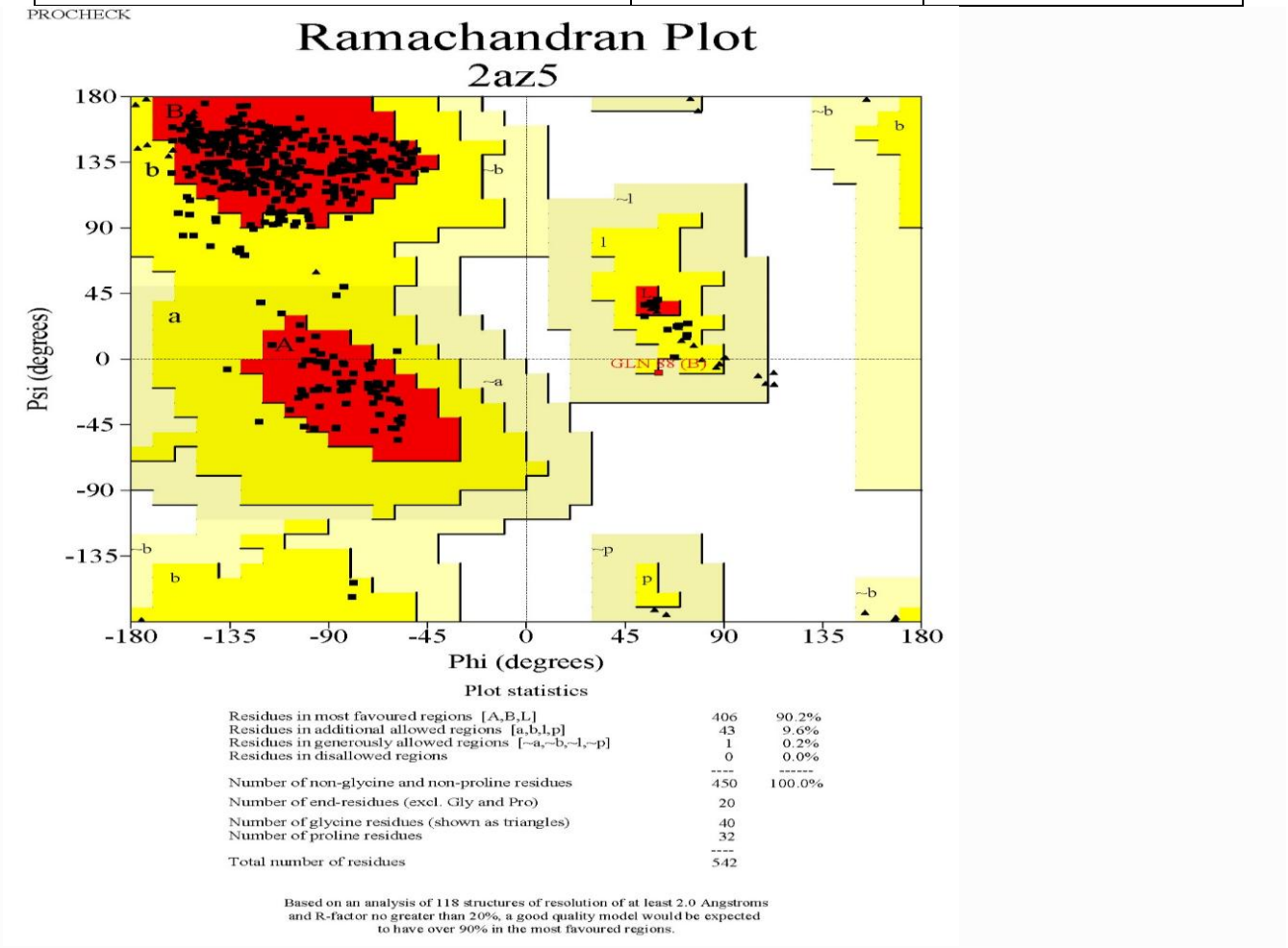

Figure 3. Ramachandran Plot 2az5 obtained from PROCHECK server

The preparation of a protein involves importing of the TNF-alpha Protein structure. Binding pocket has been verified using PDBsum server which is a Pictorial database of 3D structures in the Protein Data Bank for interactions of standard inhibitor with protein. The water molecules, unnecessary chains and ligands have been deleted and the protein were retained using Biovia Discovery Studio visualizer V21.1.0.20298. Charges were stabilized, missing residues were filled in and side chains were generated using AutoDockTools v1.5.6 spet_17_14.

The CHIMERA v1.5.3 software was used to minimize the structure of protein, using the Gasteiger charges with 1000 steepest descent steps of minimization.

Grid Generation

AutoDockTools was used for receptor grid identification. The prepared TNF-α protein was displayed in the Workspace. The volume of grid was calculated using dimensions of pocket identified from CASTp server (Computed Atlas of Surface Topography of proteins). The enclosing box was made small so that it will be consistent with the shape and character of the protein's active site and with the ligands that were expected to be docked.

Ligands Preparation

Ligand molecules were designed in MarvinSketch v21.13 and saved in 3D MOL2 format. All the three compounds were processed, and optimized by UCSF Chimera v1.15 using AM1-BCC semi-empirical force field other parameters defaults like steepest descent steps : 1000; Conjugate gradient steps 100, etc.

Molecular Docking of Target Protein with Ligands

After obtaining the ligands and enzymes, their structures were converted to pdbqt format, using the AutoDock Tools 1.5.6 program, in which all the rotatable bonds of ligands were allowed to rotate freely, and the receptor were considered rigid. For docking studies, we used the AutoDock Vina 1.1.1, with 1 ˚A of spacing between the grid points. The grid box was centred on the active site of the enzyme with high resolution, allowing the program to search for additional places of probable interactions between the ligands and the receptor. Other configurations were considered default. The XYZ coordinates 41.81 X 23.95 X 240.11, and size of the grid box is 20 X 20 X 20 A^0. The redockings were performed with the same configurations of the previous performed dockings.

Visualization:

Results obtained after Autodock Vina processing were subjected to make a complex using Biovia Discovery Studio visualizer. Interactions and binding energies of test compounds were compared with standard inhibitor.

Result:

All three compounds were prepared to dock with the Crystal Structure of TNF-alpha (PDB id

2AZ5). The selected chemical structure of the three important ligands were shown in Fig.

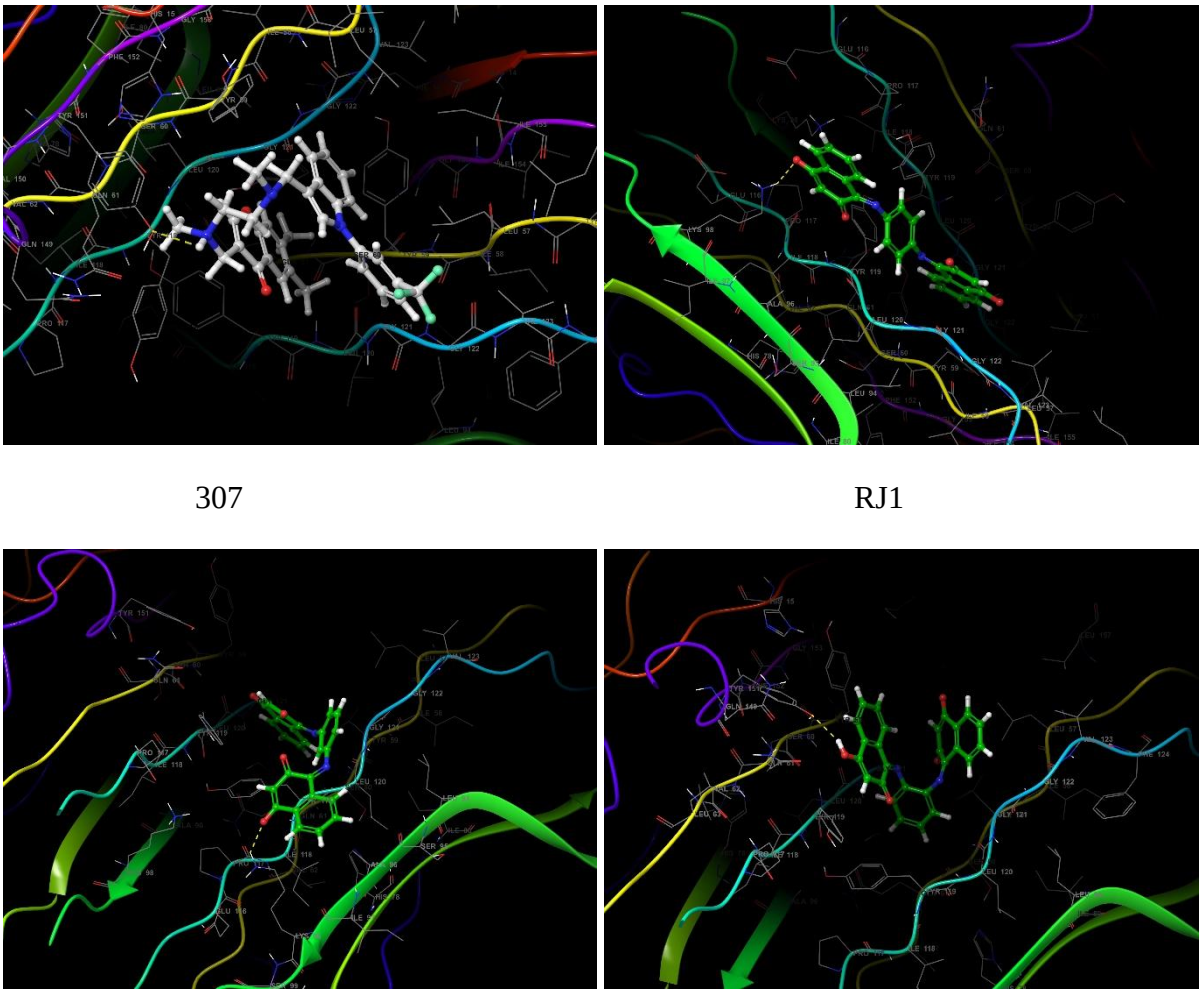

307 RJ1

RJ2 RJ3

Figure 4. Docked conformation of ligands with 2AZ5 obtained from Maestro V12.8

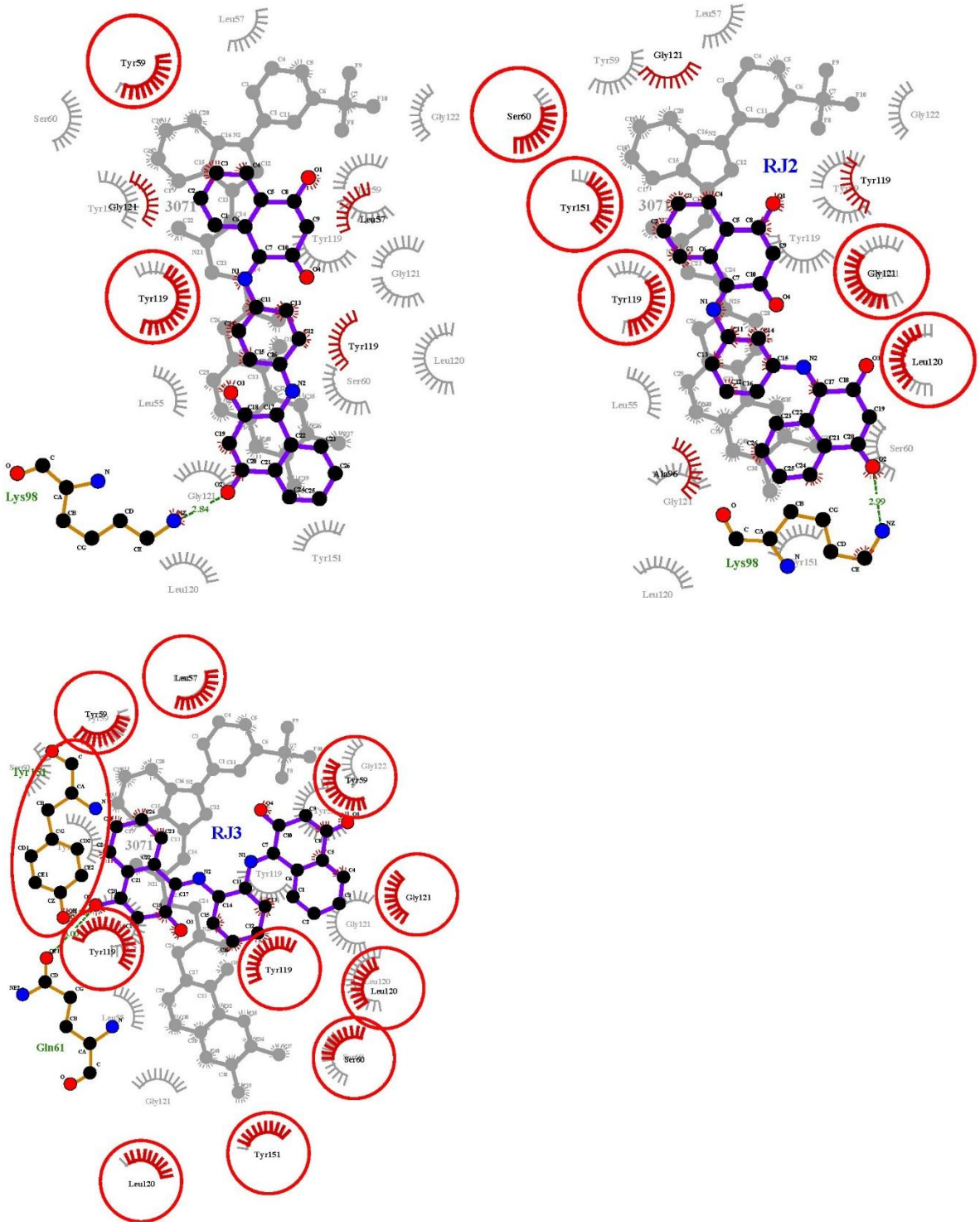

Figure 5. Overlapped 2D interactions images of designed compound compareds RJ1, RJ2, RJ3 with standard inhibitor 307 at binding pocket of TNF-α.

Table 4. Docking Score and intermolecular interactions of ligands against TNF-α (PDB id 2AZ5) using LigPlot v1.4.5, PLIP server, Maestro V12.8 and Biovia Discovery studio visualizer..

Name of compound	**Binding energy**	**Type of interaction**	**Residue id**	**Distance (in A^0)**
307 (standard)	-6.772	Hydrophobic	LEU57A LEU57B LEU57B TYR59A GLN61B TYR119B TYR119B TYR151B	3.52 3.9 3.77 3.89 3.93 3.93 3.62 3.4
		Hydrogen bond	TYR151A	2.45
		π-Stacking	TYR119B	5.44
		Π-Cation Interactins	TYR59A	4.58
RJ1	-4.6	Hydrophobic i Interactions	TYR59B TYR59B TYR119A TYR119A TYR119B	3.45 3.63 3.6 3.77 3.48
		Hydrogen bond	LYS98B	2.84
RJ2	-5.418	Hydrophobic	TYR59B	3.99

		Interactions	ALA96B TYR119B TYR151B	3.76 3.89 3.77
		Hydrogen bond	LYS98B	2.98
		Pi-Pi stacking	TYR119A	5.32
RJ3	-6.408	Hydrophobic Interactions	LEU57B LEU57B TYR59A TYR59A TYR59B TYR119A TYR119B	3.97 3.6 3.45 3.88 3.75 3.52 3.67
		Hydrogen bond	TYR151A	3.25

All the three compounds were found to be binding with the TNF-α (PDB id 2AZ5) and were used for further docking studies. The binding energy, type of interaction and their distances, interacted residues of protein with docked compounds are exhibited in Table. Compound id RJ3 exhibited good binding energy (-6.408) and formed 1 H-bond with target as compared to standard inhibitor 307 (-6.772) forming hydrogen bond with same residue (TYR151A) of TNF-α (PDB id 2AZ5). The other two compounds RJ1 and RJ2 also having moderate binding affinity with protein -4.6 and -5.418 respectively. When compared hydrogen bonds RJ1 and RJ2, first having strong interactions than second as distance of bond is smaller in RJ1. From the above results it's confirmed that the compound RJ3 was found to be best among the three compounds selected for the study, as it recorded the formation of one hydrogen bond and also exhibited a good binding energy.

Molecular docking studies :

Molecular docking studies were performed to provide a theoretical perspective for possible molecular interactions of AB-series compounds and reference/ standard (lawsone) molecules with the target

proteins [12].

The theoretical binding affinities were determined by energy minimization from docking calculation results. Molecular docking calculations were performed on Autodocktools version 4.2. energy minimization done using chimera, and molecular visualization of docking results were carried out by using the maestro.

Preparation of AB-series (ZG 1-7) and model inhibitor molecules for molecular docking was performed with MarvinSketch software. Before the docking process, the drawing and editing of the novel AB-series compounds in SD File format was done with the MarvinSketch suit program. These molecular structures have been protonated, added charges, and conformation minimization was performed with the root mean square gradient (RMS 0.001 kcal/mol/A2) by using the MMFF94 Forcefield parameters, which can be accessed in Energy Minimization protocols of these software[11]

Docking studies of AB-series compounds were carried out for important target structure named SARS-COV main protease from corona virus. The X-ray crystal structures as three-dimensional coordinates of these target proteins was obtained from the Research Collaboratory for Structural Bioinformatics (RCSB) Protein Data Bank. For use in docking calculations, structures with PDB ID 2ALV was chosen as crystal structure model corresponding to target protein. Structural defects in target protein were eliminated automatically with the DeepView - Swiss-Pdb Viewer V 4.1 software provided by the SIB Swiss Institute of Bioinformatics. Then interactions of standard inhibitor supplied by depositor with protein were checked using PDBsum (Pictorial database of 3D structures in the Protein Data Bank) online server of European Bioinformatics Institute, UK from where position of ligand was noted. Other unnecessary entries present in pdb file were removed manually using textpad 8 software.

AutodockTools version 1.5.6 was used to optimize 3D module of protein. Then energy minimization of the system was performed with UCSF Chimera 1.12 using AMBER FF14SB by considering 1000 steepest descent steps & 100 conjugate gradient steps. Possible ligand binding site in the minimized protein were determined by Computed Atlas of Surface Topography of proteins (CASTp) server.

Molecular docking studies of selected compounds into protein targets were carried out using AutoDock Vina. Docking studies were conducted on SARS-CoV-2 main protease. For docking studies, proteins were pre-processed by removal of all water and addition of kollman charges. Hydrogen bond

(H-bond) optimization was done and Gasteiger charges were added to it using AutoDock MGL tools 1.5.6. A receptor grid-box was generated by AutoGrid4 with grid box dimensions of 60 Å × 80 Å × 60 Å with spacing of 1 Å centering around hotspot residues Lys31, Glu35, Asp38, and Lys353 for ACE2 protein. Grid box for S-RBD was also set with spacing of 0.442 Å and dimensions of 62 Å × 82 Å × 82 Å centering around residues Leu455, Phe486, Asn487, Gln493, and Ser494. Lamarckian Genetic Algorithm (GA) in combination of grid based energy evaluation method was used for docking. The program was run for a total number of 50 Genetic algorithm runs. Other parameters were set as default and the final result obtained was analyzed manually by PyMol and LigPlot.

Docking of AB-series compounds and model inhibitors to the active site of these targets proteins was performed via AutodockTools 4.2 using the default docking calculation parameters. The average score of the top 10 final docking poses defined by the binding minimum energy (kcal/mol) for each compound was used as the final molecular docking score results. London dG scoring function was used for docking calculations. The London dG scoring function estimates the free energy of binding the ligand at a particular pose in a target structure. This scoring function is explained in detail in the user manual of the MOE software. After the initial scoring function for the obtained docking poses, the GBVI/WSA ΔG scoring function was used as the final docking scoring methodology. The GBVI/WSA dG is a forcefield-based scoring function, which estimates the free energy of binding of the ligand from a given pose [42]. This scoring function is explained in detail in the user manual of the MOE software.

Acknowledgement

The authors are thankful to SPPU Pune, B R Gholap College Sangavi for availability of all facilities for the synthesis and molecular docking.

References

1. Synthesis and Characterisation of Be(II) and Mg(II) complexes of 3-halolawsonemonoximes., **S. D. Gaikwad**, D. G. Kanse, V. D. Kelkar and B. A. Kulkarni. *Synth. React. Inorg. Met. Org. Chem.*, 26 (9), 77-87 (1996) **IF – 0.57**
2. Antimicrobial Activity of Thiosemicarbazone Derivatives Of Lawsone And Its Nickel Complexes,***Sanjay Gaikwad** and Charushila Gaikwad, *J. Chem. Pharm. Research*, Vol 2, Issue 4 , pp 106-111(2010
3. Synthesis and Structural Study of Yttrium (III) Complexes with Derivatives of Vitamin K3 Analog, **Sanjay Gaikwad**, *J. Appli. Chem.*, 7(6), 1565-1569, (2018),ISSN 2278 1862, IF 1.29

4. Isolation,identification and characterisation of lawsone from henna leaves powder with soxhlet apparatus, Mehrdad Mahkam,Mendi Nabati,Hadl=ieh Kafshboran ,Chemistry department ,Azarbaijan Shahid University,Tabriz,Iran.

5. Andrade et.al. Reported the synthesis and antibacterial activity of 2-amino -1,2 naphthaquinone derivatives.It ahs been shown that incorporation of amino groups into 1,4 naphthaquionone structure often results in an increase in their anticancer ,antibacterial ,antiparasitic and molluscicidal activity.(ref.6,10,40,41,46,47,50,55,59)

6. Sharma U.Katoch D.,Sood S,Kumar N.,Singh B,Thakur A.,Gulati A.: Synthesis,antobacterial and anti fungal activity of 2-amino,1,4 naphthaquinone using silica supported perchloric acid ($HClO_4.SiO_2$) as a mild recyclable and highly efficient heterogeneous catalysts Indian J.Chem-2013,Nov.52B,1431-1140.
7. F.Radt (E d .), " Elsevier 's Encyclopaedia of Organic Chemistry " Series III, Vol. 1 2 B , Elsevier, Amsterdam (1 9 5 2)
8. V. D . Kelkar, " Studies in Metal Chelates of Some Isomeric Halo hydroxynaphthoquinone s ", Ph. D . Thesis, University o f Poona (1979)
9. N . J. Sonawane, " Studies on Metal Complexes of Some Naphthoquinone Derivatives ", Ph. D . Thesis, University o f Po ona (1 9 8 1)
10. L .N . Aizenberg, A . I. Suprunenko,T. A . Bogdanovaskaya and R . S. Aizenberg, Tr. Kishinev ., Sel'Skohor Inst., 26 , 159 (1962) (C.A .59:8100b)
11. Marcello Nicoletti, ... Giovanna Palazzino, in Studies in Natural Products Chemistry, 2012
12. Naphthaquinones : Biological properties and synthesis of lawsone and derivatives,structural review.
13. Lluvia Itzel LÓPEZ LÓPEZ Ph.D.*,Departamentos de Química orgánica y Productos naturales. Facultad de Ciencias Químicas, Universidad Autónoma de Coahuila, Blvd. V. Carranza e Ing. José Cárdenas Valdés. C.P. 25280. Saltillo, Coahuila, México.
14. Synthesis, biological activity and docking calculations of bis-naphthoquinone derivatives from Lawsone ,Muhmmad Tarik Riaz,Muhmmad Yakub,Zahid Shafik, Institute of Chemical Sciences, Organic Chemistry Division, Bahauddin Zakariya University, Multan 60800, Pakistan

Paper 62

Copper Phthalocyanine Based Humidity Sensor

Ashok Datir[a], Naseem Deshpande[b]

[a]Agasti Arts, Commerce and Dadasaheb Rupwate Science College, Akole, Ahmednagar, Maharashtra

[b]Abeda Inamdar Senior College of Arts, Science and Commerce, Pune, Maharashtra

Abstract:

Copper phthalocyanine (CuPc) is synthesized using chemical method and characterized by UV visible and Fourier Transformation InfraRed (FTIR) characterization techniques. Sample is prepared in the form of pellets. Humidity sensing property of the samples is studied using two probe techniques with monitoring change in resistance of the samples. These samples have excellent stability against heat, heat, air and hence it has considerable attention for environmentally stable humidity sensors. The electrical properties of these samples were investigated at room temperature and at normal atmospheric pressure from 20 % to 90 % relative humidity. It was observed that the samples ensure good response and recovery for humidity sensing.

Key words: Copper Phthalocyanine, sensitivity, response time, recovery time, sensor

Introduction:

Today progress of mankind is directly or indirectly dependent on advanced materials which perform better and open dimensions. The domain of electronic materials was mostly confined to the simple inorganic compounds and metallic elements.

Phenomena such as metallic conduction, magnetism and superconductivity implicitly implied the study of metals and inorganic material. Although non-metallic materials are gradually replacing metallic ones in various domains at present the dominant material in the electronic industry is still silicon. Today organic polymeric materials occupy a position as a structural material.

Metal shows good conductivity of electrical charges above 10^2 S/cm. Semiconductors which have an electrical conductivity of 10^2 to 10^{-8} S/cm are the sources of transistors, integrated circuits, solid state laser and detectors. They are the control constitutes of most electronic systems. Now, highly engineered materials are vital to the progress of the electronic industry. The field of material science is entered a period of unprecedented intellectual challenge and productivity. Organic semiconductors, as a class of materials science, are in the forefront to facilitate materials science to emerge as a coherent field.

In a systematic search for new and potentially useful structures based on theory of empiricism, a multitude of phthalocyanines were synthesized and quasi one-dimensional structures were built by co-facially stacking the phthalocyanine molecules.

CuPc and its polymers possess extended conjugated structures and show interesting optical, electrical and electrochemical properties. Their remarkable thermal stability and their ability to form good quality films, the process with their molecular and crystal structures can be modified to control their properties has made them very attractive materials. CuPcs are of particular interest in many different fields of basic and applied research.

Phthalocyanine behaves as molecular organic semiconductor in solid state[3]. One of the primary physical differences between these organic semiconductors (Van der Wall's bonded) and inorganic semiconductors (covalently bounded) is the extent of orbital overlap along the conducting pathway. Binding interactions by orbital overlap of the molecular organic semiconductors are about 0.1 ev. On the other hand for the inorganic semiconductors it is of several electron volts. Cu-phthalocyanines in solid state are P type conductors. This is confirmed by measurement of thermoelectric power, rectification in thin film devices and photo reduction or oxidation in photoelectrical chemical cells (Hanack and Lang, 1994). The electrical conduction behaviour in doped polymers has been extensively studied a new conduction mechanism involving coupling of electronic excitations to nonlinear conformations have been proposed. The conduction behaviour has been explained by dopant-induced bond alternation defects. Thermal treatment of organic monomers and polymers result in the formation of extended aromatic structures or planes ladder structures, and hence the heated polymers have considerably smaller band gaps and higher mobility than unheated ones. They exhibit large and stable electrical conductivity [1], and do not need external doping. Several polymers have been shown to exhibit high conductivity upon heat treatment. The conductivity of these polymers can be controlled by varying the conditions of thermal treatment. The heated systems have excellent stability in environmental conditions such as heat, light, moisture and air. The improvement in electrical conductivity occurs due to build-up of ordered polycondensed rings [2, 5], which allow charge transport through charge hopping or tunnelling between the aromatized rings. The charge carriers are generated through the formation of radical defects formed during the thermal treatment. These materials show excellent adhesion to ceramics, metals, silicon and other semi conducting materials and hence find potential applications for the fabrication of electronic devices and as matrix materials for advances composites, electromagnetic interference shielding materials for computers and sensitive circuitry.

Experimental:

The phthalic anhydride-urea route of synthesis of copper phthalocyanine is simple and can be easily carried out in the laboratory. So the synthesis of copper phthalocyanine is carried out using this route. The reaction scheme of this synthesis method is shown in figure 1.

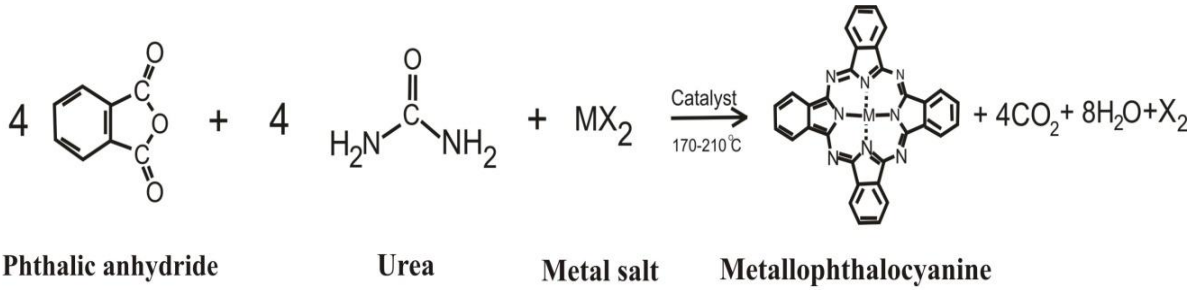

Figure 1: Reaction scheme used for synthesis of copper phthalocyanine (M = Cu).

Figure 1 shows the reaction scheme used for preparation of copper phthalocyanine [6]. CuPc is prepared by chemical method by adding phthalic anhydride into urea with copper salt. Ammonium molybdate is used as a catalyst to enhance the rate of reaction.

Synthesised material is characterized by UV visible spectroscopy for synthesized material conformation. Absorption spectra (UV-Vis) are obtained using Absorption spectrometer JASCO V-607. Synthesised MPc powders were dissolved in N-N dimethyl formamide (DMF) and electronic spectrum of the solution was recorded using UV-Vis spectrometer in the wavelength range of 200 nm – 800 nm. Infrared spectroscopy of synthesized powder is performed at room temperature using JASCO FT/IR-6100 type A in the spectral range 2000 cm^{-1} - 400 cm^{-1} by mixing synthesized material with IR-grad Pottasium Bromide (KBr) powder.

Sensitivity measurement for humidity is carried out using two probe techniques in a specially designed humidity chamber. Two silver probe contacts are used for the measurements. Relative humidity is measured by standard meter and is confirmed by calibrating with dry and wet bulb thermometer. Controlled humidity is maintained in a static humidity chamber.

Result:

The absorption bands in the region of 275 nm to 210 nm called the S-band, may be due to d-π* transition (Figure 2). The broad absorption band in the UV region is preceded by the UV absorption band edge of the phthalocyanine molecule. The other band appears in the visible region between 500 nm to 750 nm. This band is named as Q-band. Absorption due to

π-π* transitions is reported to appear in the visible region at wavelengths between 500 nm and 750 nm (Q band). Results obtained from the absorption spectra of CuPc shows the λ_{max} values of 547 nm.

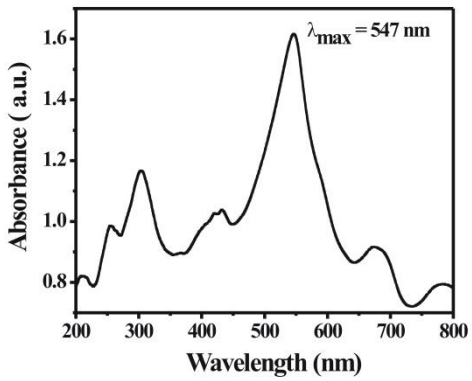

Figure 2: UV-Visible absorption spectra of CuPc

FTIR absorption spectra were studied so as to confirm the structure. Figure 3 shows the FTIR spectra of copperphthalocyanine. A series of weak absorption observed between 1700 cm^{-1} and 2000 cm^{-1} is due to the aromatic compound which is same for all metallophthalocyanines. The macromolecule shows band characteristic of phthalocyanine skeleton at 750 to 760, 885 to 915, 915 to 975, 1015 to 1070 and 1140 to 1150 cm^{-1}. As the macromolecule has COOH group, it show the characteristic band of the C=O group at 1690 and 1710 cm^{-1}.

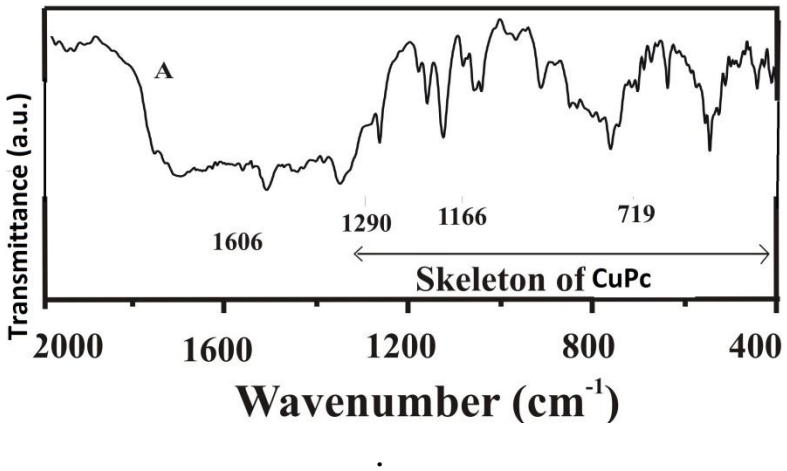

.

Figure 3: FTIR spectra of CuPc

Figure 4 shows a plot of electrical resistance of CuPc versus relative humidity from 20 percent to 90 percent.

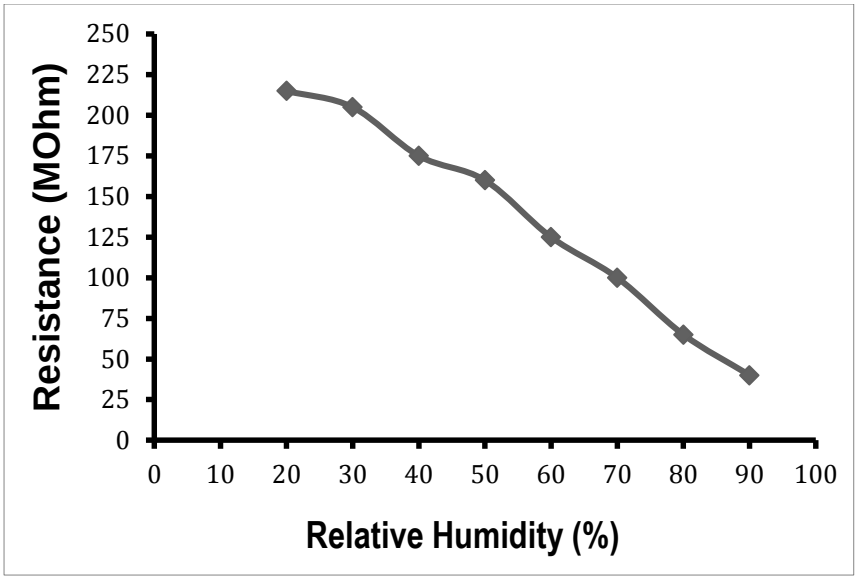

Figure 4: Resistance change with change in relative humidity.

Conclusion:

CuPc is synthesized and confirmed with characterization. These samples showed response for humidity as resistance change and observed that the variation in resistance is 220 MOhm to 40 MOhm for the change of relative humidity from 20 percent to 90 percent.

References:

[1] Hanack, M., 1989, New Aspects of Organic Chemistry I, Yoshida, Z., Shiba, T. and Oshiro, Y. (Eds), Verlag Chemie, Weinheim.

[2] Chakane S., Jain S., and Bhoraskar, S.V., 2001, Synthesis, characterization, and humidity sensing of metallophtalocyanines, SPIE, 4235, pp. 298 304.

[3] Hanack, M. and Lang, M., 1994, Adv. Matr 6, 819. Hanack, M. and Lang, M., 1995, Chemtracts, Org. Chem. 8, 131.

[4] Jain, S., Chakane, S., Samui, A.B., Krishnamurthy, V.N. and Bhoraskar, S.V., 2003, Humidity sensing with weak acid-doped polyaniline and its composites, Sensors and Actuators B, 96, pp. 124-129. Venkatachalam, S., Vijaynathan, V. and Krishnamurthy,

[5] V.N., 1996, Metallophtalocyanines Polyneric (Overview), Polyneric Materials Encyclopedia, CRC Press, Boca Raton, SL, pp. 4221-4232.

[6] **A. M. Datir**, V. S. Ghole, Pankaj Koinkar, S. D. Chakane, " Nitrogen Dioxide Gas Sensor Based on Cobalt and Nickel Phthalocyanine Working at Room Temperature", *International Journal of Modern Physics B*, Vol. 25, No. 31 (2011) 4190–4193. DOI: 10.1142/S0217979211066556.

Paper 63

Green Synthesis of ZnO Nanoparticles Using *Sugarcane Juice* for LPG Sensing Applications

Avadhut V. Kardile[1], M. H. Moulavi[1], Ramakant P. Joshi[2], Pandit N. Shelke[2] Ravindra U. Mene[2]*

[1] PDEA's, Annasaheb Waghire College, Otur Tal: Junnar, Pune,(M.S.) India.
[2]PDEA's, Annasaheb Magar Mahavidyalaya, Hadapsar, Pune, (M.S.) India.

Abstract

In the present work, we have successfully synthesized ZnO nanoparticles (NPs) by *sugarcane stem* using green synthesis method. Structural, morphological and optical characteristics of ZnO NPs are examined by X-ray diffraction (XRD), scanning electron microscopy (SEM), and ultraviolet-visible spectroscopy (UV–Vis). XRD reveals hexagonal wurtzite structure with average crystallite size of 30 nm. SEM images depict the uniformly distributed spherical nanoparticles. The optical measurements showed band gap is 3.15 eV. Synthesized ZnO NPs are investigated for its LPG gas sensing study together with operating temperature, response/recovery time and gas uptake capacity. The detail examination of LPG sensing study demonstrates the operating temperature 220ºC with gas response of 91%, with fast response/recovery times 90/70 sec. respectively. In addition, the LPG gas uptake capacity remained sensible up to 9,000 ppm. Ultimately, we conclude that the green synthesis route, to fabricate sensor devices is encouraging as it is cost-effective, eco-friendly and simple.

Keywords: Green synthesis; ZnO; XRD; UV-Vis; SEM; Gas Sensor;

1.Introduction

Nanomaterials display a wide range of unique physicochemical properties that are well-known to originate from the high surface area and nanoscale size of their constitutional components, called nanoparticles (NPs) [1]. NPs are a wide range of materials with dimensions below 100 nm, which can be used in various applications, such as medical, pharmaceutical, manufacturing and materials, environmental, electronics, energy collection, and mechanical industries, due to their multiple properties [2–5]. Wherein, metal oxide NPs have gained great attention among researchers for nano-device applications [6]. Among a large variety of metal oxides, zinc oxide (ZnO) NPs has superficially secured a special place in scientific and technological domains. ZnO is an n-type semiconductor having special features such as wide and direct band-gap (3.37 eV), large exaction binding energy (60 meV), high electron mobility,

chemical/thermal stability, and good transparency. Hence it have various front-line applications in the field of solar cells, gas sensors, field emission devices, capacitors, coatings, sunscreen lotion, cosmetic and medicated creams [7-9].

Over the years, a wide number of physical, chemical and hybrid synthetic methods have been developed and employed to obtain ZnO NPs.[10-15]. Usually, these preparation methods face several limitations, such as the high cost of equipment, usage/emission of highly toxic and hazardous materials, impurities, high temperature/pressure conditions, and additional use of capping agents, stabilizers [16]. To overcome these limitations, green chemistry procedures gaining importance as they are safe and eco-friendly methods, inexpensive, do not produce toxic by-products, and produce clean nanomaterials.

Hence the main emphasis of researchers is developing simple and green methods for synthesizing ZnO NPs [17]. According to the literature, several types of fruit and plants extracts has been used for the synthesis of ZnO NPs such as *Tabernaemontana divaricata, Citrus maxima (Pomelo), Aristolochia indica, Echinacea spp.,* Mentha longifolia, *Salvadora oleoides, Boswellia ovalifoliolata, Limonia acidissima, Cochlospermum religiosum,* and *Conyza canadensis* for various application including photo catalytic properties, antimicrobial activity, gas sensor etc., [18-29].

In the present work, we herein report, a simple, cost-effective and environment sustainable green approach for the synthesis of ZnO NPs using *sugarcane stem* extract for LPG sensing application. As synthesized, ZnO NPs are characterized for their structural, morphological and optical properties and further employed for detailed investigation of operating temperature, response/recovery time and uptake capacity for LPG gas sensing applications.

2. Experimental and Characterization Technique

2.1 Green synthesis of ZnO NPs using sugarcane stem

The schematic representation of the ZnO NPs by green synthesis using *sugarcane stem* is shown in Figure 1. Initially, fresh *sugarcane stem* is collected from agriculture field and cut into small pieces by sharp blade. Further it is washed with distilled water and dry in sunlight for two hour. Thereafter, 10 gm of dried *sugarcane stem* dipped in to 1M zinc acetate solution for specific period of 24 hrs to 48 hrs. Zinc acetate solution is absorbed by the *sugarcane stem* wherein complex reaction is occurred. Then solution is filtered and separated *sugarcane stem* dried under infrared lamp for 3-4 hours. Subsequently *sugarcane stem* is sintered at 800 ^{o}C for 3

hrs and crushed in to powder form. As prepared powder is used to prepare sensor matrix in the form of thick film by screen printing on glass substrate is reported in our earlier work [30].

Figure 1: Experimental Scheme of the ZnO NPs by green synthesis using *sugarcane stem*

The prepared films are further used for structural and morphological characterizations. The structural and surface characterization is carried out using XRD, SEM and UV analysis. X-ray diffraction pattern is recorded with a Bruker AXS Germany (Model D8 Advanced) having CuKα (λ= 1.54 Å) incident radiation. The surface morphology and elemental analysis is visualized by means of Scanning Electron Microscope (FE-SEM Hitachi S-4800) with EDAX. UV–Visible absorption spectra is obtained by a Shimadzu UV-3600 spectrophotometer.

The electrical and gas sensing characteristics are monitored using a home built static gas sensing system reported in our earlier work [30]. The sensor matrix in the form of thick film is typically 1 cm x 1.5 cm in dimension, which is placed on the heating plate in the test chamber where it is preheated at the required temperature using a temperature controller to remove the humidity effect. The two probe dc measurement technique is used to measure the electrical resistance of film in air atmosphere and in the presence of test gas. Silver paste contacts are applied at the edges of the film separated by 1 cm, as top electrodes whose ohmic nature is tested within ± 10 V. The desired gas concentration inside the system is achieved by injecting a known volume of the LPG gas. Measurement of the voltage across the reference resistance is followed by measurement of sensor resistance in air and gas (LPG) atmosphere as a function of temperature. The change in resistance of the sensor, due to the presence of LPG gas, is noted in Gas response (%), calculated using classical relations,

Gas response (%) = [$R_g - R_a$] / R_a * 100 = (Δ R/ R_a * 100) (1)

where R_g and R_a are the resistances measured in gas and air, respectively.

3. Results and Discussion

3.1. X-ray, SEM and UV analysis

Figure 2 (a) shows the X-Ray diffractogram of ZnO NPs obtained from *sugarcane stem* by green synthesis. Peak positions indexed to (100), (002), (101), (102), (110) (103), (112) and (201) observed at 2θ values such as 31.98º, 34.67º, 36.48º, 47.71º, 56.79º, 63.08º, 68.21º, 69.24º, respectively. All the reflections are observed commonly in ZnO, which support the formation of hexagonal wurtzite type structure of ZnO films [JCPDS (76-0704)]. As the width of the peak increases the size of particle decreases, which is attributed to the nano size of the present material [31]. The average crystallite size of as synthesized ZnO NPs are calculated from the full-width half maximum (FWHM) of all the obtained peaks using the Debye–Scherrer formula and it is found to be 30 nm.

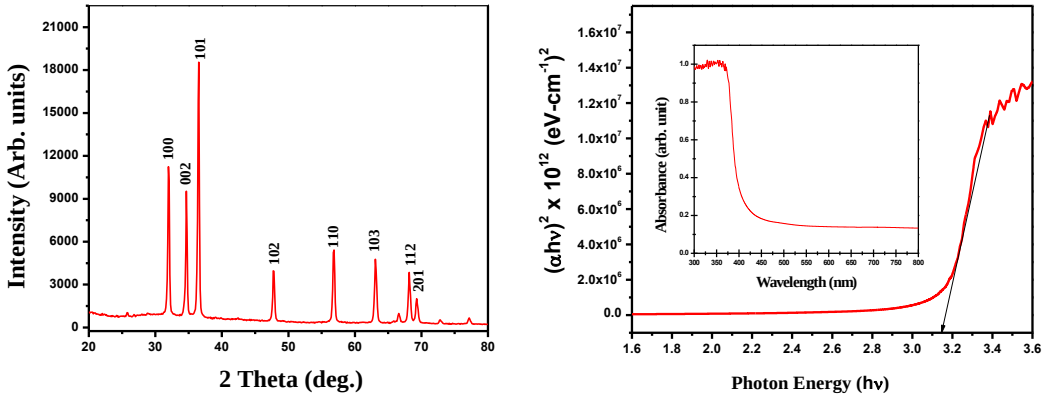

Figure 2: (a) The X-ray diffraction pattern of ZnO NR. **(b)** UV-Visible Spectra of Tauc's plot and absorption spectra (inset) for ZnO NR.

The optical study is performed to evaluate the optical properties of the ZnO NPs as shown in Figure 2 (b). The band gap of the samples are estimated by extrapolation of the linear relationship between $(\alpha h\nu)^2$ and photon energy ($h\nu$). The direct band gap (Eg) values are determined from the intercept of $(\alpha h\nu)^2$ vs ($h\nu$) curve. The band gap obtained using the variation showed the value 3.15 eV which is in good agreement with the reported value of ZnO [32]. Moreover, the absorption peak at 360 nm as shown in figure 2(b) (inset) which is blue shifted.

Thus, a strong blue shift in the absorption spectra gives the predication that ZnO must be smaller than the bohr radius of exciton [33], which confirms the formation of ZnO particle in nanoscale.

Figure 3(a-b) shows the SEM images of two magnifications for ZnO NPs obtained through novel green synthesis of *sugarcane stem*. It illustrates the presence of thickly aggregated spherical ZnO NPs spread over many regions. Moreover, the size distribution histogram revealed that green synthesized ZnO NPs are in the range of 20-40 nm which is in good agreement with the X-ray analysis. The elemental composition of ZnO NPs is also confirmed by EDAX analysis as shown in figure 3(c). This spectrum not only confirmed the occurrence of the Zn and O elements but also verified the relative purity of the material synthesized. Precisely, the EDAX analyses showed the elemental composition of Zn with 73.85% and O with 26.15%; however, the theoretical stoichiometric mass% of Zn and O are 80.3% and 19.7% respectively [34]. The deviations in the experimental data seen from that of the theoretical one can be attributed due to the presence of some organic residue and/or other impurity coming from the starting precursor in minute quantities.

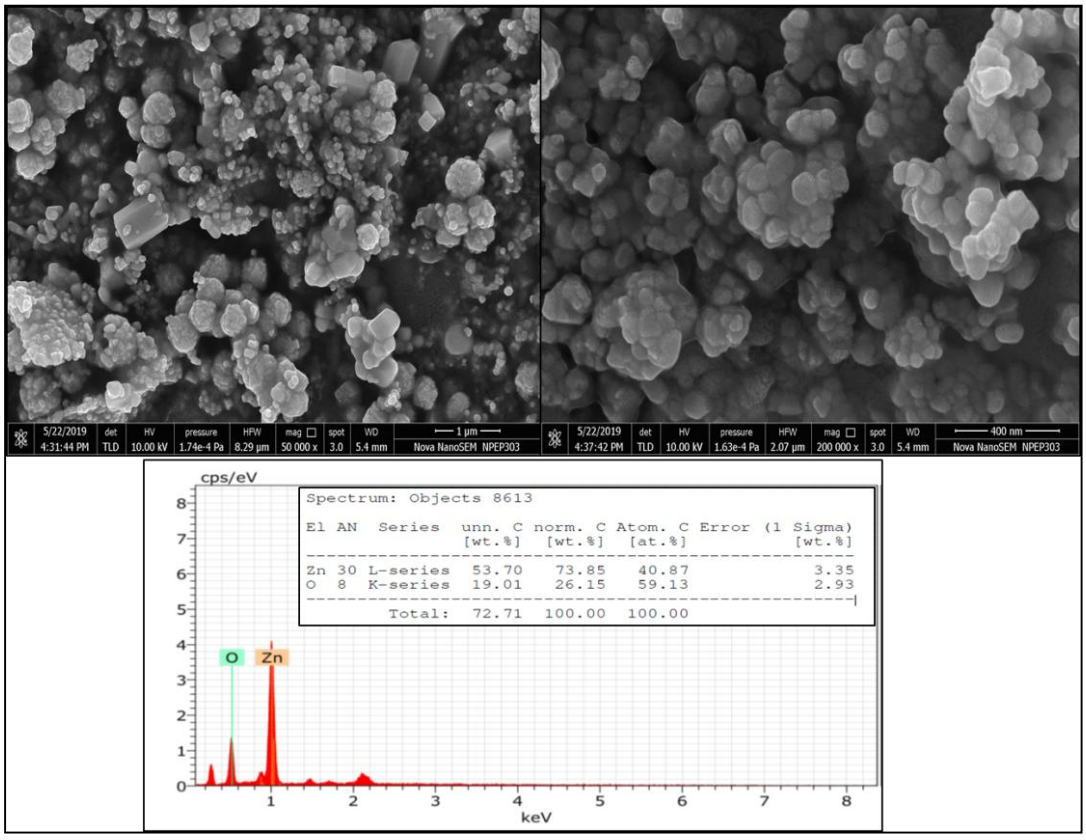

Figure 3. (a-b) The SEM Images of green synthesized ZnO NPs at two magnifications, **(c)** EDAX spectra

3.2. LPG Sensing performance of Green synthesis ZnO NPs(Temperature optimization, response-recovery time and Gas uptake capacity)

Figure 4 (a) depicts the variation of the gas response as a function of temperature in LPG gas atmosphere, with fixed gas concentration of 1000 ppm. It is observed that gas response remains very low initially and increases as a function of temperature in the range of 150-220°C and further decreases with rise in temperature. It possesses a maximum gas response of 91 % at an operating temperature 220°C for LPG gas. The variation in gas response with respect to time (sec) in response to 1000 ppm of LPG for ZnO NPs held at operating temperature 220°C is showed in figure 4 (b). When the sensor is exposed to gas atmosphere, gas response is found to be increase with time which later on remained constant with further increase in time. Upon exposure to air, the reduction in gas response is observed. From the figure, it can be concluded that the response and recovery time of ZnO film for LPG gas is found to be ~90 and 70 sec.

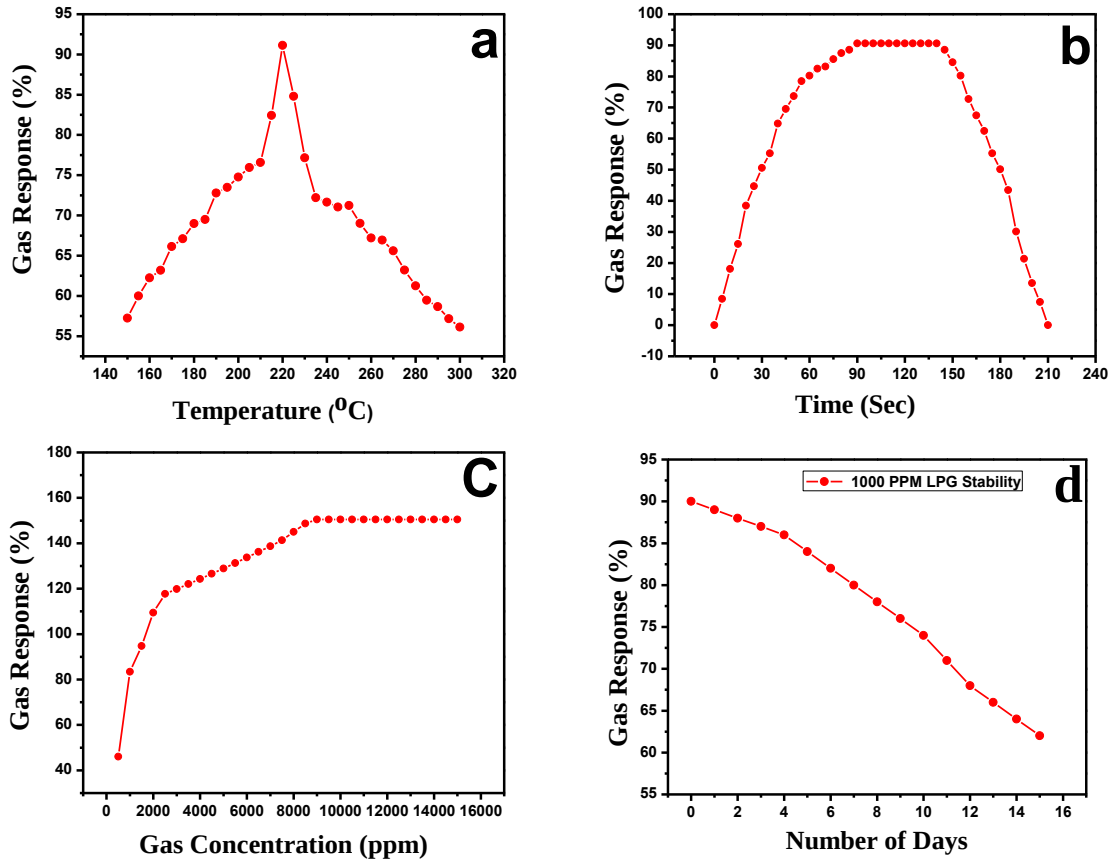

Figure 4. (a) The variation of Gas response (%) with respect to operating temperature at 1000 ppm of LPG gas concentration. **(b)** Response and Recovery plot at 220^{o}C operating temperature. **(c)** Variation of Gas response (%) with respect to LPG gas concentration. **(d)** Long term stability curve of ZnO for 1000 ppm of LPG gas concentration.

Figure 4 (c) shows the variation in gas response with variable LPG gas concentration in the range of 500 ppm to 15,000 ppm. From the figure, it can be concluded that the behavior of gas response as a function of gas concentration shows three main regions. The first region shows sharp initial rise in gas response up to 2500 ppm (high sensitivity region). The second is intermediate region, shows nearly linear increase in gas response, and third region is the saturation region in which the sensor completely saturates. The rate of increase in gas response is relatively larger up to 9000 ppm for LPG. Afterwards, increase in gas concentration, the sensor gets completely saturated. It may be due to the mono/multi-layer adsorption of gas molecules on the surface that could cover the whole surface of the film. The excess gas molecules cannot reach surface active sites of the sensor; hence the gas response at higher concentration not expected to increase further. Therefore it can be concluded that the green synthesized ZnO NPs can monitor the LPG gas up to 9000 ppm concentration respectively. In addition, stability of the gas sensor is very important aspect to assess the long term gas sensing performance. Therefore we have studied the stability curve of ZnO NPs for LPG as shown in Fig. 4(d). It is observed that the gas response of ZnO NPs remains nearly stable up to 15 days which conclude its steady gas response even after its long term exposure.

4. Conclusions

In this study, ZnO NPs are successfully prepared through green synthesis method using *sugarcane stem* extract. Structural, optical and morphological studies are confirmed using XRD, UV and SEM analysis respectively. X-ray analysis confirmed the formation of ZnO hexagonal wurtzite structure with a crystallite size of 30 nm. Uniformly aggregated spherical ZnO NPs is visualized by SEM. The optical characteristics showed the wide band gap 3.15 eV. The organized study of LPG sensing has demonstrated 91% maximum gas responses at operating temperature 220^{o}C. The fast response and recovery time of 90 and 70 sec, proves its possibility to be employed as gas sensor. The maximum gas uptake capacity for LPG remained sensible up to up to 9000 ppm. In summary, we conclude that simple, cost-effective and eco-friendly green synthesized ZnO sensor would be a potential candidate for LPG sensors.

Acknowledgement

Thanks to Prof. S. G. Gosavi, SPPU, Pune, for providing SEM facility and fruitful discussion. This work is carried out under minor research project (F.No.F-47-1058/14 (GENERAL/64/WRO/XIIth Plan 2017) sanctioned by University Grants Commission (UGC), New Delhi, India.

References

[1] Kim, Dohyung, Joaquin Resasco, Yi Yu, Abdullah Mohamed Asiri, and Peidong Yang. "Synergistic geometric and electronic effects for electrochemical reduction of carbon dioxide using gold–copper bimetallic nanoparticles." *Nature communications* 5, no. 1 (2014): 1-8.

[2] Khan, Ibrahim, Khalid Saeed, and Idrees Khan. "Nanoparticles: Properties, applications and toxicities." *Arabian journal of chemistry* 12, no. 7 (2019): 908-931.

[3] Saleh, T.A.; Gupta, V.K. Chapter 4—Synthesis, Classification, and Properties of Nanomaterials. In Nanomaterial and Polymer Membranes; Saleh, T.A., Gupta, V.K., Eds.; Elsevier: Amsterdam, The Netherlands, (2016): 83–133. ISBN 978-0-12-804703-3.

[4] Guleria, Apurav, Suman Neogy, Bhakti S. Raorane, and Soumyakanti Adhikari. "Room temperature ionic liquid assisted rapid synthesis of amorphous Se nanoparticles: Their prolonged stabilization and antioxidant studies." *Materials Chemistry and Physics* 253 (2020): 123369.

[5] Sudha, P.N.; Sangeetha, K.; Vijayalakshmi, K.; Barhoum, A. Chapter 12—Nanomaterials history, classification, unique properties, production and market. In Emerging Applications of Nanoparticles and Architecture Nanostructures; Barhoum, A., Makhlouf, A.S.H., Eds.; Micro and Nano Technologies; Elsevier: Amsterdam, The Netherlands, (2018): 341–384. ISBN 978-0-323-51254-1.

[6] Wang, Chengxiang, Longwei Yin, Luyuan Zhang, Dong Xiang, and Rui Gao. "Metal oxide gas sensors: sensitivity and influencing factors." *sensors* 10, no. 3 (2010): 2088-2106.

[7] Comini, E., C. Baratto, G. Faglia, M. Ferroni, Alberto Vomiero, and G. Sberveglieri. "Quasi-one dimensional metal oxide semiconductors: Preparation, characterization and application as chemical sensors." *Progress in Materials Science* 54, no. 1 (2009): 1-67.

[8] Giri, P. K., S. Bhattacharyya, B. Chetia, Satchi Kumari, Dilip K. Singh, and P. K. Iyer. "High-yield chemical synthesis of hexagonal ZnO nanoparticles and nanorods with excellent optical properties." *Journal of Nanoscience and Nanotechnology* 11 (2011): 1-6.

[9] Thomas, Deepu, Simon Augustine, Kishor Kumar Sadasivuni, Deepalekshmi Ponnamma, Ahmad Yaser Alhaddad, John-John Cabibihan, and K. A. Vijayalakshmi. "Microtron irradiation induced tuning of band gap and photoresponse of Al-ZnO thin films synthesized by mSILAR." *Journal of Electronic Materials* 45, no. 10 (2016): 4847-4853.

[10] Vasei, H. Vahdat, S. M. Masoudpanah, M. Adeli, and M. R. Aboutalebi. "Solution combustion synthesis of ZnO powders using various surfactants as fuel." *Journal of Sol-Gel Science and Technology* 89, no. 2 (2019): 586-593.

[11] Zare, Mina, K. Namratha, K. Byrappa, D. M. Surendra, S. Yallappa, and Basavaraj Hungund. "Surfactant assisted solvothermal synthesis of ZnO nanoparticles and study of their antimicrobial and antioxidant properties." *Journal of materials science & technology* 34, no. 6 (2018): 1035-1043.

[12] Lin, Kuo-Feng, Hsin-Ming Cheng, Hsu-Cheng Hsu, Li-Jiaun Lin, and Wen-Feng Hsieh. "Band gap variation of size-controlled ZnO quantum dots synthesized by sol–gel method." *Chemical Physics Letters* 409, no. 4-6 (2005): 208-211.

[13] Khan, Ziaul Raza, Mohd Shoeb Khan, Mohammad Zulfequar, and Mohd Shahid Khan. "Optical and structural properties of ZnO thin films fabricated by sol-gel method." *Materials Sciences and applications* 2, no. 5 (2011): 340-345.

[14] Kołodziejczak-Radzimska, Agnieszka, and Teofil Jesionowski. "Zinc oxide—from synthesis to application: a review." *Materials* 7, no. 4 (2014): 2833-2881.

[15] Ba-Abbad, Muneer M., Abdul Amir H. Kadhum, Abu Bakar Mohamad, Mohd S. Takriff, and Kamaruzzaman Sopian. "Visible light photocatalytic activity of Fe3+-doped ZnO nanoparticle prepared via sol–gel technique." *Chemosphere* 91, no. 11 (2013): 1604-1611.

[16] Yusof, Hidayat Mohd, Rosfarizan Mohamad, and Uswatun Hasanah Zaidan. "Microbial synthesis of zinc oxide nanoparticles and their potential application as an antimicrobial agent and a feed supplement in animal industry: a review." *Journal of animal science and biotechnology* 10, no. 1 (2019): 1-22.

[17] Awwad, Akl M., Mohammad W. Amer, Nidà M. Salem, and Amany O. Abdeen. "Green synthesis of zinc oxide nanoparticles (ZnO-NPs) using Ailanthus altissima fruit extracts and antibacterial activity." *Chem. Int* 6, no. 3 (2020): 151-159.

[18] Patil, Bheemanagouda N., and Tarikere C. Taranath. "Limonia acidissima L. leaf mediated synthesis of zinc oxide nanoparticles: a potent tool against Mycobacterium tuberculosis." *International journal of mycobacteriology* 5, no. 2 (2016): 197-204.

[19] Kumar, HK Narendra, N. Chandra Mohana, B. R. Nuthan, K. P. Ramesha, D. Rakshith, N. Geetha, and Sreedharamurthy Satish. "Phyto-mediated synthesis of zinc oxide nanoparticles using aqueous plant extract of Ocimum americanum and evaluation of its bioactivity." *SN Applied Sciences* 1, no. 6 (2019): 1-9.

[20] Raja, A., S. Ashokkumar, R. Pavithra Marthandam, J. Jayachandiran, Chandra Prasad Khatiwada, K. Kaviyarasu, R. Ganapathi Raman, and M. Swaminathan. "Eco-friendly preparation of zinc oxide nanoparticles using Tabernaemontana divaricata and its photocatalytic and antimicrobial activity." *Journal of Photochemistry and Photobiology B: Biology* 181 (2018): 53-58.

[21] Pavithra, N. S., K. Lingaraju, G. K. Raghu, and G. Nagaraju. "Citrus maxima (Pomelo) juice mediated eco-friendly synthesis of ZnO nanoparticles: applications to photocatalytic, electrochemical sensor and antibacterial activities." *Spectrochimica Acta Part A: Molecular and Biomolecular Spectroscopy* 185 (2017): 11-19.

[22] Steffy, Katherin, Ganesan Shanthi, Anson S. Maroky, and Sachidanandan Selvakumar. "Enhanced antibacterial effects of green synthesized ZnO NPs using Aristolochia indica against Multi-drug resistant bacterial pathogens from Diabetic Foot Ulcer." *Journal of infection and public health* 11, no. 4 (2018): 463-471.

[23] Attar, Azade, and Melda Altikatoglu Yapaoz. "Biomimetic synthesis, characterization and antibacterial efficacy of ZnO and Au nanoparticles using echinacea flower extract precursor." *Materials Research Express* 5, no. 5 (2018): 055403.

[24] Mohammadi-Aloucheh, Ramin, Aziz Habibi-Yangjeh, Abolfazl Bayrami, Saeid Latifi-Navid, and Asadollah Asadi. "Green synthesis of ZnO and ZnO/CuO nanocomposites in Mentha longifolia leaf extract: characterization and their application as anti-bacterial agents." *Journal of Materials Science: Materials in Electronics* 29, no. 16 (2018): 13596-13605.

[25] Karaköse, Ercan, and Hakan Çolak. "Structural, electrical, and antimicrobial characterization of green synthesized ZnO nanorods from aqueous Mentha extract." *MRS Communications* 8, no. 2 (2018): 577-585.

[26] Padalia, Hemali, Shipra Baluja, and Sumitra Chanda. "Effect of pH on size and antibacterial activity of Salvadora oleoides leaf extract-mediated synthesis of zinc oxide nanoparticles." *Bionanoscience* 7, no. 1 (2017): 40-49.

[27] Supraja, N., T. N. V. K. V. Prasad, T. Giridhara Krishna, and E. David. "Synthesis, characterization, and evaluation of the antimicrobial efficacy of Boswellia ovalifoliolata stem bark-extract-mediated zinc oxide nanoparticles." *Applied Nanoscience* 6, no. 4 (2016): 581-590.

[28] Zare, Elham, Shahram Pourseyedi, Mehrdad Khatami, and Esmaeel Darezereshki. "Simple biosynthesis of zinc oxide nanoparticles using nature's source, and it's in vitro bio-activity." *Journal of Molecular Structure* 1146 (2017): 96-103.

[29] Bala, Niranjan, S. Saha, M. Chakraborty, M. Maiti, S. Das, R. Basu, and P. Nandy. "Green synthesis of zinc oxide nanoparticles using Hibiscus subdariffa leaf extract: effect of temperature on synthesis, anti-bacterial activity and anti-diabetic activity." *RSC Advances* 5, no. 7 (2015): 4993-5003.

[30] Mene, Ravindra U., Megha P. Mahabole, and Rajendra S. Khairnar. "Surface modified hydroxyapatite thick films for CO2 gas sensing application: Effect of swift heavy ion irradiation." *Radiation Physics and Chemistry* 80, no. 6 (2011): 682-687.

[31] Goutham, Solleti, Sukhpreet Kaur, Kishor Kumar Sadasivuni, Jayanta Kumar Bal, Naradala Jayarambabu, Devarai Santhosh Kumar, and Kalagadda Venkateswara Rao. "Nanostructured ZnO gas sensors obtained by green method and combustion technique." *Materials Science in Semiconductor Processing* 57 (2017): 110-115.

[32] Oladiran, Awodugba Ayodeji, and Ilyas Abdul-Mojeed Olabisi. "Synthesis and characterization of ZnO nanoparticles with zinc chloride as zinc source." *IOSR Journal of Applied Physics* 2, no. 2 (2013).

[33] Yeow, S. C., W. L. Ong, A. S. W. Wong, and G. W. Ho. "Template-free synthesis and gas sensing properties of well-controlled porous tin oxide nanospheres." *Sensors and Actuators B: Chemical* 143, no. 1 (2009): 295-301.

[34] Narayana, Ashwath, Sachin A. Bhat, Almas Fathima, S. V. Lokesh, Sandeep G. Surya, and C. V. Yelamaggad. "Green and low-cost synthesis of zinc oxide nanoparticles and their application in transistor-based carbon monoxide sensing." *RSC Advances* 10, no. 23 (2020): 13532-13542.

Paper 64

A Brief Review on Ethnomedicinal Plants used by Tribal Healers for the Maintenance of Primary Healthcare in India.

Roopa Vishwanath Sangvikar

Department of Botany, Microbiology and Biotechnology, NES Science College, Nanded

Abstract:

The traditional medicine based on ethnomedicinal plants in India presents a strong relationship belonging to natural remedies, health, diet, and folk healing practice recognized by tribal healers. The present study aims to carry out an ethnobotanical review on medicinal plant species used by tribal healers in India including information on plant species, plant part used, mode of consumption as well as medical uses. Earlier published data in research journals, textbooks, websites, and databases written in pharmacological evidence of Indian ethnomedicinal plants were based on gathering information. The present review work reported that 58 plant species belonging to 30 different families have been used by Indian tribal healers. Fabaceae has the highest number of plant species (07) followed by Amaranthaceae and Euphorbiaceae with 04 plant species in each. The inventoried plant species in the current work are frequently used for the treatment of primary healthcare and to ensure the medication safety of tribal healers. The most used preparation method of plant drugs, which is used in Indian Alternative medicine was decoction and paste of plant parts. The leaves (36%), underground parts (root/bulb/tuber) (15%), bark (11%), fruit (7%), seeds (7%), latex (6%), and flowers (5%) were the most useful plant parts in natural preparation in Indian traditional medicine in a percentage as reported in the present review work. The studied ethnomedicinal plant species have been extensively effective medicines for diarrhea and dysentery, oral healthcare, snakebite and cuts, burns, and wound healing potential.

Key words: Ethnomedicinal plants, tribal healers, primary health care.

Introduction:. ...

India has a rich traditional plant-based knowledge of health care. Plant based herbal drugs are in great demand in both developing and the developed countries in primary healthcare due to their great efficacy and little or no side effects. In India, the indigenous system of medicine namely ayurvedic, siddha and unani have been in existence since several years. A large number of plants, plant extracts, decoctions, or pastes are used by tribal healers and folklore traditions in India for the treatment of diarrhea, oral problems, snakebites, cuts, and wounds [1-3]. Several tribal groups have been using several plants or plant products for medicinal preparations and these medicines are known as ethnomedicines [4]. It is estimated that around 200,000 plant species are known all over the world. The World Health Organization (1978), has estimated that 80% of the populations of developing countries rely on traditional

medicines, mostly plant drugs, for their primary health care needs [5]. In India, 65 % of the population relies on ethnomedicine for their health care needs [6].

India is one of the twelve mega-biodiversity countries of the world, which having rich vegetation with a wide variety of plants with high medicinal values. Over 550 tribal communities are covered under 227 ethnic groups residing in about 5000 villages of India in different forests and vegetation types [7]. The uses of different parts of plants by the tribal healers of the plains or hilly areas in different aspects have been studied by several workers [8]. Our country has a vast ethnomedicinal and folklore wealth. The indigenous groups possess their own distinct culture, religious rites, food habit, and rich knowledge of traditional medicine [9]. Medicinal plants had a considerable global impact in recent years. Due to various human activities such as deforestation, urbanization, rapid industrialization, and other developmental activities causing a fast reduction in both natural vegetation and traditional culture in India [10].

Therefore, the current review was conducted to gather information about the ethnomedicinal plants used by tribal healers for the maintenance of primary health care, such as to highlight the description of medicinal plants including local name, the parts used, mode of consumption as well as traditional uses.

Materials and methods:

Study area:

India is a Southern Asia. It has the 2nd largest population in the world. Speaking of area, India is the 7th largest country in the world. It lies on the Indian Plate, which is the northern part of the Indo-Australian Plate. India spreads over an area of about 3.28 million sq. km. The mainland of India extends between 8°4′ and 37°6′ N latitude and 68°7′ and 97°25′ E longitude.

Data collection:

In the present brief review, the data collected from previously published research journals, textbooks, websites, databases and folklore information written in pharmacological profiles and traditional uses of Indian medicinal plants were checked for collecting information.

Results and discussion:

The fruits of the present review of ethnomedicinal plants used in traditional medicine in India are summarised in Table 1.

The present survey reported that 58 plant species springing from 30 different families have been used in different continents of India (Table 1). Fabaceae has the highest number of plant species (07) Followed by Euphorbiaceae and Amaranthaceae with 04 plant species. The remaining families were represented by one or two species each (Figure 1). The present data confers that these families were mostly used by the tribal healers in India for primary health care as traditional medicine. Data presented in Table 1 shows several plant species,

frequently used for the treatment of various illnesses associated with diarrhea and dysentery, oral health problems, snakebite and skin cut, wounds, and skin burn. The most cited plant families in the present work were Fabaceae, Amaranthaceae, Euphorbiaceae, Asteraceae, Liliaceae, Meliaceae, and Caesalpinaceae. It was reported that herbal medicine used traditionally for disease treatment, also used as a precursor for the development of several promising drugs [59]. The present work highlights these practices from an ethnopharmacological survey by targeting 58 ethnomedicinal plant species frequently used by almost all tribal healers of India. (Table 1).

Fig.1 Showing Name of studied Families

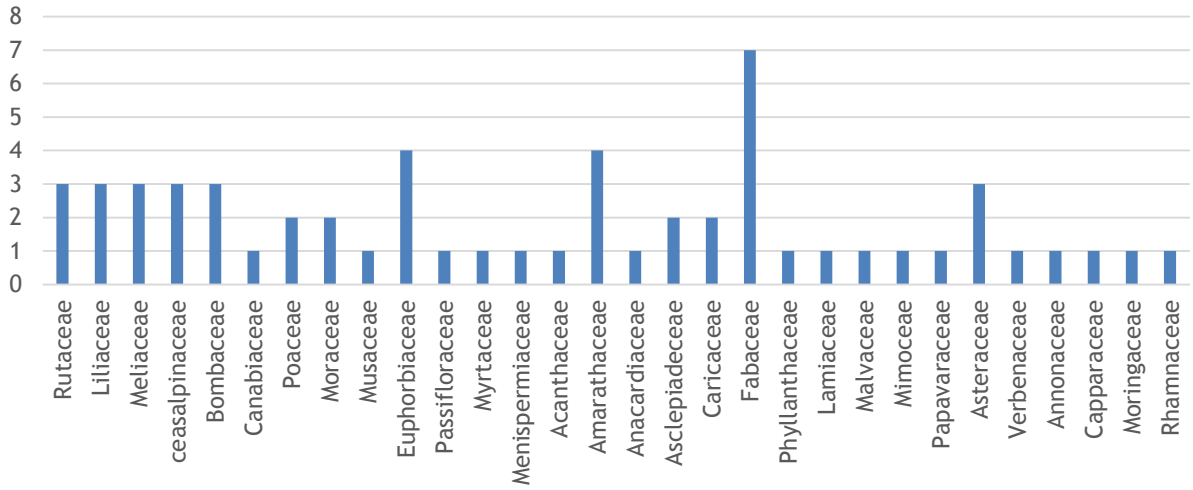

According to our review report, the commonly used preparation methods of plant drugs in Indian medicine were the decoction of leaves. Plant part paste is mixed with other plant parts as a remedies use was also documented with lower values.

Present review reported that 58 ethnomedicinal plants species survey was carried out from previous literature, which belongs to 30 different families and it was apparent that leaves (n=26) were the most used part in the mode of consumption followed by underground parts (n=11) (root/bulb/tuber), bark (n=08), stem (n=05), fruits (n=05), seeds (n=05), flowers (n=04), latex (n=04) and whole plant (n=04) respectively showed in Figure 2.

Fig. 2 Showing Different Plant part used

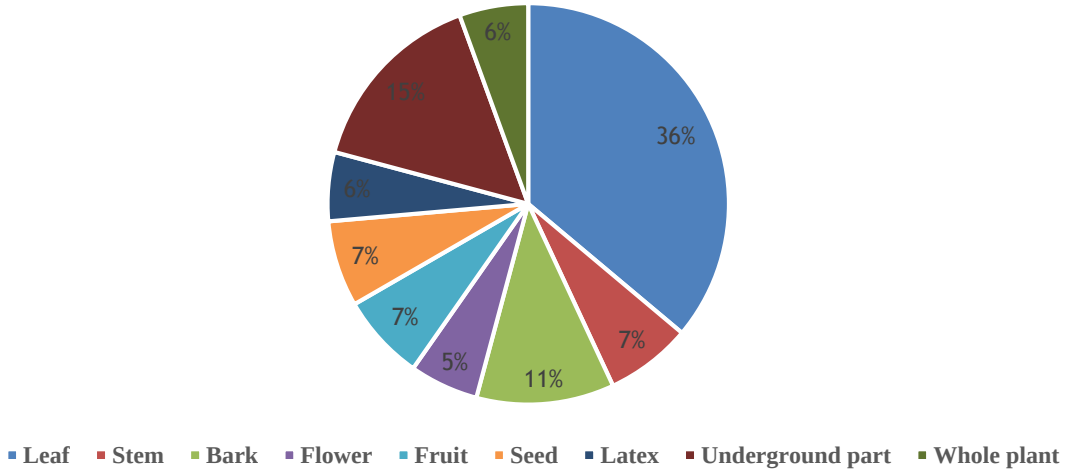

The different plant parts of *A. marmelos* [11], *A. racemosus* [11], *A. indica* [12], *B. variegata* [12], *B. ceiba* [12], *C. sativa* [11], *C. medica* [12,13], *C. lacryma* [14], *F. benghalensis* [15], *M. paradisiaca* [15], *P. parvifolius* [16], *P. edulis* [17], *P. guajava* [11,12], and *T. cordifolia* [15] have been extensively reported as effective remedy for the treatment of diarrhea and dysentery. Some very common plants like *A. aspera* [18], *A. viridis* [19], *M. indica* [18,20], *C. procera* [18], *B. ceiba* [21], *T. indica* [22], *C. tora* [23], *C. papaya* [20], *C. cajan* [11], *E. officinalis* [24], *R. communis* [18], *A. precatorius* [25,26], *P. pinnata* [18], *O. sanctum* [27], *G. herbaceum* [28], *A. indica* [22,29], and *A. arabica* [30] reported primarily for the treatment of oral health care.

Ethnomedicinal plant species such as *A. precatorius* [31,32], *A. aspera* [33-35], *A. marmelos* [35,36], *A. lebbeck* [37,38,45], *A. cepa* [31,39], *A. sativum* [40], *A. spinosus* [41], *A. viridis* [42], *A. mexicana* [31,43], *A. indica* [31,44,45], *B. ceiba* [37,45], *B. monosperma* [43,46], *C. procera* [47], *C. papaya* [36], *E. prostrata* [31], *C. rotundus* [31], *T. procumbens* [48], and *V. negundo* [31,32] reported for the treatment of snakebites. Some other plant species like *A. squamosa* [49], *A. precatorius* [50], *C. viscosa* [51], *E. hirta* [51,52], *F. racemosa* [53], *J. gossypifolia* [51,54], *M. oleifera* [55,56], *Z. oenoplias* [57], and *T. patula* [51,58] have been extensively reported in Ayurveda, Siddha and Unani systems of medicines for their cuts, burns and wound healing potential.

Conclusion:

All the ethnomedicinal plant species reported in the current review work have been used in Indian traditional medicine for the treatment of different human diseases such as diarrhea and dysentery, oral health, snakebite and cut, wound and skin burn. However, the investigated plant species in the current review need further studies covering specific screening of natural products, pharmacological and biological activities as well as a safety control. Present data Open window for Researches to use it and develop novel drugs as well as, to continue studying the effects of extracts and isolated phytochemicals derived from these plants for their health benefits, in important diseases.

Table 1: List of Ethnomedicinal plant species used by tribal healers for maintaining primary Healthcare in India.

Ethnomedicinal Plants used for the treatment of Diarrhea and Dysentery:						
Sr. No.	**Botanical Name**	**Common Name**	**Family**	**Plant Part Used**	**Mode of Consumption**	**References**
1.	*Aegele marmelos* Linn.	Belpatra	Rutaceae	Fruit	The fruit pulp is together boiled and filtered with fruits of *Punica granatum* L. and leaves of *Psidium guajava* L. The filtrate after mixing along with sugar and water is taken to get a cure for chronic dysentery and diarrhea. Dose: 5 teaspoons for adults and 2 teaspoons for children (three times daily).	11
2.	*Asparagus racemosus* Willd.	Shatavari	Liliaceae	Roots	The mixture of ground *Asparagus racemosus* and *Byttneria pilosa* together with the boiled bark of *Myrica esculenta* and is given altogether to cure dysentery.	11
3.	*Azadirachta indica* Juss.	Neem	Meliaceae	Leaf	Boiled leaf extracts are used for the treatment of diarrhea and dysentery.	12
4.	*Bauhinia variegata* Linn.	Kolhari	Caesalpiniaceae	Flower	Flowers are boiled and eaten for 6-7 days to treat piles and dysentery.	12
5.	*Bombax ceiba* Linn.	Katshevari	Bombaceae	Bark	Aqueous extracts mixed along with curd are used to check blood dysentery.	12
6.	Cannabis sativa Linn.	Kena	Cannabinaceae	Leaf	Leaves are ground with water and a filter. The filtrate is given to cure dysentery. Dose: 2 teaspoons twice daily.	11
7.	*Citrus medica* Linn.	Kadulimb	Rutaceae	Root	Preserved rind is used for diarrhea and dysentery.	12,13
8.	*Coix lacryma* Linn.	Ranjondhla	Poaceae	Leaf	Leaf juice is taken in diarrhea and dysentery.	14
9.	*Ficus benghalensis* Linn.	Vad	Moraceae	Leaf	Powdered leaves mixed with curd and used for the treatment of diarrhea.	15
10.	*Musa paradisiaca* Linn.	Banana	Musaceae	Fruit	Plant juice or crushed raw fruit mixed with curd is taken orally 2-3 times	15

					daily to treat diarrhea and dysentery.	
11.	*Phyllanthus parvifolius* Ham.	Inkplant	Euphorbiaceae	Whole plant	Treatment of diarrhea.	16
12.	*Passiflora edulis* Sims.	Krashnaful	Passifloraceae	Leaf	Leaf juice is given in dysentery. Dose: Half cup twice daily, till cured.	17
13.	*Psidium guajava* Linn.	Peru	Myrtaceae	Leaf	Leaves are crushed and the extracts are drunk in case of chronic dysentery. Sometimes the leaves are ground with the peels of raw mango and bark of *Rubus ellipticus* or with the leaves of *Passiflora edulis* and rhizome of *Curcuma longa* and the juice obtained from these mixtures are given to cure blood dysentery. Dose: 2 teaspoons twice daily after food till cured.	11,12
14.	*Tinospora cordifolia* Hook. f.	Gulvel	Menispermaceae	Leaf & bark	Decoction of leaves and bark in equal amounts is taken orally thrice daily in the treatment of diarrhea and dysentery.	15
Ethnomedicinal Plants used for the treatment of Oral Health:						
15.	*Achyranthes aspera* L.	Aghada	Acanthaceae	Stem	Stem used as a toothbrush, ash of the plant is used as tooth powder; to relieve pyorrhea and toothache.	18
16.	*Amaranthus viridis* L.	Math	Amaranthaceae	Stem	Toothache.	19
17.	*Mangifera indica* L.	Mango	Anacardiaceae	Small stem & latex	The toothbrush of the small stem is used to cure toothache and latex is applied to relieve gingivitis.	18,20
18.	*Calotropis procera* L.	Ruchaki	Asclepiadaceae	Root	Paste of root is applied as a toothpaste toothbrush to cure toothache Ash of the root is used to remove pus from gums.	18
19.	*Bombax ceiba* L.	Katshevari	Bombaceae	Bark	Bark used for toothache.	21
20.	*Tamarindus indica* L.	Imali / Chinch	Caesalpiniaceae	Bark	Bark powder is used as tooth powder.	22
21.	*Cassia tora* Linn.	Tarota	Caesalpiniaceae	Leaf	Leaf decoction is given for children with teething.	23
22.	*Carica papaya* L.	Papaya	Caricaceae	Latex	Latex is used to cure toothache and mouth ulcers.	20
23.	*Cajanus cajan* L.	Tur	Fabaceae	Fruit	Fruit used for toothache.	11

24.	*Emblica officinalis* L.	Amla	Phyllanthaceae	Small stem	Twig is worn into the neck to cure toothache.	24
25.	*Ricinus communis* L.	Karadi	Euphorbiaceae	Seed	Cotyledon is fried in mustard oil and the smoke is emitted by this process is inhaled for toothache.	18
26.	*Abrus precatorius* L.	Gunj	Fabaceae	Leaf	Leaves are chewed to get relief from toothache.	25, 26
27.	*Pongamia pinnata* Linn.	Karanj	Fabaceae	Leaf	Tender leaf twigs are chewed to cure toothache.	18
28.	*Ocimum sanctum* L.	Tulsi	Lamiaceae	Leaf	Leaves are chewed to induce saliva secretion, which keeps the mouth fresh.	27
29.	*Gossypium herbaceum* L.	Kapas	Malvaceae	Seed	Burned seed powder/ash is used for toothache.	28
30.	*Azadirachta indica* Juss.	Neem	Meliaceae	Flower	Tender twigs are used as a toothbrush. Flowers for mouth infections and bleeding of gums.	22, 29
31.	*Acacia arabica* Willd.	Babul	Mimosaceae	Bark	The bark is used for Gum diseases and mouth ulcers.	30
Ethnomedicinal Plants used for the treatment of Snakebite:						
32.	*Abrus precatorius* Linn	Gunj	Fabaceae	Seed, leaf & root	2–3 g of fresh leaves or roots with seeds are made into a paste and consumed along with cold water or cow's milk. (Two times a day for 5–7 d to cure any poisonous bite, as well as root powder applied topically.)	31, 32
33.	*Achyranthes aspera* Linn.	Aghada	Amaranthaceae	Whole plant	The whole plant extract or root extract is given orally as well as the paste obtained from the root has been used (for 3 weeks).	33, 34, 45
34.	*Aegle marmelos* Linn.	Belpatra	Rutaceae	Leaf & root	Decoction/extract (twice a day up to 5 days) of the leaves is given orally or root bark extract is administered internally for every 4 hours up to 3 days.	35, 36
35.	*Albizia lebbeck* Linn.	Siris	Fabaceae	Bark	Paste of bark is used.	37, 38, 45
36.	*Allium cepa* Linn.	Onion	Liliaceae	Bulb	Paste taken from fresh skin bulb for external application (5 days).	31, 39
37.	*Allium sativum* Linn.	Garlic	Liliaceae	Bulb	The bulb is made into a paste and given orally.	40
38.	*Amaranthus spinosus* Linn	Kate math	Amaranthaceae	Leaf	Paste of leaves is applied locally.	41
39.	*Amaranthus viridis* Linn.	Math	Amaranthaceae	Leaf & stem	Leaves/stem paste are applied externally.	42

40.	*Argemone mexicana* Linn.	Bilayat	Papaveraceae	Leaf & seed	Leaf and seed decoction is given orally (7 days).	31, 43
41.	*Azadirachta indica* Juss.	Neem	Meliaceae	Leaf & flower	Decoction/paste is prepared and given orally (7 days).	31, 44, 45
42.	*Bombax ceiba* Linn.	Katshevari	Bombaceae	Flower & fruit	Paste of flowers/fruits/leaves is applied on the bitten spot.	37, 45
43.	*Butea monosperma* Lamk.	Palas	Fabaceae	Bark & seed	Bark paste applied on swelling. Paste of one seed in 10 mL lemon juice is given orally.	43, 46
44.	*Calotropis procera* L.	Ruchaki	Asclepiadaceae	Latex & Root	Leaf latex is applied to the bitten area. The root is crushed and given to drink and applied externally.	47
45.	*Carica papaya* Linn.	Papaya	Caricaceae	Fruit & latex	Unripped fruit of Carica papaya is taken and the skin is removed by slicing. Salt is then rubbed over it. The fruit is then placed over the bite with sliced portions in contact with the bite and bandaged. Few drops of latex are applied to the wound due to snakebite for quick healing.	36
46.	*Eclipta prostrata* Linn.	Bhingraj	Asteraceae	Leaf	Leaf paste is applied externally.	31
47.	*Cyperus rotundus* Linn.	Nagarmotha	Poaceae	Root & tuber	Decoction of root/tubers given orally (7 days).	31
48.	*Tridax procumbens* Linn.	Dagadful	Asteraceae	Leaf	The leaves are crushed and the juice is dripped on the wound of snakebite. Juice is taken orally after its dilution with some quantity of water.	48
49.	*Vitex negundo* Linn.	Nirgudi	Verbenaceae	Leaf & root	Leaf paste is applied over the bitten area (5 days) as well as root extract is given with warm water.	31, 32
Ethnomedicinal Plants used for the treatment of cuts, wounds, and skin burn:						
50.	*Annona squamosa* L.	Sitaphal	Annonaceae	Leaf	Fresh leaf paste is applied twice a day on wounds until cure.	49
51.	*Abrus precatorius* L.	Gunj	Fabaceae	Leaf	Leaf paste is applied on boils and wounds twice a day till cure.	50
52.	*Cleome viscosa* L.	Tilaparni	Capparaceae	Leaf	Leaf paste is applied on wounds twice a day for three days.	51
53.	*Euphorbia hirta* L.	Dudhi	Euphorbiaceae	Whole plant	The whole plant paste is applied over cuts and wounds.	51, 52

54.	*Ficus racemosa* L.	Umbar	Moraceae	Bark	Fresh plant bark paste is applied on bleeding wounds twice a day.	53
55.	*Jatropha gossypifolia* L.	Jamalghota	Euphorbiaceae	Whole plant	The whole plant paste is applied over cuts and wounds.	51, 54
56.	*Moringa oleifera* Lam.	Shevaga	Moringaceae	Leaf	Leaf paste is applied on cuts and wounds.	55, 56
57.	*Zizyphus oenoplias* (L.) Miller	Ber	Rhamnaceae	Leaf	Leaf paste is applied to wounds.	57
58.	*Tagetes patula* L.	Genda	Asteraceae	Leaf	Fresh leaf paste is applied on wounds twice a day for 3-4 d to kill germs in wounds.	51, 58

References:

1. Anonymous, Epidemic diarrhea due to Vibrio cholera. *Weekly Epidemic Rec*. 1979; 16:121.
2. UNESCO. Culture and Health, Orientation texts- World Decade for Cultural Development Documents CLT/DEC. PRO-1996, Paris, France. 29.
3. Shashi SS. Encyclopedia of Indian tribes. New Delhi: Anmol Publications Pvt. Ltd; 1994, p. 16-27.
4. Pushpangadan P, Atal CK. Ethno-medico-botanical investigations in Kerala I. Some primitive tribes of western ghats and their herbal medicines. *J Ethnopharmacol* 1984; 11:59-77.
5. World health organization (WHO). The promotion and development of traditional medicine. *Technical report series* 622, 1978.
6. Rajasekharan S, Pushpangadan P, Biju SD. Folk Medicines of Kerala – A Study on Native Traditional Folk Healing Art and its Practitioners. New Delhi, Deep Publications, New Delhi (ed. S. K. Jain), 1996.
7. Sikarwar RLS. Ethnogynaecological uses of plants new to India. *Ethnobotany* 2002; 14:112-115.
8. Jain SK. Dictionary of Indian folk medicines and ethnobotany. New Delhi: Deep Publications; 1991.
9. Upadhye A, Kumbhojkar MS, Vartak VD. Observations in wild plants used in folk medicine in the rural areas of the Kolhapur district. *Anc Sci Life* 1986; 6: 119-121.
10. Bhattacharjee S.K. Handbook of medicinal plants. Jaipur: Pointer Publishers; 2001, p. 18-25.
11. Ahmed AA, Borthakur SK. Ethnobotanical Wisdom of the Khasis (Hynniew Treps) of Meghalaya. Bishen Singh, Mahendra Pal Singh, editors. *Dehradun- 01: India*; 2005. p. 114-47.
12. Frlht.org.in. Medicinal plants conservation and sustainable utilization- Meghalaya, India. Annexure- C. Meghalaya: 2003 p. 55-75.
13. Laloo RC, Kharlukhi S, Jeeva S, Mishra BP. Status of medicinal plants in the disturbed and the undisturbed sacred forest of Meghalaya, Northeast India: Population structure and regeneration efficacy of some important species. *Curr Sci*.2006; 90:225-32.
14. Hynniewta SR, Yogendra K. Herbal remedies among the Khasi traditional healers and village folks in Meghalaya. *Indian J Tradit Knowl* 2008; 7:581-6.
15. Jaiswal V. Cultures and ethnobotany of Jaintia tribal community of Meghalaya, Northeast India- A mini-review. *Indian J Tradit Knowl* 2010; 9:38-44.
16. Laloo RC, Kharlukhi S, Jeeva S, Mishra BP. Status of medicinal plants in the disturbed and the undisturbed sacred forest of Meghalaya, Northeast India: Population structure and regeneration efficacy of some important species. *Curr Sci*.2006; 90:225-32.

17. Ahmed AA, Borthakur SK. Ethnobotanical Wisdom of the Khasis (Hynniew Treps) of Meghalaya. Bishen Singh, Mahendra Pal Singh, editors. Dehradun- 01: India; 2005. p. 114-47.
18. Badgujar SB, Mahajan RT, Kosalge SB. Traditional Practice for Oral Health Care in Nandurbar District of Maharashtra. India *Ethnobotaical Leaflets*, 2008; 12:1137-44.
19. Vanila D, Ghanthikumar S, Manickam VS. Ethnomedicinal Uses of Plants in the Plains Area of the Tirunelveli-District, Tamil Nadu, India. *Ethnobotanical Leaflets,* 2008; 12:1198-1205.
20. Achuta NS, Sharad S, Rawat AKS. An ethnobotanical study of medicinal plants of Rewa districts. Madhya Pradesh. Indian journal of traditional knowledge 2010; 9(1):191-202.
21. Dowlathabad MR, Rao BUVU, Sudharshanam G. EthnoMedico-Botanical Studies from Rayalaseema Region of Southern Eastern Ghats, Andhra Pradesh, India. *Ethnobotanical Leaflets,* 2006; 10:198-207.
22. Natarajan D, Balaguru B, Nagamurugan N, Soosairaj S, Natarajan E. Ethno-medical-botanical survey in the Malliagainatham village, Kandankathri taluk, Pudukottai district, Tamilnadu. *Indian J of traditional knowledge*, 2010; 9(1):768-774.
23. Katewa SS, Galav PK. Traditional Herbal Medicines from Shekhawati Region of Rajasthan. Indian J of traditional knowledge 2005; 4(3):237-245.
24. Akilesh KTDD, Tewari JP. Ethnomedicinal knowledge among Tharutribe of Devipatan division. *Indian Journal of Ttraditional Knowledge,* 2006; 5(3):310-313.
25. Pandi KP, Ayyanar M, Ignacimuthu S. Medicinal plants used by Malasar tribes of Coimbatore district, Tamilnadu. *Indian Journal of Traditional Knowledge* 2007;6579-582.
26. Umapriya, Rajendran, Aravindhan, Binu Thomas, Maharajan. Traditional medication of namakal district, Tamil Nadu. *Global J of Pharmacology* 2010; 4(3):107-110.
27. Kadhirvel K, Ramya S, Palin SST, Veera RA, Rajasekaran C. Ethnomedicinal Survey on Plants used by Tribals in Chitteri Hills. *Environ We Int. J. Sci.* 2010;35-46.
28. Koche DK, Shirsat RP, Syed I, Mohd. Nafees, Zingare AK, Donode KA. Ethnomedicinal Survey of Nagzira Wild Life Sanctuary, District Gondia (M.S.) India- Part II. *Ethnobotanical Leaflets*,2008; 12:532-37.
29. Chellaiah M, Muniappan A, Nagappan R, Savarimuthu I. Medicinal plants used by traditional healers in Kancheepuram District of Tamil Nadu, *India. Journal of Ethnobio and Ethnomed*.2006; 2:43.
30. Jain DL, Baheti AM, Jain SR, Khandelwal KR. Use of medicinal plants among tribes in the Satpuda region of Dhule and Jalgoan districts of Maharashtra- A ethnobotanical survey. *Indian journal of traditional knowledge.* 2010;9(1):152-157.

31. R.P. Samy, M.M. Thwin, P. Gopalakrishnakone, S. Ignacimuthu Ethnobotanical survey of folk plants for the treatment of snakebites in Southern part of Tamilnadu, India. *J Ethnopharmacol*, 115 (2008), pp. 302-312.
32. J.M. Yabesh, S. Prabhu, S. Vijayakumar An ethnobotanical study of medicinal plants used by traditional healers in the silent valley of Kerala, India. *J Ethnopharmacol*, 154 (2014), pp. 774-789.
33. N.P. Rajith, V.S. Ramachandran Ethnomedicines of Kurichyas, Kannur district, Western Ghats, Kerala. *Indian J Nat Prod Resour*, 1 (2010), pp. 249-253.
34. D.G. Bhadange Harnessing plant biodiversity of forests of Akola and Washim District of Maharashtra for medicinal use. *Int J Adv Biotechnol Res*, 2 (2011), pp. 350-356.
35. N. Nagaraju, K.N. Rao. A survey of plant crude drugs of Rayalaseema, Andhra Pradesh, India. *J Ethnopharmacol*, 29 (1990), pp. 137-158.
36. A.V. Khan, Q.U. Ahmed, M.W. Khan, A.A. Khan. Herbal cure for poisons and poisonous bites from Western Uttar Pradesh, India. *Asian Pacific J Trop Dis*, 4 (2014), pp. S116-S120.
37. R. Jitin, S.P. Singh, A. Naz. An ethnomedicinal survey of Orchha Wildlife Sanctuary region of Tikamgarh District, Madhya Pradesh, India. *J Bot Research*, 4 (2013), pp. 31-34.
38. A.S. Khalkho, P.R. Sahu, S. Kumari, S. Alam. Studies on ethnomedicinal uses and formulation of herbal drugs from medicinal plants of Ranchi District—a survey. *Am J Ethnomed*, 2 (2015), pp. 284-296.
39. C. Alagesaboopathi. Ethnomedicinal plants used for the treatment of snake bites by Malayali tribals and rural people in Salem district, Tamilnadu, India. *Int J Biosci*, 3 (2013), pp. 42-53.
40. S. Sarkhel. Ethnobotanical survey of folklore plants used in the treatment of snakebite in Paschim Medinipur district, West Bengal. *Asian Pacific J Trop Biomed*, 4 (2014), pp. 416-420.
41. M.B. Krishna, S. Mythili, K.S. Kumar, B. Ravinder, T. Murali. Ethnobotanical survey of medicinal plants in Khammam District, Andhra Pradesh, India. *Int J Appl Biol Pharm Techno*l, 2 (2011), pp. 366-370.
42. S.K. Basha. Traditional use of plants against snakebite in Sugali tribes of Yerramalais of Kurnool district, Andhra Pradesh, India. *Asian Pacific J Trop Biomed*, 2 (2012), pp. S575-S579.
43. N. Kumar, R. Choyal. Traditional phytotherapy for snake bites by the local rural people of Hamirpur district in Himachal Pradesh (India). *Biol Forum*, 4 (2012), pp. 98-106.
44. T. Thirumalai, E.K. Elumalai, S.V. Therasa, B. Senthilkumar, E. David. Ethnobotanical survey of folklore plants for the treatment of jaundice and snakebites in Vellore districts of Tamilnadu, India. *Ethnobotany Leaflets*, 14 (2010), pp. 529-536.

45. E. Lulekal, Z. Asfaw, E. Kelbessa, P. VanDamme. Ethnomedicinal study of plants used for human ailments in Ankober District, North Shewa Zone, Amhara Region, Ethiopia. *J Ethnobiol Ethnomed*, 63 (2013), pp. 1-13.
46. S. Jeetendra, A.D. Kumar. Ethnomedicinal plants used by tribal communities for the treatment of snakebite in West Nimar, MP, India, *ISCA J Biol Sci*, 1 (2012), pp. 77-79.
47. P. Mahishi, B.H. Srinivasa, M.B. Shivanna. Medicinal plant wealth of local communities in some villages in Shimoga District of Karnataka, India, *J Ethnopharmacol*, 98 (2005), pp. 307-312.
48. C.P. Kala. Aboriginal uses and management of ethnobotanical species in deciduous forests of Chhattisgarh state in India, *J Ethnobiol Ethnomed*, 5 (2009), pp. 1-9.
49. Dash, S.S., Misra, M.K., 1999. Taxonomic survey and systematic census of economic plants of Narayana Patna Hills of Koraput Dist., Orissa. *Journal of Economic and Taxonomic Botany*, 23, 473–498.
50. Bhatt, D.C., Mitaliya, K.D., Mehta, S.K., Joshi, P.N., 2002. Notes on some ethnomedicinal plants of Paccham Hills of Kachh district. *Gujarat Ethnobotany*, 14, 34–35.
51. Girach, R.D., Singh, S., Brahmam, M., Misra, M.K., 1999. Traditional treatment of skin diseases in Bhadrak District, Orissa. *Journal of Economic and Taxonomic Botany*, 23, 499–504.
52. Upadhyaya, O.P., Kumar, K., Tiwari, R.K., 1998. Skin treatments of Bihar plants. Pharmaceutical Biology 36, 20–24.
53. Punjani, B.L., 2002. Ethnobotanical aspects of some plants of Aravali Hills in North Gujarat. *Ancient Science of Life*, 21, 268–280.
54. Pal, D.C., Jain, S.K., 1997. Tribal Medicine. Naya Prakash Publishers, Calcutta - 6.
55. Das, S.N., 1997. A study on the Ethnobotany of Karauli & Sawai, Madhapur Districts, Rajasthan. *Journal of Economic and Taxonomic Botany*, 21,587–605.
56. Begum, D., Nath, S.C., 2000. Ethnobotanical review of medicinal plants used for skin diseases and related problems in Northeastern India, *Journal of Herbs, Spices and Medicinal Plants* 7, 55–93.
57. Singh, A.K., Raghubansi, A.S., Singh, J.S., 2002. Medical ethnobotany of the tribals of Sonaghati of Sonbhadra district, Uttar Pradesh, India. *Journal of Ethnopharmacology*, 81, 31–41.
58. Sharma, H.K., Chhangte, L., Dolui, A.K., 2001. Traditional medicinal plants in Mizoram, India. *Fitoterapia*, 72, 146–161.
59. Balunas, M.J., Kinghorn, A.D., 2005. Drug discovery from medicinal plants. *Life Sci*., 78, 431–441.

***

PAPER 65

AIR ION CONCENTRATIONS AND POLLUTION INDEX FOR IRRIGATED AND NON- IRRIGATED VEGETATION AREAS AT RURAL STATION KHATAV (16.57^{O}N, 74.31^{O}E)

Gajanan Patil[1a*], Subhash Pawar[2b], Jalindar Bhosale[3c], Prachi Patil[4d], Pratik Patil[5e]

[1] Secondary school & Jr. College, Bhilawadi, Maharashtra, India.

[2] A.C.S. College, Palus, Maharashtra, India.

[3] Dr. Bapuji Salunkhe College, Miraj, Maharashtra, India.

[4]Institute of Chemical Technology, Jalana, Maharashtra, India.

[5]Willingdon College, Sangli, , Maharashtra, India.

Abstract:

Atoms, molecules or molecule clusters that have a net electric charge and electric conductivity are called air ions. Cosmic rays, radon exhalation, ionization, photosynthesis and lighting excitation provide the energy required to produce air ions. Air ions generation near the ground varies mostly with 222 Radon and its progenies concentrations. Negative air ions are helpful for a human being, also called air vitamins. As compared to non-irrigated vegetation areas, irrigated vegetation areas of Grapes, Sugarcane, Maize and Papaya show remarkable variation in ion concentrations. Temperature, humidity, photosynthesis and respiration plays an important role in the generation of air ions. Negative air ions produce a natural healing effect. The pollution index is also less than one so the air quality is beneficial for humans and animals also.

Keywords: Pollution index, Irrigated field, Ion counter, Air ions, Ionization, Radon exhalation.

Introduction: - Air ions are generated by removing or adding an electron in the ionization process. There are two types of air ions. i.e., positive and negative Positive air ions are produced by different sources of ionization whereas negative air ions are produced by the attachment of electrons to the neutral molecules present in the atmosphere. Air ions are a constituent part of our atmosphere, they are small, large and intermediate depending upon their size and mobility. Air ions produce an effect on living organisms. The positive ions cause headache, insomnia, fatigue, joint ache, high blood pressure, nervousness [1]. Due to the presence of negative air ions, we feel good, happy and relaxed also breathe easy which increases work productivity, mood and peaceful sleep [2]. live organisms including humans and plants are affected by the balance and concentration of atmospheric particles [3K].

These air ions are generated by natural as well as artificial activities. Negative and positive air ions are produced by cosmic rays, ultraviolet rays, hydrolysis of water, plant tip discharge, the photovoltaic effect of green plants, volcanic eruptions, lightning, corona discharge, combustion in vehicles, thunderstorms are sources of air ions generation [4]. Radon is the main source of air ion production near the ground surface [5]. The daily cycle of ionization is triggered by gamma and cosmic radiations and some energetic minerals ground also contribute to formation of air ions. Typically,35ev energy is required to produce ion pair in the atmosphere [6].

The siphoning activity made during happening close to the plant roots eliminates air contamination and is changed over into plant food. The charges between the earth and the climate

are moved via air particles. The transporters of negative charges rush into the ionosphere while positive air particles move to the surface, where they come into contact with plants, higher the negative charge of the plants, the more the positive particles it ingests. Plants respond to change the electric capability of the general climate. The pumping action created during transpiration near the plant roots removes air pollution and is converted into plant food. the charges between the earth and the atmosphere are transferred by air ions. The carriers of negative charges rush into the ionosphere while positive air ions move to the surface, where they come into contact with plants higher the negative charge of the plants, the more the positive ions it absorbs. plants react to change the electric potential of the surrounding environment [7].

Instrumentation and Methodology

The instrument used for the measurement of air ion concentration is Gerdien condenser-based air ion counter which is designed and developed at A.C.S. College, Palus (India) with courtesy of IITM Pune [8]. Air ion concentration is directly proportional to ionic current is principle behind this instrument. This instrument is used to operate in at rural station Khatav (16.57^{O}N, 74.31^{O}E). Air ion concentration is measured in Banana, Maize, Papaya and Grapes and in empty unused place. Field location is nearabout 250km south of Pune. It is 3km away from river Yerala. A 6 feet road having frequency of 5 to 6 vehicle per hour passes near it.

Figure 1 shows instrumental setup used for the measurement of air ions in Sugarcane, Guava, Onion, Turmeric and Maize vegetation area. Instrumental setup contains Gerdien cylinder, Fan, Power supply, Digital multimeter, Data logger, Laptop and aluminum box containing operational amplifier ADC549JH and its circuit used to convert current to voltage. The whole instrument is kept in caged box for its safety and protection. Rishcom software is used for data acquisition and interpretation for irrigated and non-irrigated vegetation area. For irrigated field has system of artificial watering any time. For irrigation system surface, drip, subsurface and sprinkler systems are used. For non-irrigated vegetation area there is no artificial system of watering.

Data collected for six months. Since measurement of positive and negative air ions is not possible simultaneously with this instrument, readings are taken for alternate days as per convenience. Sugarcane, Maize, Turmeric Guava, Banana and Papaya are cash crops so they are cultivated in more proportion in Maharashtra, Utter Pradesh and Karnataka.

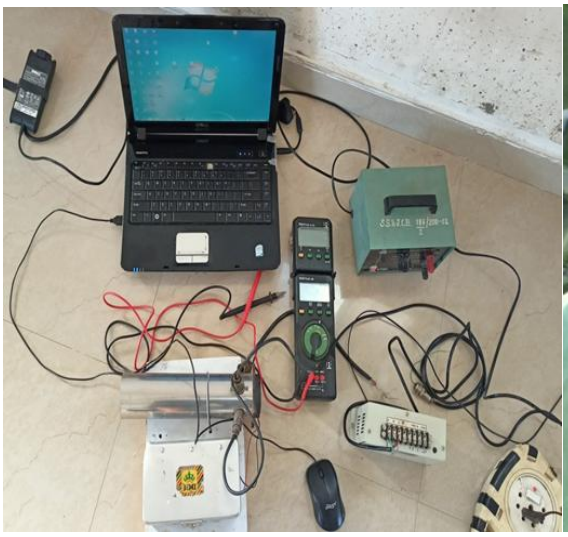

Figure 1 Experimental setup. **Figure 2 Banana Vegetation area.**

Figure 2 shows Banana vegetation area at rural station Khatav. Figure 3 shows Papaya vegetation area with instrument in caged box. Maize vegetation area is shown by figure 4.

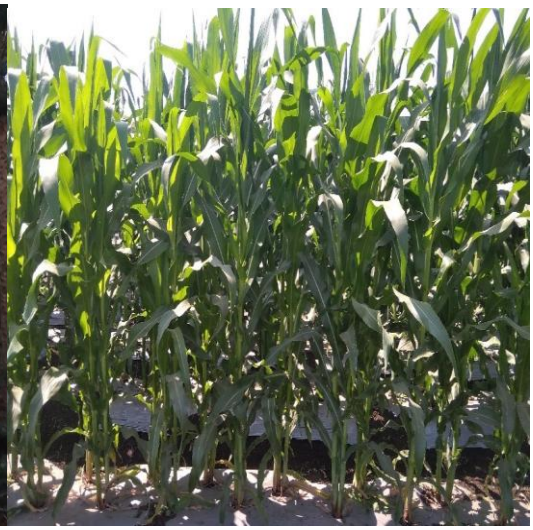

Figure 3 Papaya with instrumental box. **Figure 4 Maize vegetation area.**

Data collected from December 2018 to March 2019. Since measurement of positive and negative air ions is not possible simultaneously with this instrument, readings are taken for alternate days as per convenience. Sugarcane, Maize, Turmeric Guava and Papaya are cash crops so they are cultivated in more proportion in Maharashtra, Utter Pradesh and Karnataka. The pollution index is also calculated which is the ration of number of positive air ions to the number of negative air ions. It should be less than one for good air quality and beneficial for human beings as well as animals. Pollution index greater than means air quality is not good. It is harmful for human beings. Thus, pollution index can be treated as tool for measurement of air quality in rural and urban civil and vegetation areas.

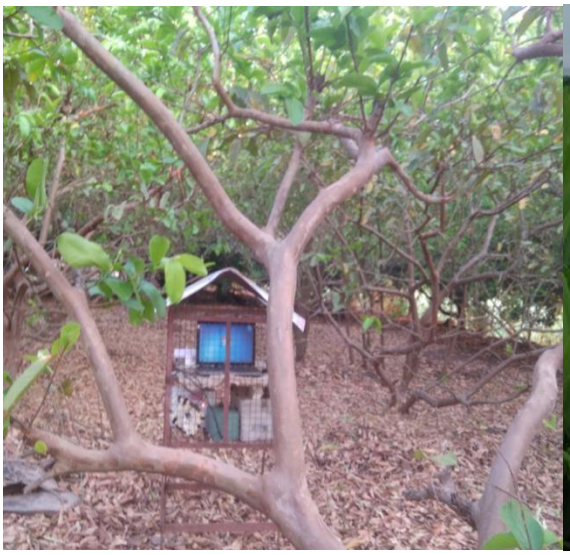

Figure 5 Instrumental setup in Guava

Figure 6 Turmeric vegetation area.

Figure 7 Sugarcane vegetation Area

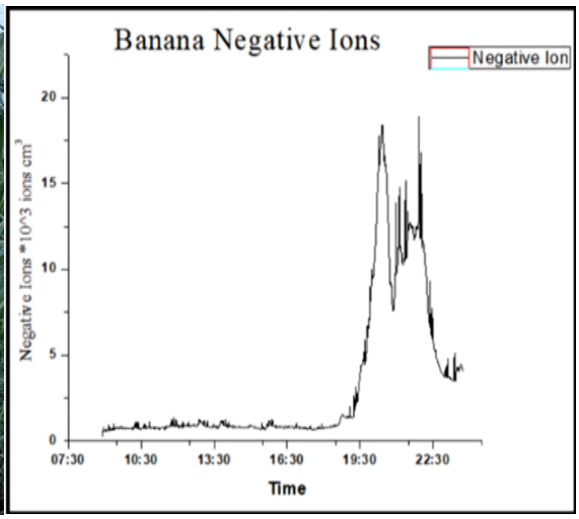

Figure 8 Banana vegetation area negative ion.

Radon222 radiation, transpiration, photosynthesis and respiration are main sources for generation of air ions by plants. Temperature and humidity also affect the concentration of air ions. Air quality is determined from proportion of positive and negative air ion concentrations. Positive air ions are nothing but aerosols. The soil at observatory is completely black. Air ion concentrations is measured by giving water irrigation system to these plants and difference is observed. Energy required for the formation of air ions by emission of alpha, beta and gamma rays are National Research Council Staff [9] has given ionization rates for different sources, they are shown in the table 1.

Ionization Source	Altitude From ground surface.	Ionization Rate in per second per cubic cm
Cosmic Rays	100 to 3000 metre above ground surface	1 to 2
α- emission from	Few centimetres above	1 to 4

ground	ground surface	
β- emission from ground	Few meters above ground surface	0.1 to 10
γ- emission from ground	Few hundred meters above ground	1 to 6
Radiation of Radon and its progenies	1 to 2 meter above ground surface	1 to 20

Table 1 shows ionization rate from different sources.

From the it is clear that ion production due to radon and its progenies is large as compared to cosmic rays. Ion concentration in vegetation areas depends upon photosynthesis, respiration and transpiration.

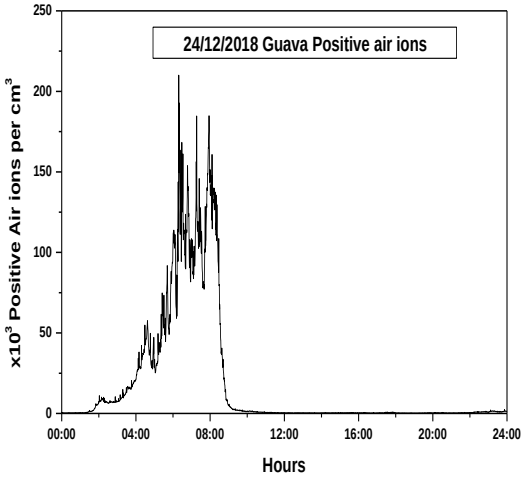

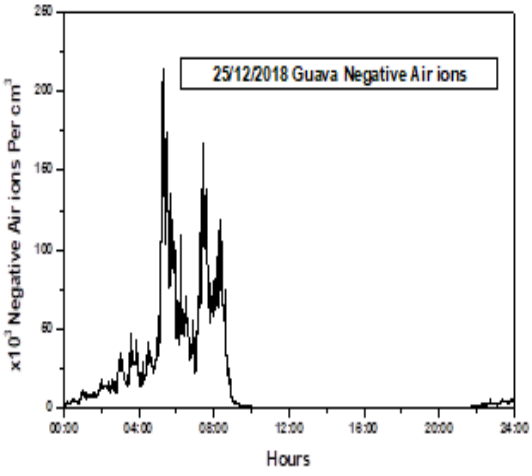

Figure 7 Positive ions in Guava vegetation area. **Figure 8 Negative air ions in Guava vegetation area**

Result and Discussion

In irrigated vegetation area air ion concentration is increases due to cuticle and stomatal transpiration of plants. It is found that negative air ion concentration is more in the morning period between 4 to 9 am afterwards it decreases due to human activities and transportation of vehicles which increases aerosols. The photosynthesis is oxidation-reduction process in which oxygen is released and carbon dioxide is taken by plants is given by Brown [10]

$$6CO_2 + 6H_2O \xrightarrow[\text{Chlorophyll}]{\text{Light energy}} C_6H_{12}O_6 + 6O_2$$

$$C_6H_{12}O_6 + 6O_2 \longrightarrow C_6O_2 + 6H_2O + \text{Heat}$$

Figure 9 Negative air ions in Maize

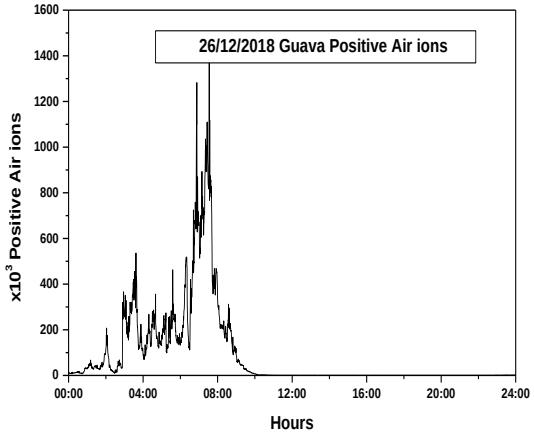

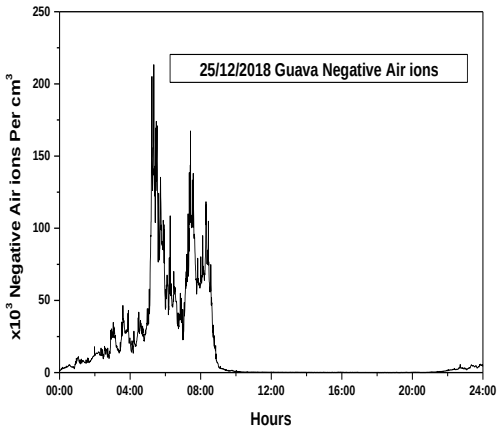

Figure 10 Positive air ions in Guava **Figure 11 Negative air ions in Guava**

Respiration is exothermic reaction in which heat is evolved. In this process carbon dioxide is released in the atmosphere. The reaction is given by.

$$C_6H_{12}O_6 + 6O_2 \longrightarrow 6CO_2 + 6H_2O + Heat$$

In transpiration water vapour is released in the atmosphere through cuticle and stomatal transpiration process. This water vapour has dissolved radon222. Thus, oxygen, carbon dioxide released in the process of photosynthesis and respiration receives ionization energy from radon or from any other sources like cosmic rays, lightning thunderstorm or other radiations. As a result, there is increase in the concentration of air ions in the irrigated vegetation area. So that air ion concentration is more in irrigated vegetation area compared with non-irrigated vegetation area.

The vegetation area of sugarcane, Maize, Papaya turmeric, Guava, Banana and empty space (non-irrigated area) with their positive and negative air ion concentration is given in table no.2. The air ion assessment coefficient (C.I.) is the ratio of number negative air ions to the 1000 times pollution index [11]. Air quality is best when CI > 1. Air is clean when CI is between 0.70 to 1.0. Air has average quality when CI lies between 0.50 to 0.69. Air quality is below average when CI lies between 0.30 to 0.49. Air is polluted when CI is in between 0.19 to 0.29. Air is polluted when CI lies below 0.19. This means for high value of CI indicates pure and fresh air quality useful for human being.

Vegetation Area	Botanical Name	Variety	Average positive air ions	Average negative air ions	Pollution index	Air assessment coefficient (CI)
Sugarcane	Saccharum officinarum	CO86032	4500	5020	0.90	5.60

Maize	Zea mays L	Prabhat	3520	6210	0.57	10.96
Papaya	Carica papaya	Pusa drawf	1440	2520	0.57	4.41
Turmeric	Curcuma longa	Rajapore	3930	5360	0.73	7.31
Guava	Psidium guajava	Psidium guajava	17500	18000	0.97	18.51
Banana	Musa	Basrai	2600	3140	0.83	3.79
Empty Space	Nil	Nil	900	1150	0.78	1.47

Table 2 Vegetation area, air ions and pollution index with C.I.

Temperature and humidity also related to air ion concentration. As temperature increases then humidity decreases and air ion concentration also decreases. The relation between air ion concentration and humidity is somewhat direly proportional. Figure 12 shows the graph of humidity and temperature.

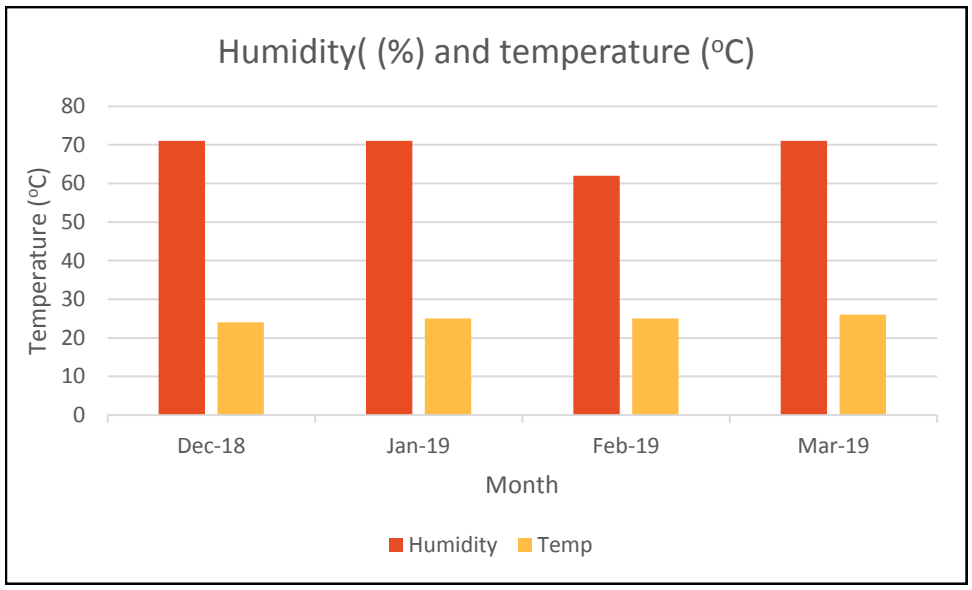

Figure12 shows humidity and temperature graph.

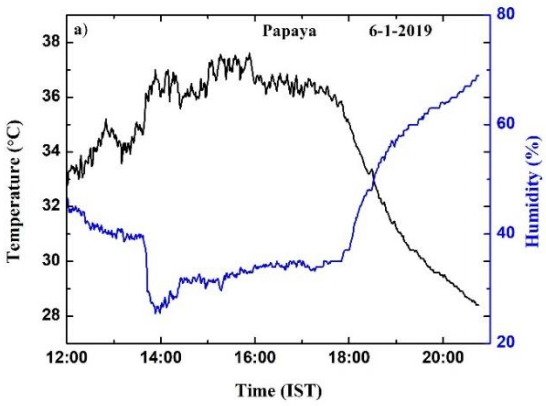

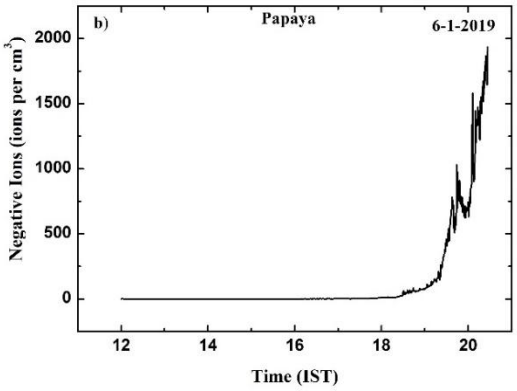

Figure 13 humidity and temperature graph **Figure 14 Papaya negative ions**

Figure 13 and14 shows the graph shows relation of negative air ions related with temperature with humidity for irrigated papaya vegetation area. It also found that when water is given in large quantity by surface irrigation method, concentration is decreased due to chock off of roots of plants. For irrigated (watered) vegetation areas, the concentration of air ions has increased day by day. But in the case of non-irrigated vegetation areas, the concentration of air ions was seen almost unchanged. Transpiration, Radon exhalation and vaporization might be responsible for it. The concentration of negative air ions which are beneficial for a human being was found more in the morning period than that of the afternoon period.

This study concludes that the air quality can vary with the irrigated as well as non-irrigated vegetation areas. When the vegetation area is irrigated fully then the rate of ion production is less because roots of crops do work properly and evaporation of water is large with the increase in temperature. As water soaks or its water content decrease then processes of transpiration, photosynthesis and respiration become speedier and air ion concentration increases. In non - irrigated vegetation areas the rate of ion generation is normal. But when there are cracks in the soil then radon 220 gas is released from the ground through these cervices, emission of radiation gives energy for atoms to generate more ions in the atmosphere. Subhash et. al, also found that morning period is rich in air ion concentration at rural station Ramanandnagar (India) [12]. Air ion concentration at rural station Bhilawadi also found that sugarcane vegetation area has larger negative air ions in the morning period as compared afternoon period [13]. Average concentration of air ions found more negative air ions at Alpine waterfalls [14]. By condition of neutrality, air ions are always balanced [15].

$\sum n_i z_i = 0$ where n_i – means number of charges and Z_i – means charge number. Thus, total charge is also balanced in the environment. Figure 15,16,17and 18 shows average number of positive and negative air ions in the irrigated and non-irrigated vegetation area and pollution index. Pollution index is less than one hence air quality is good.

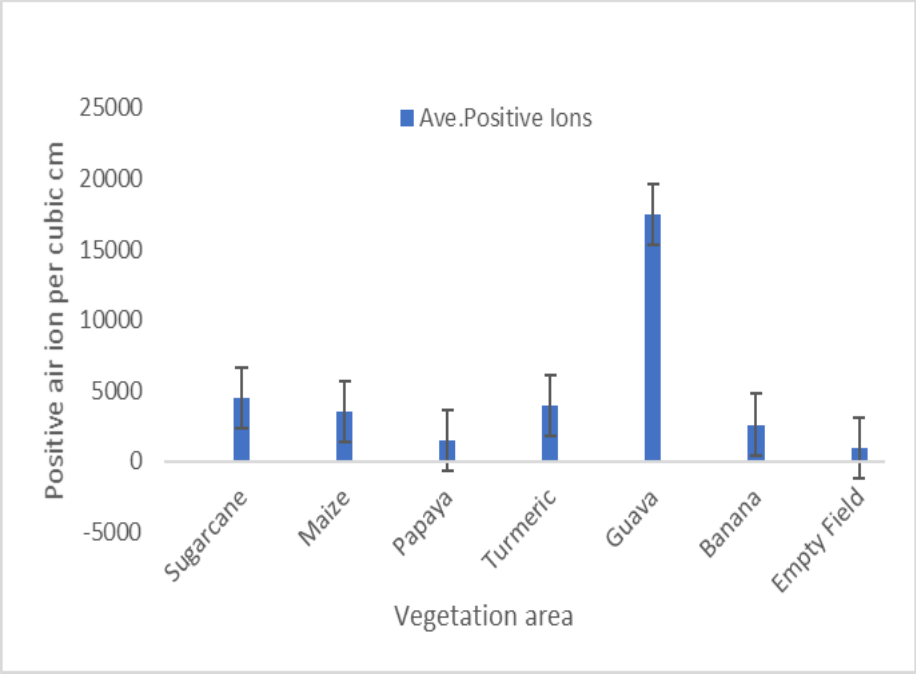

Figure 15 shows average positive air ion concentration of different vegetation area.

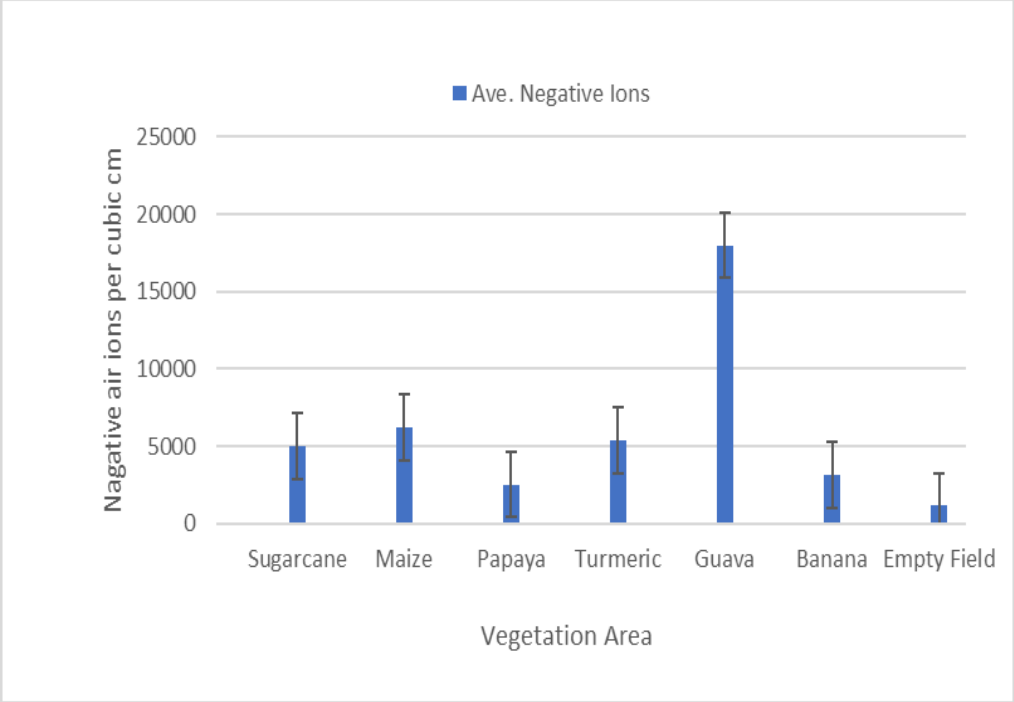

Figure 16 shows average negative air ion concentration in different vegetation area.

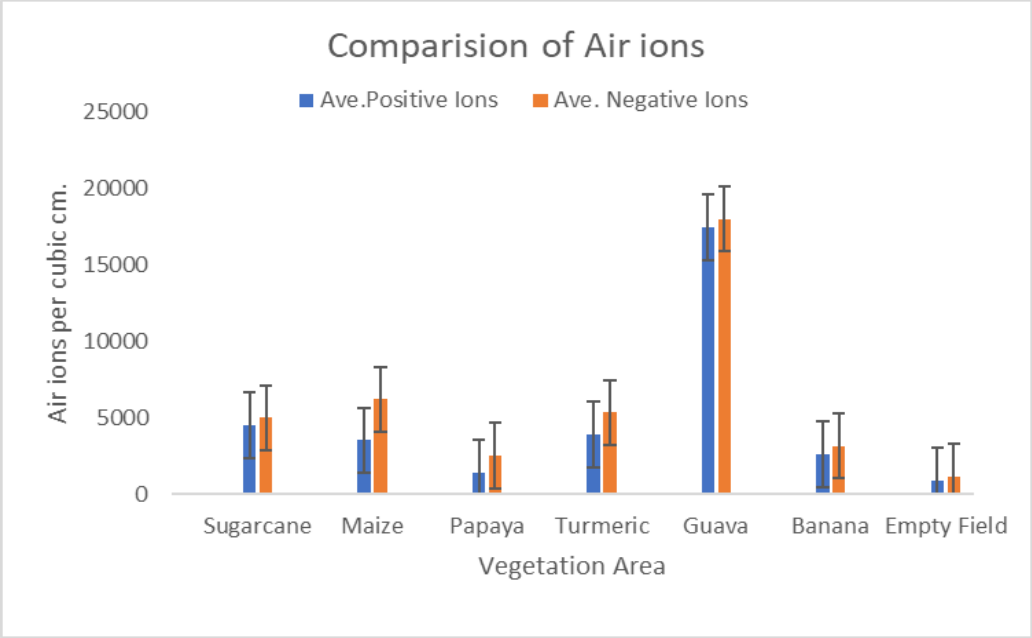

Figure 17 Comparison of air ions in irrigated and non-irrigated (empty field)

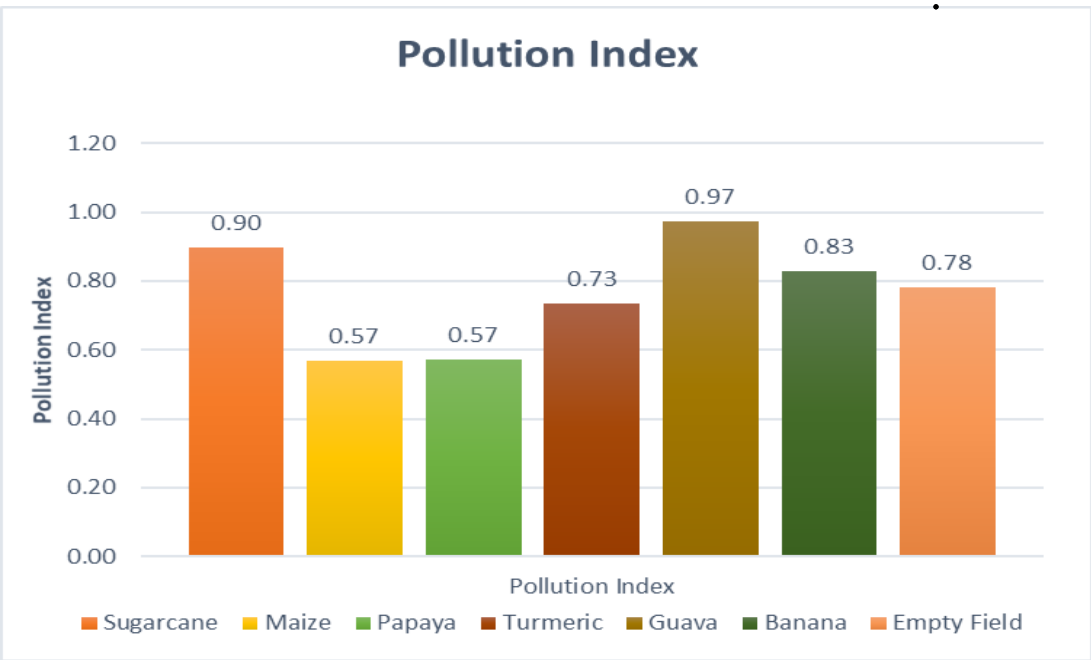

Figure 18 pollution index for Irrigated and non-irrigated vegetation area at rural station Khatav

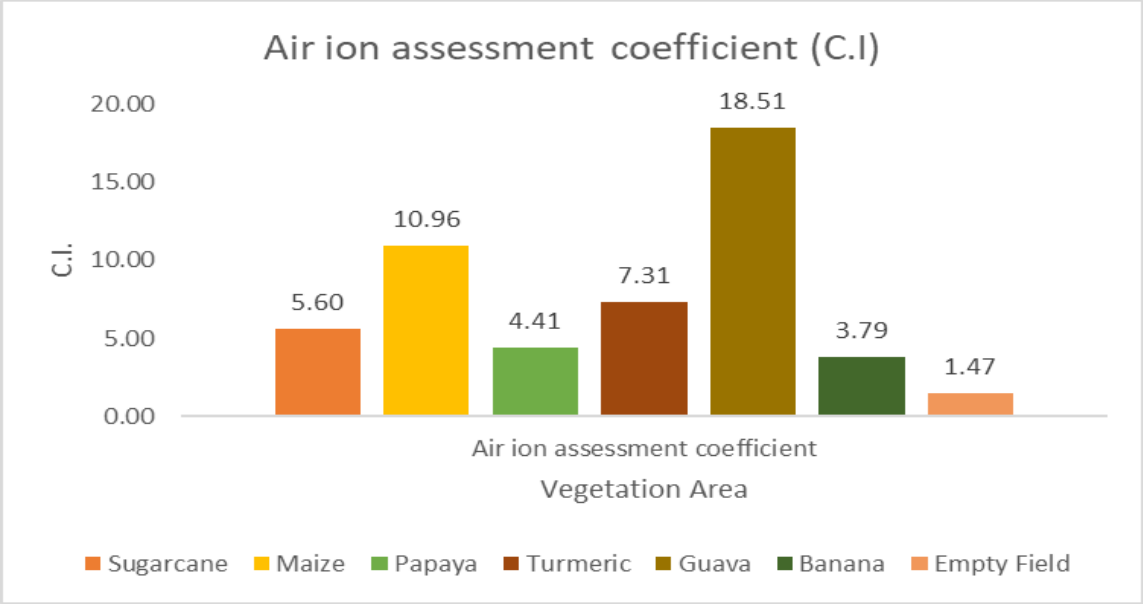

Figure 19 air ion assessment coefficient for irrigated and non-irrigated vegetation area at rural station Khatav

Air ion assessment coefficient is shown in the figure 19. For better air quality CI must be greater than one. Thus, concentration of air ions is different for different vegetation in irrigated area.

Conclusion.

At the rural station Khatav, irrigated vegetation area of sugarcane, banana, Guava, Maize, Turmeric is found to be rich in the air ion concentration as compared non-irrigated (empty field). Pollution index is less than so air quality is good and beneficial for human being. Air ion assessment coefficient is also greater than which indicates that air is good and rich in negative air ion concentration. Pollution index and CI can be considered as air quality indicator which will be useful not only for rural but also for urban areas.

References

[1] A.A. Polyakova: Charles University in Prague,284(2010).

[2] S.R, O, Honger: Charles University in Prague,284(2005).

[3] J. Smallwood: Reviews the literature on the biological effects of air ions in an

Electrostatic solutions report commissioned by Ecstatic ltd,11(2016).

[4] A.K. Kamra: Geophysics Res.,77. (1972), p5858-5869.

[5] A. S. Hussein: Environmental physics conference, Aswan (2008).

[6] Jesse, W.P. and Sadaukis, J. 'Absolute energy to produce an ion pair by beta

particles from S35', Phys. Rev., Vol. 107, No. 3, pp.766–771(1957).

[7] B.C. Wolverton, Anne Johnson, Keith Bounds: National Aeronautics and Space Administration John Stennis Space Centre Science and Technology Laboratory Stennis Space Center, by NASA,11(2016).

[8] Patil G.B., Pawar S.D., Bhosale J. L., Air Ion Counter Design Using Gerdien Condenser, IOP Conf. series: Journal of Physics: conf. series 1172(2019)

[9] National Research Council Staff, The Earth's Electrical Environment, Washington. USA: National Academies Press, (1986).

[10] Brown, LeMay, Burslen. Chemistry The Central science, ISBN0-13-048450-4,958. (1977).

[11] Chunyang zhu, Peng Ji and Shuhua Li. Effects of urban green belts on the air, temperature, humidity and air quality, Journal of Environmental Engineering and Landscape Management,25,39-55. (2017).

[12] Pawar S. D., Meena, G., Jadhav, D. B., Weekday and weekend air ion variation at Rural Station Ramanandnagar (17^0 2, N,74^0E), India, Aerosol and Air Quality Research, 10, 154-166 (2011).

[13] Gajanan Patil.,Subhash Pawar.,Onkar Gurav.,Jalindar Bhosale.,Sonali Rananananavare,Variation in atmospheric air ionand its index of pollution during morning time (00:00 to 08:00 IST) in the sugarcane area at rural station Bhilawadi ($16{\cdot}5^0$N,74.2^0E), Int. J. Environment and Sustainable Development, Vol. 20, No. 2, (2021).

[14] P. Kolartz., M. Gaisberger., P.Madl.,W.Hofmann.,M.Ritter.,H.Hartl,Characterization of ions at Alpine waterfalls, Atmospheric Chemistry and Physics,12,3687-3697 (2012).

[15] Sitar,J. Aerial ions and our health. In conference on Humans in Their Earthly and Cosmic Environment. Upice, Czech Republic,10-174(2006).

Paper 66

Morphological And Electrical Properties of spray deposited $CdSe_{0.3}Te_{0.7}$ thin film

Mr. A.D. Kanwate[a], Dr. E. U. Masumdar[b]

[a,b] *Thin Films and Materials Science Research Laboratory, Department of Physics, Shahu college, Latur, Maharashtra, India.*

Abstract:

The $CdSe_{0.3}Te_{0.7}$ thin film was deposited by using spray deposition techniques having substrate temperature 300^0C. We studied morphological and electrical properties of deposited $CdSe_{0.3}Te_{0.7}$ thin film through SEM, EDAX and two probe measurements techniques. The SEM micrograph of $CdSe_{0.3}Te_{0.7}$ thin film looks like leaf structure composed of large number of flake-like thin micro-particles. From EDAX analysis conform that, the presence of Cd, Se and Te in prepared film with elemental stoichiometry of Cd, Se and Te were 54.49%, 9.12% and 36.39% respectively. The electrical resistivity of the film at room temperature was 1 $x10^6$ Ωcm.

Keywords: Morphological, Electrical, Spray techniques.

1. Introduction:

The II–VI semiconducting materials are very interesting and potential candidate for this ever-advancing technological fields, recently ternary alloys of semiconducting materials have received much attention in the fields of optoelectronic devices and solar energy conversion owing to their properties of band gap and lattice constant modulation by composition and other growth parameters [1, 2].The cadmium chalcogenides CdSeTe has received much attention as it is used in devices such as solar cells, photoconductors, solar control applications and thin film transistors due to by obtaining desired crystal structure and tailored optical bandgap by changing the concentration of Se and Te [3-5].

Surendra K. Shinde et.al [6] have deposited $CdSe_{0.6}Te_{0.4}$ thin film on stainless steel and ITO coated glass substrate by using electrodeposition method. From XRD analysis shows that the films were polycrystalline nature with hexagonal crystal structure. FE-SEM studies reveal that the entire substrate surface was covered with $CdSe_{0.6}Te_{0.4}$ nano-nest. In optical absorption study shows the presence of direct transition and calculated band gap of the film was Eg = 1.7 eV. Further photovoltaic activity of $CdSe_{0.6}Te_{0.4}$ films were studied. The efficiency and fill factor of these PEC cells were found to be 0.64% and 0.49 respectively. A. Kathalingam et.al [7] investigated $CdSe_xTe_{1-x}$ thin films by electrochemical deposition with variation of x = 0.2, 0.4, 0.6 and 0.8. The

XRD pattern of CdSeTe thin film at composition x = 0.58 shows polycrystalline hexagonal crystal structure with average crystalline size found that 200nm.From optical study revealed that, the bandgap of the film varied between 1.48 to 1.69 eV with compositions varied from 0.2 to 0.8. N. Muthukumarasamy et.al [8] have deposited $CdSe_{0.7}Te_{0.3}$ and $CdSe_{0.15}Te_{0.85}$ by hot wall deposition. The XRD pattern of $CdSe_{0.7}Te_{0.3}$ film exhibits hexagonal structure and $CdSe_{0.15}Te_{0.85}$ film exhibits cubic zinc blende structure.

So far in literature, there was no one deposited CdSeTe thin film with spray pyrolysis techniques. In our study, first time we trying to deposited CdSeTe thin film with the help of homemade spray pyrolysis techniques. The deposited film characterized through morphological, compositional and electrical with the help of SEM, EDAX and two probe measurement techniques respectively.

2. Experimental Setup:

The CdSeTe thin film deposited on silica glass by using homemade spray pyrolysis techniques with deposition temperature 300^0C. For deposition glass substrate were boiled in chromic acid for 15 min. & washed with lebalene and distilled water, also substrates were ultrasonically cleaned for 10 min. The precursor were used for deposition as 0.025M equimolar 15ml solution of Cadmium Chloride ($CdCl_2.H_2O$) in double distilled water, 4.5ml solution of Selenium Dioxide (SeO_2) &10.5ml solution of Tellurium Dioxide (TeO_2) in double distilled water and ammonia. The Triethanolamine (TEA) used as complexing agents and Hydrazine hydrate used for reduction agent. The total 30ml solution were mixed together and used for deposition with spray rate 4ml/sec. onto a glass substrate. Compressed air pressure was used as carrier gas to spraying a solution. The as-grown sample was thin, uniform, smooth and tightly adherent to the substrate support. The colour of the deposited film was dark brown.

The thickness of the deposited film was measured by gravimetric weight by difference method using sensitive microbalance and that was found 355nm. The surface morphology of the film was observed using scanning electron microscope (JOEL-JSM 5600 operating at accelerating voltage of 15 and 200kV). Elemental chemical compositions were studied by an energy dispersive X-ray spectrometer (Bruker EDAX, X Flash 6130). The electrical properties was studied by two probe measurement (Keithley Model 2400).

3. Characterization:

3.1 Scanning Electron Microscopy (SEM):

The scanning electron microscopy is used to obtain information about surface topography of the deposited film. The scanning electron microscopy image of resultant $CdSe_{0.3}Te_{0.7}$ film given in

Fig.1. The SEM micrograph of $CdSe_{0.3}Te_{0.7}$ thin film looks like leaf structure composed of large number of flake-like thin micro-particles with different sizes ranging from 1.681 to 2.836 µm. Thus there was not agreement with grain sizes calculated from SEM and XRD [9]. This may be due to two or more grains fusing together to form the cluster type of structure [10]. The SEM image also exhibits porous nature with small roughness at the surface of $CdSe_{0.3}Te_{0.7}$ film.

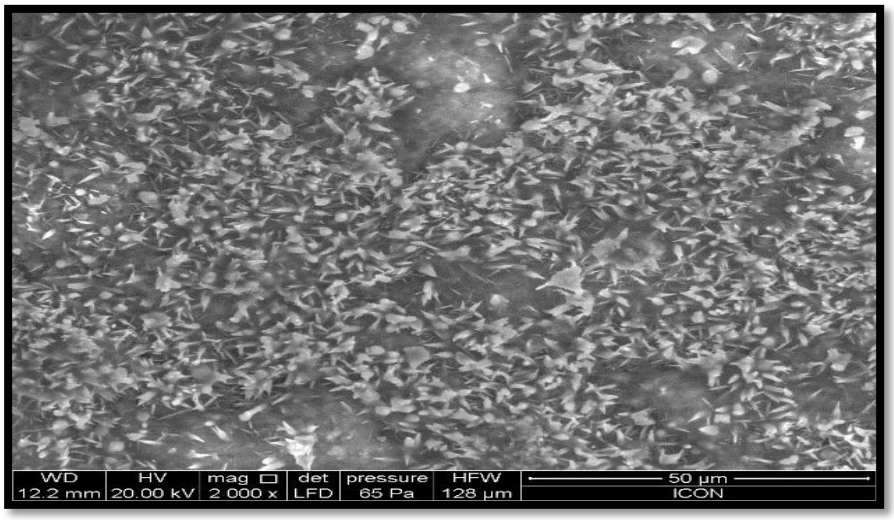

Fig.1: FSEM image of deposited $CdSe_{0.3}Te_{0.7}$ thin film

3.2 Energy Dissipative X- ray Analysis (EDAX):

The compositional analysis of the $CdSe_{0.3}Te_{0.7}$ thin film deposited at optimized preparative parameters is carried out by the EDAX technique. Fig.2 shows typical EDAX pattern of spray deposited $CdSe_{0.3}Te_{0.7}$ thin film at substrate temperature 300^0C. The presence of well-defined peaks related to Cd, Se and Te confirms the successful preparation of CdSeTe film with average atomic stoichiometry of Cd, Se and Te were 54.49%, 9.12% and 36.39% respectively, which shows slight rich in Cd and Te. The average weight and atomic percentage of Cd, Se and Te is shown in Table 1.

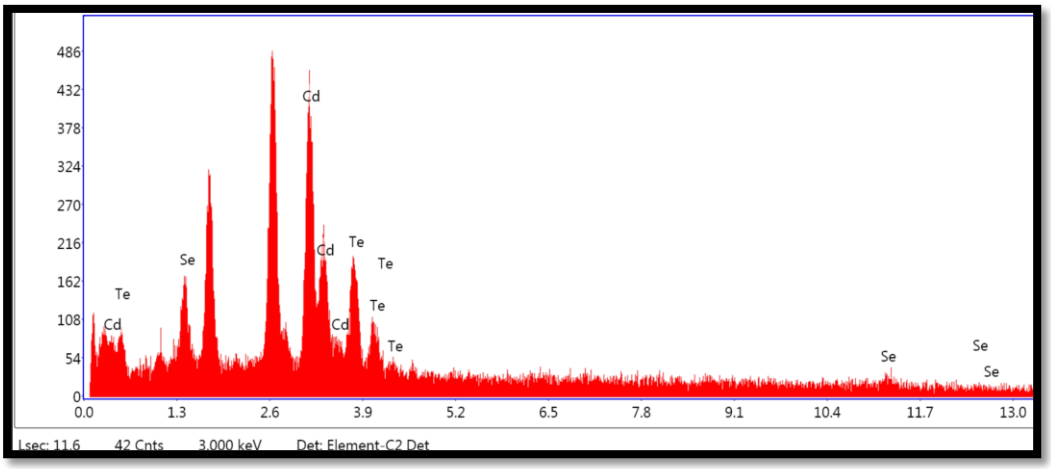

Fig.2: EDAX pattern of $CdSe_{0.3}Te_{0.7}$ thin film

Table 1: Elements composition of $CdSe_{0.3}Te_{0.7}$ thin film

Element	Weight %	Atomic %	Net Int.	Error %	Kratio	Z	R	A	F
CdL	53.31	54.49	372.31	4.50	0.5381	1.0189	0.9977	0.9662	1.0252
TeL	40.42	36.39	158.78	14.00	0.3174	0.9646	1.0157	0.8003	1.0173
SeK	6.27	9.12	7.10	63.56	0.0823	1.1008	0.9670	0.9747	1.2230

3.3 Electrical Properties:

The electrical resistivity of the $CdSe_{0.3}Te_{0.7}$ thin film deposited at 300^0C substrate temperatures was measured using a standard DC two-point probe method in temperature range 300-500K. The electrical resistivity of $CdSe_{0.3}Te_{0.7}$ thin film was calculated by relation [11];

$$\rho = 2\pi s \frac{V}{I} \quad \ldots\ldots\ldots\ldots\ldots\ldots\ldots\ldots\ldots\ldots\ldots (1)$$

Where s is distance between two probes, the V was kept constant and I measured with varying temperature. Fig.3 shows the relationship between the inverse absolute temperature of the cooling cycle and log (resistivity). Resistivity decreases with increasing temperature, shows the typical semiconductor nature of the sample [12]. The value of resistivity at room temperature was found that 1 x10^6 Ωcm. These results have been reported in one of our previous work. The higher value of resistivity may be due to nanocrystalline nature of the film, discontinuity at surface boundary, imperfection and dislocation of the film. Due to grain boundary discontinuities the internuclear space effectively increases and increases the height of the grain boundary potential resulting in a decrease in carrier concentration as well as mobility and hence the electrical resistivity increases [13, 14].

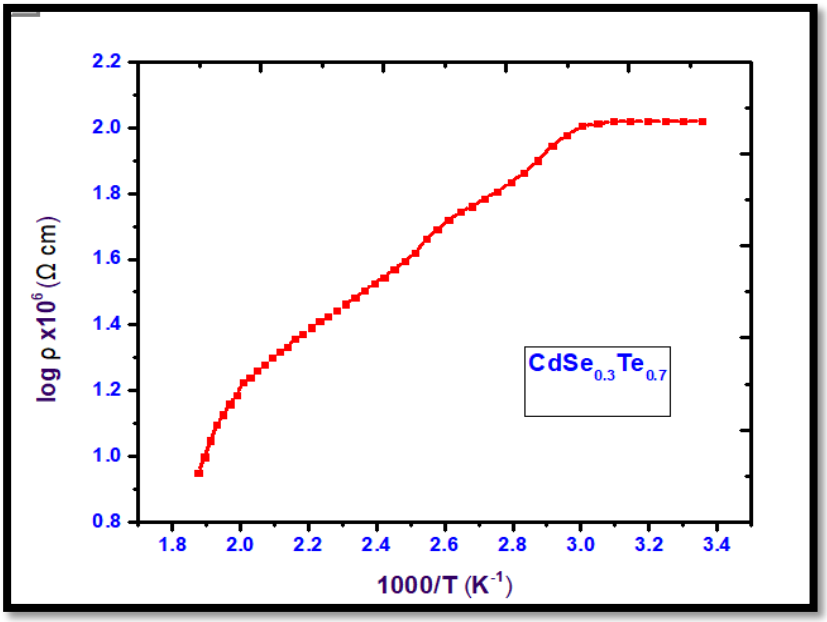

Fig.3: Variation of verses log ρ vs inverse temperature

3.4 Conclusion:

In recent years cadmium chalcogenide compounds have been extensively investigated because of their potential applications in solar energy conversion with different methods. But we successfully first time demonstrated synthesis of $CdSe_{0.3}Te_{0.7}$ thin film by homemade spray pyrolysis technique. The homemade spray pyrolysis technique is simple, cost effective and easy for deposition of ternary materials with desired parameters. The spray deposited $CdSe_{0.3}Te_{0.7}$ thin film have leading material in the field of opto-electronics, photo-voltaic devices because bandgap of the film near in optical spectrum reported in previous paper [15].The SEM image of $CdSe_{0.3}Te_{0.7}$ thin film shows leaf of large number of flakes thin micro-particles. In EDAX pattern conforms the presence of Cd, Se, and Te materials. The electrical resistivity of the film at room temperature was found to be 1 $x10^6$ Ωcm.

References:

1) V. Saaminathan, K.R. Murali, Physica B 373 (2006) 233–239.
2) A.S. Khomane, P.P. Hankare, Journal of Alloys and Compounds 489 (2010) 605–608.
3) P.D. More, G.S. Shahane, L.P. Deshmukh, P.N. Bhosale, Materials Chemistry and Physics 80 (2003) 48–54.
4) K.R. Murali, Materials Science in Semiconductor Processing 13 (2010) 193–198.
5) K.R. Murali, B. Jayasuthaa, Solar Energy 83 (2009) 891–895.
6) Surendra K. Shinde, Jagannath V. Thombare, Deepak P. Dubal, Vijay J. Fulari, Applied Surface Science 282 (2013) 561– 565.
7) A. Kathalingam, Mi-Ra Kim, Yeon-Sik Chae, Jin-Koo Rhee, S. Thanikaikarasan, T. Mahalingam, Journal of Alloys and Compounds 505 (2010) 758–761.
8) N. Muthukumarasamy, S. Velumani, R. Balasundaraprabhu, S. Jayakumar, M.D. Kannan, Journal of Vacuum 84 (2010) 1216–1219.
9) A. D. Kanwate, E. U. Masumdar, Volume XII, Number 8, ISSN: 2319-7129, Edu. World (2018) 296-300.
10) S. Mahato, A.K. Kar, J. Elec. Che. 742, (2015), 23–29.
11) S. Erat, H. Metin, M. Ari, Mater. Chem. Phys.111 (2008)114.
12) K. Chaudhari, N. Gosavi, N. Deshpande, S. Gosavi, J. Sci.: Advanced Materials and Devices 1, (2016), 476-481.
13) A. Purohit, S. Chander, S.P. Nehra, M.S. Dhaka, Physica E 69 (2015) 342–348.
14) P.A. Chate, D.J. Sathe, P.P. Hankare, S.D. Lakade, V.D. Bhabad, Journal of Alloys and Compounds 552 (2013) 40–43.
15) S.K. Shinde, D.P.Dubal, G.S.Ghodake, V.J.Fulari, Materials Letters 126 (2014) 17–19.
16) K.R. Murali, Materials Science in Semiconductor Processing 13 (2010) 193–198.
17) S.K. Shinde, G.S.Ghodake, D.P.Dubal, G.M.Lohar, D.S.Lee, V.J.Fulari, Ceramics International 40 (2014) 11519–11524.
18) N. Muthukumarasamy, S. Velumani, R. Balasundaraprabhu, S. Jayakumar, M.D. Kannan, Journal of Vacuum 84 (2010) 1216–1219.
19) N. Muthukumarasamy, R. Balasundaraprabhu, S. Jayakumar, M.D. Kannan, Materials Chemistry and Physics 102 (2007) 86–91.

20) N. Muthukumarasamy, R. Balasundaraprabhu, S. Jayakumar, M.D. Kannan, Materials Science and Engineering B 137 (2007) 1–4.
21) N. Muthukumarasamy, S. Jayakumar, M.D. Kannan, R. Balasundaraprabhu, Solar Energy 83 (2009) 522–526.
22) F.Z. Amir, K. Clark, E. Maldonado, W.P. Kirk, J.C. Jiang, J.W. Ager III, K.M. Yu, W. Walukiewicz, Journal of Crystal Growth 310 (2008) 1081-1087.
23) Ling Liu, Xiaoliang Xu, Tian Luo, Yansong Liu, Zhou Yang, Jiemei Lei, Solid State Communications 152 (2012) 1103–1107.
24) R. Sathyamoorthy, P. Sudhagar, R. Saravana Kumar, P.Matheswaran, Ranjith G. Nair, Physica B 406 (2011) 715–719
25) V. Saaminathan, K.R. Murali, Physica B 373 (2006) 233–239.
26) T.V. Torchynska, Journal of Luminescence 137 (2013) 157–161.
27) Lifang Liao, Hua Zhang, Xinhua Zhong, Journal of Luminescence 131 (2011) 322–327.
28) T.V.Torchynska, J.L.Casas Espinola, J.A.Jaramillo Gómez, J.Douda , K.Gazarian PhysicaE51(2013)55–59.
29) N. Muthukumarasamy, S. Jayakumar, M.D. Kannan, R. Balasundaraprabhu, P. Ramanathaswamy, Journal of Crystal Growth 263 (2004) 308–315.
30) T.G. Kryshtab, L.V. Borkovska, O.F. Kolomys, N.O. Korsunska, V.V. Strelchuk, L.P. Germash, R.Yu. Pechers'ka, G. Chornokur, S.S. Ostapenko, C.M. Phelan, O.L. Stroyuk, Superlattices and Microstructures 51 (2012) 353–362.
31) Lokendra Kumar, Beer Pal Singh, Aparna Misra, S.C.K. Misra, T.P. Sharma, Physica B 363 (2005) 102–109.
32) K. R. Murali, V. Subramanian, K. Srinivasan, Journal of Materials Science 34 (1999) 3417 – 3419.
33) L. Hannachi, N. Bouarissa, Superlattices and Microstructures 44 (2008) 794-801.
34) X. Zheng, D. Kuciauskas, J. Moseley, E. Colegrove, D. S. Albin, H. Moutinho, J. N. Duenow,T. Ablekim,1S. P. Harvey, A. Ferguson, and W. K. Metzger, APL Mater. **7**, 071112 (2019); doi: 10.1063/1.5098459 Accepted: 13 June 2019.
35) AL. Hannachi, N. Bouarissa, Superlattices and Microstructures 44 (2008) 794-801.
36) K.R. Murali, P. Thirumoorthy, C. Kannan, V. Sengodan, Solar Energy 83 (2009) 14–20.
37) Ali Hussain Reshak, I.V. Kityk, R. Khenata, S. Auluck, Journal of Alloys and Compounds 509 (2011) 6737-6750.
38) N. Muthukumarasamy, S. Jayakumar, M.D. Kannan, R. Balasundaraprabhu, P. Ramanathaswamy, Journal of Crystal Growth 263 (2004) 308-315.
39) Zhen Wan, Weiling Luan, Shan-tung Tu, Journal of Colloid and Interface Science 356 (2011) 78–85.
40) S. Ouendadji, S. Ghemid, H. Meradji, F.El Haj Hassan, Computational Materials Science 50 (2011) 1460–1466.
41) Lokendra Kumar, Beer Pal Singh, Aparna Misra, S.C.K. Misra, T.P. Sharma, Physica B 363 (2005) 102–109.

Paper 67

Life table and intrinsic rate of increase in Lepidopteran pest *Hypsa producta*

Vishnu Y. Kadam[1], Rajendra V. Salunkhe[2*], Sanjay K. Gaikwad[3] and Sambhajirao H. Bhosale[4]

1. Department of Zoology, Bharati Vidyapeeth's Matoshri Bayabai Shripatrao Kadam Kanya Mahavidyalaya, Kadegaon Dist. Sangli
2. Department of Zoology, Arts, Science and Commerce College, Indapur, District Pune-Maharashtra, India. Author for correspondence
3. Department of Cell and Molecular Biology, Rajiv Gandhi Institute of IT and Biotechnology, Bharati Vidyapeeth, Pune, Maharashtra, India.
4. Department of Zoology, Shankarrao Mohite Mahavidyalaya, Akluj, Dist. Solapur, Maharashtra, India.

Abstract:-

Hipsa producta is the Lepidopteran insect pest is forest pest which acts as defoliator of *A. excelsa.* Therefore life table and intrinsic rate increase have been studied. The first adult mortality was noted on 5th day. Average period of immature stages was 30 days. Maximum mean progeny production per day, mx was 26 on the 3rd day. The immate capacity for increase was found to be 0.141 per female per day and population of *H. producta* multiplied 76.76 times in generation 'T' of 30.78 days.

Key words- *Alianthus excelsa, H. producta,* life table, intrinsic rate of increase.

Introduction:-

The estimate of rate of growth of the pest have tremendous importance in pest management. The estimates of the rate of growth of the pests have tremandous importance in pest management (Howe, 1953). In a given environment an individual living animal shows its own characteristics qualitatively and quantitatively at longevity and fecundity. The value of development, are determined in part by the environment and in part by inherent characteristics of the living animal itself. According to Thompson (1924) the inherent characteristics of the animals are collectively called the 'innate capacity for increase". He visualised the first mathematical method for population dynamics. Later, Lotka (1925) derived the function for "the intrinsic rate of natural increase' and then Birch (1948) used the same for animal ecology and for the insect populations. In the present study the life tables were constructed according to Birch (1948) as elaborated by Howe (1952) and Watson (1964) .

Review of literature indicates that life table studies have been attempted in different orders of insects by several workers, noteworthy amongst them refers to Morris & Miller (1954) on Choristoneura fumiferana (Lepidoptera), Stark (1959) on Recurvaia starki (Lepidoptera), Richards & Waloff (1961) on Phytodecta olivacea (Coleoptera), Le Roux et al.,(1963) on Spilonota ocellana (Lepidoptera); Waloff (1968) on Sitona recansteinansis Herbst (Coleoptera) and on Arytacina cenistae (Homoptera), Mcleod (1972) on Neodiprion swainei Midd. (Hymenoptera), Tamaki

et al.,(1972) on Zebra caterpillar (Lepidoptera), Bains & Shukla (1976) on Chilo partellus (Swinh.) (Lepidoptera), Bilapate & Pawar (1980) and Reddy & Bhattacharya (1988) on Helicoverpa armigera.

Material and methods:-

Intrinsic rates of increase-

Birch (1948) visualized the following equation to study intrinsic rate of natural increase.

$$\sum e^{-r} m^x l_x m_x = 1$$

Where

'e' is the base of the natural logarithms,

'x' the age of the individual in days,

*l*x the number of individual alive at age, 'x' as a portion of one, and m_x the number of female offsprings produced per female in the age interval 'x'.

The sum of the products 1x mx is the net reproductive rate,

'R_0' which is the rate of multiplication of the population in each generation measured in terms of females produced per generation.

The approximate value of cohort generation time 'Tc' was calculated as follows:

$$T_c = \frac{l_x m_x X}{l_x m_x}$$

The formula: $$r_c = \frac{\log_e R_o}{T_c}$$

provides the arbitrary value of innate capacity for increase 'r_c'.

This was an arbitrary value for rm and value of r_m Upton two decimal places was substituted in the formula until the two values of the equation were

found which lies immediately above or below 1096.6. The two values of

$$\sum e^{7-r} m^x l_x m_x = 1$$

were then plotted on the horizontal axis against their respective arbitrary r_m s on the vertical axis. The point of intersection gives the value of r_m accurate to 3 decimal places. The precise generation time 'T' was calculated as

$$T = \frac{\log_e R_0}{r_m}$$ and

the finite rate of increase (λ) was calculated as-

$\lambda = e^r m.$

Adults moths of *H. producta* reared under laboratory conditions (25 ± 2^0c, 65 ± 5 % R.H., 12 hrs. photoperiod). The laboratory culture was used for determining intrinsic rate of increase.

The life tables were prepared with the help of fecundity data and later the intrinsic rates of natural increase of population of moths were calculated. All the experiments were carried out at laboratory conditions (25 ± 2^0c, 65 ± 5 % R.H., 12 hrs. photoperiod) and replicated for ten times.

Result:-

Intrinsic rates of increase in *H. product-*

The first adult mortality was noted on the 5th day. Average period of immature stages was 30 days, Maximum mean progeny production per day, m x was 26 on the 3rd day. The innate capacity to increase was found to be 0.141 per female per day and population of *H. producta* multiplied 76.76 times in generation time 'T' of 30.78 days. Results are shown in tables 1-5.

$$T_c = \frac{1_x m_x X}{1_x m_x} = \frac{2506.34}{76.76} = 32.65$$

Where T_c is arbitrary T.

$$\frac{= \log_e R_0}{= T_c} \quad = \frac{76.76}{32.65} = 0.132$$

Where r_c is arbitrary r_m

T_c = 32.65

r_c = 0.132

Now arbitrary 'rm's are 0.11 and 0.15 where λ is the finite rate of natural increase.

r_m = 0.141 (figure)

$$T = \frac{\log_e 76.76}{0.141} = 30.78$$

T = 30.78 *days.*

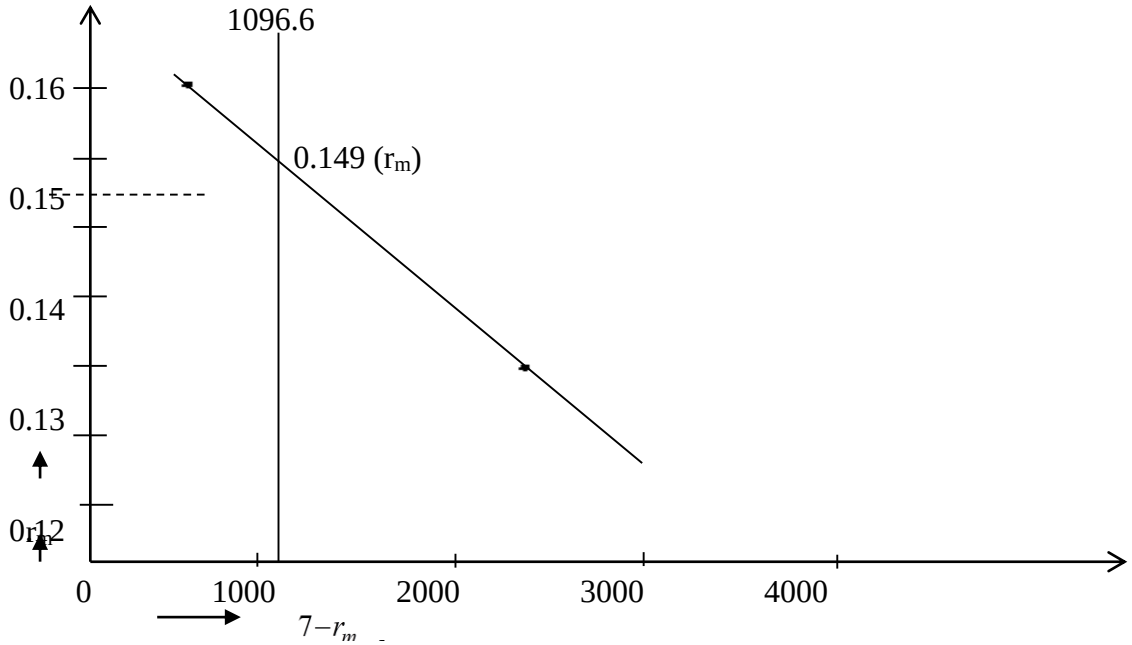

Fig.: 1 Determination of intrinsic rate of increase in *H. producta.*

Table 1: Developmental period required for females of *H. product.*

Sr. No	Egg (days)	Larva (days)	Pupa (das)	Adult formation (Total days)
1	3	20	7	30
2	3	21	7	31
3	3	21	8	32
4	3	18	8	29
5	3	21	8	32
6	3	18	7	28
7	3	21	7	31
8	3	18	7	28
9	3	18	7	28
10	3	20	8	31
Mean				30

Table 2: Daily production of progeny by mated females of *H. producta*

Replicates	Number of progeny produced /day																
Female	**1**		**2**		**3**		**4**		**5**		**6**		**7**		**Males**	**Females**	**Total**
number	**M**	**F**	**M**	**F**	**M**	**F**	**M**	**F**	**M**	**F**	**M**	**F**	**M**	**F**			
1	7	12	8	18	17	28	5	14	2	-	D	7	-	D	39	79	118
2	9	14	10	16	12	19	5	17	2	10	D	D	-	-	38	76	114
3	8	17	9	21	15	25	5	17	3	D	D		-	-	40	80	120
4	6	12	10	20	15	24	5	10	5	11	D	5	-	D	41	82	123
5	9	14	11	17	14	23	4	15	D	6	-	D	-	D	38	75	113
6	8	11	10	18	12	27	4	13	3	4	-	D	-	-	37	73	110
7	7	15	12	27	16	28	7	15	D	D	-		-	-	42	85	127
8	8	13	12	19	12	29	6	14	3	8	D	D	-	D	41	83	124
9	9	12	11	27	12	30	6	9	D	D	-		-	-	38	78	116
10	10	16	11	19	12	27	6	11	D	7	-	D	-	-	39	80	119
Mean	8.1	13.6	10.4	20.2	13.7	26.0	5.3	13.5	1.8	4.6		1.2	-	-	39.3	79.1	118.4

Table 3: Life table statistics of *H. producta*

Pivotal age (days)	Proportional live age ×	Number of female progeny per female		
x	Lx	mx	Lx mx	Lx m_xx
1-30 days immature stages				
31	1.0	13.6	13.60	421.60
32	1.0	20.2	20.20	646.40
33	1.0	26.0	26.00	858.00
34	1.0	13.5	13.50	459.00
35	0.7	4.6	3.22	112.70
36	0.2	1.2	0.24	8.64
37	0.0	0.0	0.00	0.00
			∑ 76.76	∑ 2506.34

Table 4: Provisional r_m (0.11) for *H. producta* and related values of $e^{7-r}mxl_xm_x$

x	r_{mx}	$e^{7-r}mx$	e^{7-r} mx	e^{7-r} mxl_xm_x
31	3.41	3.59	36.23	492.72
32	3.52	3.48	32.45	655.49
33	3.63	3.37	29.07	755.82
34	3.74	3.26	26.04	351.54
35	3.85	3.15	23.33	75.12
36	3.96	3.04	20.90	5.01
37	4.07	2.93	18.72	0.0
				∑ 2335.7

Table 5: Provisional r_m (0.5) for *H. producta* and related values of $e^{7-r}mxl_xm_x$

x	r_{mx}	$e^{7-r}mx$	e^{7-r} mx	e^{7-r} mxl_xm_x
31	4.65	2.33	10.48	142.52
32	4.8	2.20	9.02	182.20

33	4.95	2.05	7.76	201.76
34	5.1	1.90	6.68	90.18
35	5.25	1.75	5.75	18.51
36	5.4	1.60	4.95	1.18
37	5.55	1.45	4.26	0.0
				$\sum$ 636.35

Discussion:-

Bains and Shukla (1976) studied the life tables and intrinsic rate of increase in *Chilo partellus* (Swin.) (lepidoptera), the intrinsic rate of increase (r_m) at different temperatures were in ascending order 0.0002 (35^0C), 0.165 (32.5 ^{0}C), 0.223 (25^0C), 0.383 (27.5^0C) and 0.435 (30^0C). These conclusions showed that the rate of increase was maximum at 30^0C which should be considered to be the optimum temperature for the multiplication of this lepidopterous pest. However, the present study was not carried out at different temperature. Further observations of Bains and Shukla (1976) on the finite rate of increase per week were 4.67, 15.59, 21, 3.177 and 1.002 at 25^0C , 27.5^0C, 30^0C , 32.5^0C and 35^0C respectively, In the present study λ was calculated for each lepidopterous pests (*H. producta*,) in respect of daily increase at laboratory temperature (25 ± 2^0C, 65 ± 5 % R.H and 12 hrs. photoperiod.).

In *H. armigera,* the value of R_0 indicated that 285.06 females were produced per female during one generation. The innate capacity and finite rate for increase in numbers were 0.1210 and 1.1260 respectively. The mean duration of a generaton was 46.71 days. Under conditions of abundant space, the daily finite rate of increase of *H. armigera* was 1.1286 which enabled the insect to multiply 2.3322 times every week (Bilapate and Pawar, 1980).

According to Reddy & Bhattacharya (1988) the life expectancy (e_x) of *H. armigera* declined up to first 6 days due to egg mortality and increased upto 10^{th} day due to larval mortality. Later, with the advancement of development e_x decreased steadily till it reached 46^{th} day. This type of enhancement in e_x due to heavy mortality at any age group was also reported for *Naranga diffua* Walker, *Phyllonistis citrella* Stainton, *Creatonotus gangis* Linneaus, *S. obliqua* and *S. litura* (Singh, 1984). There was indication of the survival fraction (lx) of each cohort. Females started laying eggs after 31.5^{th} day and stopped it after 39.5^{th} day with lx values being 0.42 and 0.17 respectively. The lx decreased gradually after 4.5^{th} day due to adult mortilty.

Fecundity rate (mx) and reproductive rate (*l*x mx) of each age group showed an undulating pattern during the entire egg laying period. Such pattern was also reported for several other insects (Evans & Smith, 1952; Choudhary and Bhattacharya, 1986). Reddy and Bhattacharya (1988) studied various life parameters computed to get an overall picture of different vital statistics of *H. armigera* on maize based diet. Mean length of generation (T) indicated that this insect completed first generation in 35.5 days. Similarly, net reproductive rate (R_0), accurate estimate of intrinsic rate (r_m), finite rate of increase or the population multiplication in on unit time (λ) , time required for the population become double (DT), potential fecundity (PT) and annual ratio of increase (AR) were 46.98, 0.1090, 1.1152, 3.36, 134.40, 1.898×10^{17} respectively.

Conclusion:-

In the present study 'r_m' and 'T' of *H. producta*, were 0.141 and 30.78 days respectively. The present studies will be helpful for population dynamics of above forest pests and in deciding control strategies for them.

References:-

1. Bains, S. B. and K. K. Shukla, 1976. Effect of temperature on the development and survival of maize borer *Chilo pertellus* (Swinhoe). *Indian J. Ecol.,* 3(2), 149 – 155.
2. Birch, L. C. 1948. The intrinsic rate of natural increase in an insect population. *J. Anim. Ecol*., 17, 15-26 (W.L. 25559).
3. Bilapate, G. G., and V.M. Pawar, 1980. Life fecundity tables for *Heliothis armigera* Hubner (Lepidoptera : Noctuidae) on sorghum earhead. *Proc. Indian Acad. Sci.* (Ani. Sci.), 89 (1), 69-73. (W. L. 2555).
4. Howe, R. W. 1953. The rapid determination of intrinsic rate of increase of an insect population. *Appl. Biol.,* 40, 134-155.
5. Le Roux, E. J. 1963. Population dynamics of agricultural and forest insect pests. Mem. Ent. Soc. Can., 32, 1-103.
6. Lotka, A. J. 1925. Elements of Physical Biology. Williams and Wilkins, Baltmore Md – pp. 462.
7. Morris, R. F. and C. S. Miller, 1954. The developments of life tables for the spruce budworm. Can. J. Zool., 32, 382-301.
8. Reddy, C.G. and Bhattacharya, 1988. Life tables of *Heliothis armigera* (Hubner) on semisynthetic diets. *Indian J. Ent.*, 50 (3), 357-370.
9. Stark, R.W. 1959. Population dynamics of the lodgepole needle miner, *Nicrophorus spp* and the mite *Poecilochirus necrophori*. *J. Animi. Ecol*., 37, 417-474. (W.L. 25559).
10. Thompson, W.R. 1924. La theorie mathematique deiaction des parasites entomophages et. le. facteur du hasar du hasar d. Annls Fal. Sci. Morseilla, 2, 69-89.
11. Watson, T. F. 1964. Influence of host plant conditions on population increase of *Tetranychus tetarius* (Linnaeus). *Hilgardia*, 35, 275-322.

Paper 68

Histopathology of Prostate Gland in Terrestrial Slug *Semperula Maculata* after Acute Exposure of Zinc Chloride

Vishnu Kadam[1], Nilofar Shaikh[2], Sunil Londhe[3], Rajendra Salunkhe[4*], Sanjay Gaikwad[5]

1. Department of Zoology, Bharati Vidyapeeth's Matoshri Bayabai Shripatrao Kadam Kanya Mahavidyalaya, Kadegaon Dist. Sangli
2. Department of Zoology, D.K.A.S.C. College, Ichalkaranji Dist. Kolhapur
3. Department of Zoology, Bharati Vidyapeeths Matoshri Bayabai Shripatrao Kadam Kanya Mahavidyalaya, Kadegaon, Dist. Sangli
4. Department of Zoology, Arts, Science and Commerce College, Indapur, District Pune-Maharashtra, India. Author for correspondence
5. Department of Cell and Molecular Biology, Rajiv Gandhi Institute of IT and Biotechnology, Bharati Vidyapeeth, Pune Maharashtra, India.

Abstract:

This study enlights on terrestrial molluscan slug, *Semperula maculata*, against acute exposure of Zinc chloride ($ZnCl_2$). Histopathological changes were observed in the cellular arrangement of prostate gland. Prostate gland showed increased dilated secretory cells and damaged connective tissues were observed in the sectional view. These alterations found directly proportional to the time of exposure period. Evidence indicates that Zn degeneration and impact over the normal function and structure of prostate gland.

Key words- *Semperula, maculate*, *Morus, indica*, alcohol, prostate gland

Introduction:

Molluscan species can also represent hazards or pests for human activities. Snails and slugs can also be serious agriculture pests, and accidental or deliberate introduction of some snail species into new environments has seriously damaged some ecosystems (Kadam *et al.* 2021). Terrestrial gastropods are highly sensitive to toxic chemicals producing alterations at the cellular level (Hernadi *et al.* 1992). He also reported the mussel *Elliptio complanata*, exposure to Cu had a significant effect on the mean percentage of destabilized lysosomes in different concentration. Now a day rapid industrial development in agricultural field leads to organic and inorganic contamination from hazardous chemicals and heavy metals of aquatic and terrestrial ecosystems. These form a major group of aquatic and terrestrial contaminants showing deleterious impact on terrestrial and aquatic media (Sanchez, 2008; Davidson *et al*. 2011; pack *et al*. 2014). Heavy metals are enter in the environment through anthropogenic sources, such as industrial effluent,

traffic, smelting, combustion of fossil fuels, and certain agricultural practices (Uyear *et al*. (2009).

From above review it is clear that there is scanty information available on the effect of heavy metal on the reproductive organs i.e. on the prostate gland. Thus, the present study designed to study the effect of zinc chloride on the prostate gland of terrestrial slug.

Materials and Methods:

Experimental animals-

Adult herbivorous, hermaphrodite, terrestrial slugs *S. maculata* (Approximately of 67 cm length, 11.5 cm width and 34 g wt.) were collected from natural habitats from the village Panmala at Bedug, Miraj, district Sangli, Maharashtra, India. Animals were carried in aerated plastic bottles to the laboratory. Experimental animals were kept in open-air trough covered with aerated plastic lead covering to provide proper ventilation. Experimental animals were allowed to feed on fresh leaves of mulberry plant (*Morus indica*). All the animals were kept under controlled lab conditions of water, temperature, and fresh air for better acclimatization (Kadam *et al*. 2021).

Induction and tissue preparation-

Experimental animals, *S. maculata*, were acutely exposed to previously determined mean LC50 (377.7 ppm) concentration of $ZnCl_2$ (Londhe, 2013).Control and experimental animal were dissected after 24, 48, 72, or 96 hr., respectively, for prostate gland and fixed in Bouin's solution (75 ml picric acid + 25 ml formalin + 5 ml acetic acid) for 6-7 hr. at room temperature followed by washing with 70% ethanol for three days, dehydrated with ethanol-graded series, cleaned with xylene, and embedded in paraplast. Tissue blocks were prepared and sectioned with a rotary microtome at 6 mm thickness and for histological study (Londhe, 2013).

Histological study-

Hematoxylene and eosin technique (H&E) (Harris 1900)-

For histological study, tissue sections were dewaxed in xylene, hydrated in descending order of alcohol grades and, finally in distilled water. The sections were stained with aqueous hematoxylene for 7 minutes. Stained sections were differentiated in distilled water, dehydrated in 30%, 50%, and 70% alcohols, respectively. All sections were treated with eosin for 45 sec. Furthermore, sections were differentiated in 70% alcohol, dehydrated in 90% absolute alcohol, cleared in xylene, and mounted in Di-N-butyl phthalate in xylene (DPX).

Result and Discussion:-

Histological study-

Toxicity study related to the prostate gland was studied by applying the standard histological techniques for slug *S. maculata* exposed to $ZnCl_2$ on targeted reproductive organ i.e. prostate gland.

Prostate gland-

Light microscopic observation of the prostate gland showed the number of secretary cells embedded in thin connective tissues whereas the luminal content was found well-established at center. It covers the outer surface of the whole gland. Secretary cells were found in groups and showed an ample secretion in the luminal region (Figure). After H&E staining, secretory cells were deep blue and non-secretory ones stained red. Microscopic structure of the prostate gland was similar with the earlier observation made by Nanaware and Varute (1976).

After the 24 and 48 hours of exposure, slightly increased dilated secretory cells and damaged connective tissues were observed in the sectional view (Figure- 1). These alterations became more complicated after the 72 and 96 hours of exposure, which are photographically shown in Figure. The major alterations in prostate glands were hypertrophy of secretory cells, degenerated outer surface, and disturbed luminal content. Similar to the digestive gland, the reproductive gland is also sensitive and may be used for the biomonitoring of heavy metal pollution. After 96 hrs., the prostate gland showed changes in the structure which included the dilation of unicellular and multicellular glands, the degeneration in the muscular fiber, the dilation in secretory cells, and the disruption in the luminal content. Otitoloju, Ajikobi, and Egonmwan (2009) notice molluscs were found to have higher capacity to accumulate metals to varying degree depending upon the concentration of exposure and the type of metal. Jantataeme *et al*. (1996) studied the bioaccumulation of Pb in the intestine, prostate gland, digestive gland, ovary, albumin gland, testis, stomach, and cerebral ganglia and noted a maximal uptake in the intestine and less in the prostate gland, digestive gland ovary, and testis. Londhe and Kamble (2013) observed exposure dependent bioaccumulation of Hg and Zn in the nervous system and the gill tissue of freshwater snail *B. bengalensis*. Tanhan *et al*. (2005) noted that Cd accumulated in the proboscis, esophagus, stomach, digestive gland, rectum, and gill of snail Babylonia areolata (spotted Babylon) and was increased with the time of exposure. In the conclusion we found, The histopathological changes represented end point contamination in the terrestrial media, which will be hazardous for the survival of the terrestrial as well as aquatic fauna. The major contaminations provide an imbalance to the ecological diversity in the region.

Conclusion:

Alterations of prostate gland found directly proportional to the time of exposure period to zinc chloride. Evidences indicate that the Zn degeneration cause the normal function and structure of prostate gland. The major alterations in prostate glands were hypertrophy of secretory cells, degenerated outer surface and disturbed luminal content. Similar to the digestive gland, the reproductive gland is also sensitive and may be used for the biomonitoring of heavy metal

pollution. After 96 hrs., the prostate gland showed changes in the structure which included the dilation of unicellular and multicellular glands, the degeneration in the muscular fiber, the dilation in secretory cells and the disruption in the luminal content.

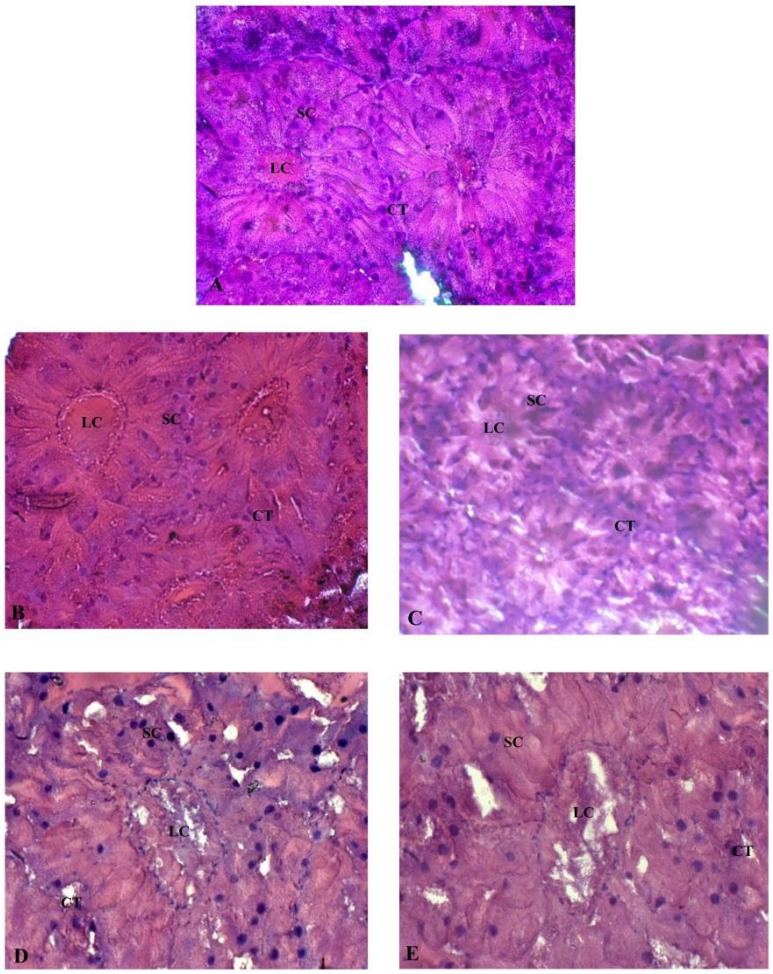

Fig-I:- $ZnCl_2$ induced alteration in Prostate gland of slug S. maculata at different exposure period. Fig. A- Control group, Fig. B- 24 hrs. , Fig. C - 48 hrs., Fig. D - 72 hrs., Fig. E - 96 hrs.

References:-

1. Davidson, M.S., M.C. Croteau, C.S. Millar, V.L. Trudeau, and D.R. Lean. 2011. "Fate and Developmental Effects of Dietary Uptake of Methylmercury in Silurana tropicalis Tadpoles." Journal of Toxicology and Environmental Health A 74: 364-379

2. Hernadi, L., L. Hiripi, A. Vehovszky, G.S. Kemenes, and K. Rozsa 1992. "Ultrastructural, Biochemincal and Electrophysiological Changes Induced by 56-dihydroxytryptamine in the CNS of the Snail Helix omatia L." Brain Research 578: 221-234.
3. Jantataeme, S., M. Kruatrachue, S. Kaewsawangsap, Y. Chitramvong, P. Sretarugsa, and E.S. Upatham. 1996. "Acute Toxicity and Bioaccumulation on Lead in the Snail, Filopaludian (Siamopaludina) Martensi martensi (Frauenfeldt)." Journal of Science Society Thailand. 22: 237-247.
4. Londhe, S.R., and N.A. Kamble. 2013. "Histopathology of Cerebro Neuronal Cells in Freshwater Snail Bellamya bengalensis: Impact on Respiratory Physiology, by Acute Poisoning of Mercuric and Zinc Chloride." Toxicological and Environmental Chemistry 95: 304-317.
5. Nanaware, S.G., and A.T. Varute. 1976. "Histochemical Studies on Mucosubstances in the Prostate Gland of the Pulmonate Snail *Semperula maculata* in Annual Breeding Aestivation Cycle." Folia Histochemica 14: 19-38.
6. Otitoloju, A.A., D.O. Ajikobi, and R.I. Egonmwan. 2009. "Histopathology and Bioaccumulation of Heavy Metals (Cu and Pb) in the Giant Land Snail, Archachatina marginata (Swainson)." Open Environmental Pollution Toxicology Journal 1: 79-88.
7. Pack, E.C., C.H. Kim, S.H. Lee, C.H. Lim, D. G. Sung, M.H. Kim, K.H. Park, S.S. Hong, K.M. Lim, D.W. Choi, and S.W. Kim. 2014. "Effects of Environmental Temperature Change on Mercury Absorption in Aquatic Organisms with Respect to Climate Warming." Journal of Toxicology and Environmental Health A 77: 1477-1490.
8. Sanchez, M.L. 2008. Causes and Effect of Heavy Metal Pollution. Hauppauge, NY: Nova Science Publishers.
9. Tanhan, P., P. Sretarugsa, P. Pokethitiyook, M. Kruatachue, and E.S. Upatham. 2005. "Histopathological Alterartion in the Edible Snail, Babylonia areolata (Spotted Babylon), in Acute and Subchronic Cadmium Poisoning." Environmental Toxicology 20: 142-149.
10. Uyear, G., E. Avcil, M. Oren, F. Karaca, and M.S. Oncel. 2009. "Determination of Heavy Metal Pollution in Zonguldak (Turkey) by Moss Analysis (Hypnam cupresssiforme)." Environmental Engineering Science 26: 1-12.

Paper 69

Reproductive cycles in two geographically separated populations of the oyster *Saccostrea cucullata* from Sindhudurg district, Maharashtra State, India.

Rajendra V. Salunkhe*, Sambhajirao H. Bhosale, Sanjay K. Gaikwad and Vishnu Y. Kadam

1. Department of Zoology, Arts, Science and Commerce College, Indapur, District Pune Author for correspondence
2. Department of Zoology, Shankarrao Mohite Mahavidyalaya, Akluj, Dist. Solapur.
Department of Cell and Molecular Biology, Rajiv Gandhi Institute of IT and Biotechnology, Bharati Vidyapeeth, Pune.
4. Department of Zoology, Bharati Vidyapeeth's Matoshri Bayabai Shripatrao Kadam Kanya Mahavidyalaya, Kadegaon Dist. Sangli

---

ABSTRACT:

Two geographically separated localities at Deogad (16^0 23' N ; 73^0 23' E) and Achra (16^0 15' N; 78^0 26' E) in Sindhudurg district of Maharashtra State ,India were selected on the basis of the differences in habitat , topography ,vegetation and local market value to study the reproductive cycles of the oyster *Saccostrea cucullata*. The maximum sizes attained by *S. cucullata* in the estuaries at Deogad and Achra were 44-45 mm shell length. However, comparatively larger sized oysters are found round the year in the estuary at Deogad than at Achra.

The environmental parameters such as tidal heights, pH, temperature, dissolved oxygen and salinity existing on the oyster beds in Deogad and Achra were recorded on every new-moon and full-moon days for a period of twelve months.

The microscopic details of the gonad tissue processed on every new moon (NM) and full moon (FM) days of each month revealed following stages ; (i) Gametogenesis ; (ii) Maturing ; (iii) Mature; (iv) Partial spawning ; (v) Complete spawning ; (vi) Recovery ;(vii) Neutral . The gonads of twenty oysters were staged for males and females separately on each NM and FM days and percentage of the males and females in these different stages were calculated.

The study on reproductive cycle in male oysters of *S. cucullata* from Deogad showed that many oysters were in gametogenesis stage in entire June and once again on November NM. Maturing stage was seen on March NM, May FM, July NM and again on November FM and in entire December. Many oysters were in mature stage on March FM, April FM and July FM and again on January NM. Most of oysters were under spent stage on March FM, in entire August and September, and on January FM. Many oysters were under recovery stage on May NM and in entire October. Most of the samples collected in entire February and on April NM showed prominent neutral stage. The female oysters showed that the gametogenesis was dominant on March NM, in entire June and on November NM; maximum on NM of March and on November. The maturing stage was dominant in entire April and May and on July NM and December NM. Oysters under spent condition were dominant on April NM and December FM, and all the gametes were released in entire August, September and on October NM. The recovery stage was recorded

in many oysters on October FM and January FM, while the neutral stage was recorded in entire February.

The male oysters from Achra showed gametogenesis stage on March NM, April FM and June NM. The maturing stage was seen in most oysters on April FM, June FM, July NM, September NM and FM. The mature stage was very conspicuous on July FM and November NM. Most oysters were in the spent stage on May FM , August NM ,October NM and December FM. Oysters under recovery stage were in high percentage on December NM , January NM and February FM. The neutral condition was most prominent in many oysters on March NM and January FM. The female oysters at Achra showed that many oysters under the gametogenesis appeared on April NM, June NM and December FM. The maturing condition in oysters was dominant on April FM, June FM, August FM, entire September and on February NM. Many oysters in mature stage occurred on October NM and November NM. The spent stage in oysters was dominant on December NM, In entire May and on July FM. The recovery stage was recorded in December NM, while the neutral stage in oysters was dominant on January FM and March NM. These different stages of the gonads have been correlated with the changes in environmental conditions over the oyster beds from the two localities. The results are discussed in the light of possible impact of the environment on reproductive events.

Key words: *S. cucullata*, Deogad, Achra, FM, NM, gametogenesis

INTRODUCTION :

Along the west coast of India the backwaters and estuaries are very extensive and play an important role for food production. These are widely scattered and have an area of 30.7 lakhs acres (Mitra, 1970) from which Maharashtra coast constitutes 3.0 lakhs acres combining together 2.0 lakh acres for brackish water and 1.0 lakhs acre for estuaries. These backwater and estuaries are very productive along the coast and are being used for various purposes. They are the breeding grounds of various species of marine and estuarine communities (Dwivedi, 1973).An extensive literature have been reviewed by Sastry (1979), Nagabhushanam and Mane (1991) and Mane (1997) on the oysters from different geographical locations.

Fig. 1: Map showing the coast of Maharashtra state

Two geographically separated localities at Deogad (16^0 23' N ; 73^0 23' E) and Achra (16^0 15' N; 78^0 26' E) in Sindhudurg district of Maharashtra State ,India (**Fig.1**) were selected on the basis of the differences in habitat, topography ,vegetation and local market value to study the reproductive cycles of the oyster *Saccostrea cucullata*. The maximum sizes attained by *S. cucullata* (**Fig.2**) in the estuaries at Deogad and Achra were 44-45 mm shell length. However, comparatively larger sized oysters are found round the year in the estuary at Deogad than at Achra. The estuary at Achra is comparatively deeper than at Deogad but the estuary at Deogad is wider than at Achra.

Fig. 2: Shells of *Saccostrea cucullata*

The topography of the oyster beds on the rocks in these two localities in mixed soil of mud and sand. In Deogad mangrove vegetation exits near the oyster bed and at Achra it is away from the oyster bed. The oyster beds in the intertidal zone in Deogad get exposed to atmospheric air from comparatively a longer period than those at Achra, where it is situated in the subtidal zone. The oyster bed in Achra gets exposed to atmospheric air during in neap tides. Both the estuaries are free from water pollution and no mechanical fishing operation occurs. The water is fairly clean on the oyster beds. The environmental parameters such as tidal heights, pH, temperature, dissolved oxygen and salinity existing on the oyster beds in Deogad and Achra were recorded on every new-moon and full-moon days for a period of twelve months.

MATERIALS AND METHODS :

Environmental parameters: Temperature, salinity, dissolved oxygen and pH on the oyster habitats at Deogad and Achra were recorded on full-moon and new-moon days. The samples of sea water were drawn just before the collection of these oysters and analysed immediately. Samples were collected for determination of dissolved oxygen in 250 ml DO bottles and oxygen was fixed by adding alkali iodide for further analysis by Wrinkler's method, azide modification. The temperature of sea water was recorded with the help of standard centigrade thermometer ^{0}C.pH was recorded with the help of standard BDH pH paper strips. Salinity was measured according to the method given by Parson *et al*. (1984). The replicates of these determinations on each fortnight were used in calculation. The height of the tide was recorded from chartdatum.

Changes in the gonads: *Saccostrea cucullata* (44-45 mm shell length) were collected from the fixed localities at Deogad and Achra in Sindhudurg district. Twenty oysters were collected on low tide of every new-moon and full-moon days for a period of twelve months. The oysters were brought to the laboratory and shucked for the flesh .The gonad was dissected and fixed in Bouin's Hollande preservatives prepared in sea water for further paraffin preparations for histological study. The paraffin blocks were cut at 7 μm thickness and stained with Mallory's triple. The observations were made under VT-20 Labo Video Scan microscope on television and whenever necessary photomicrographs were taken after measurements of the gonad contents.

RESULTS:

The environmental parameters such as tidal heights, pH, temperature, dissolved oxygen and salinity existing on the oyster beds in Deogad and Achra were recorded on every new-moon and full-moon days for a period of twelve months (**Figs. 3** and **4**).

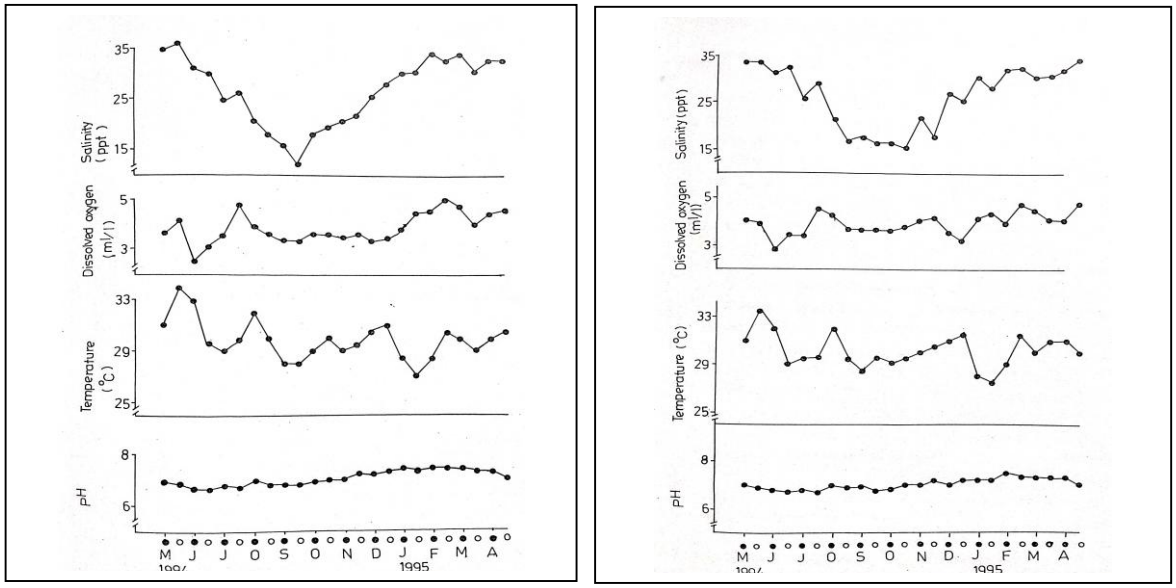

Fig. 3 and 4: Fortnight variations in the physicochemical parameters from the habitat of S.cucullata in the estuary of Deogad and Achra

The tidal heights differed in these two localities. Generally, the new-moon tidal heights were comparatively higher than the successive full-moon tides in both the estuaries during May to October and vice-versa in the remaining period. The pH of sea water for the oyster bed is from 6.7 to 7.5. Generally, the maximum pH values were recorded in summer season, whereas minimum pH values were recorded in monsoon in both localities. Fortnight variations in temperature showed almost similar patterns in both the localities, i.e. from 27.0 ^{0}C to 34.0 ^{0}C. The minimum temperature was recorded in June, whereas maximum was observed in May in both localities. The second peak of high temperature was recorded in December at both the localities. The fortnight variations in the dissolved oxygen content of sea water in the estuaries at Deogad and Achra also showed a similar pattern, at Deogad it was ranged from 2.53 to 5.07 ml/l and at Achra it was ranged between 2.81 and 4.79 ml/l. The salinity showed comparatively similar trend of variations, in Deogad it ranged between 12.84 and 35.91 ppt, while in Achra the values ranged from 15.40 to 34.63 ppt. The maximum salinity values coincided with summer season, while minimum values coincided with monsoon and influx of freshwater. The influx of freshwater in the estuary at Deogad is more than at Achra.

The oyster density is high in Deogad than at Achra in all the season (Figs**. 5** and **6**). The maximum density in both the estuaries was in May and minimum in January at Deogad and in August at Achra. The oyster in Deogad showed population density 98$\pm$17.14 individuals /m^2 in May. In August it was 81$\pm$19.60 individuals/m^2.In October it was 81$\pm$ 16.32 indiduals/m^2 and in January 70$\pm$13.88 individuals/m^2. In the estuary at Achra the population density of oyster was observed 62 $\pm$ 8.98 individuals/m^2 in May, i.e. in the summer season, whereas in August, i.e. the monsoon, it was 46 $\pm$ 13.88 individuals/m^2. In October, i.e. the post-monsoon season, it was recorded 52 $\pm$ 7.34 individuals/m^2 and 48 $\pm$8.98 individuals/m^2 in January, i.e. in winter season.

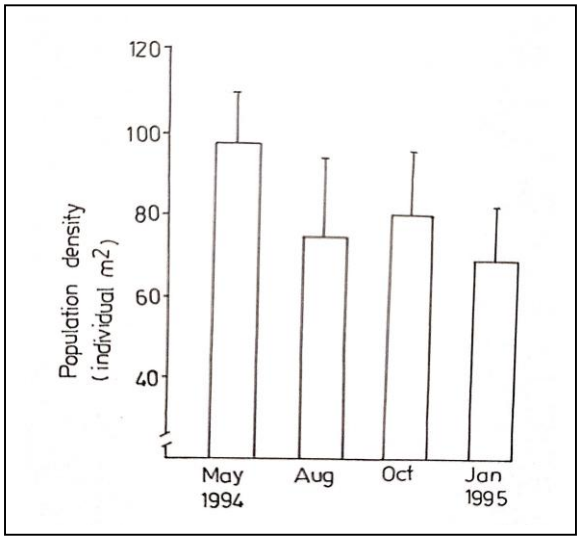

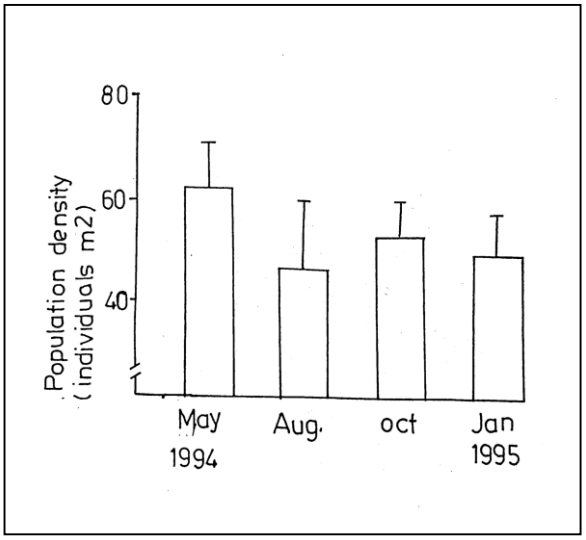

Fig. 5 and 6: Seasonal variations in the population density of *S. cucullata* from the estuary at Deogad and Achra. [Bar represents ± S.D.]

The gonads of twenty oysters were staged for males and females separately on each NM and FM days and percentage of the males and females in the different stages were calculated . The results are shown in **Figs. 7** to **10**.

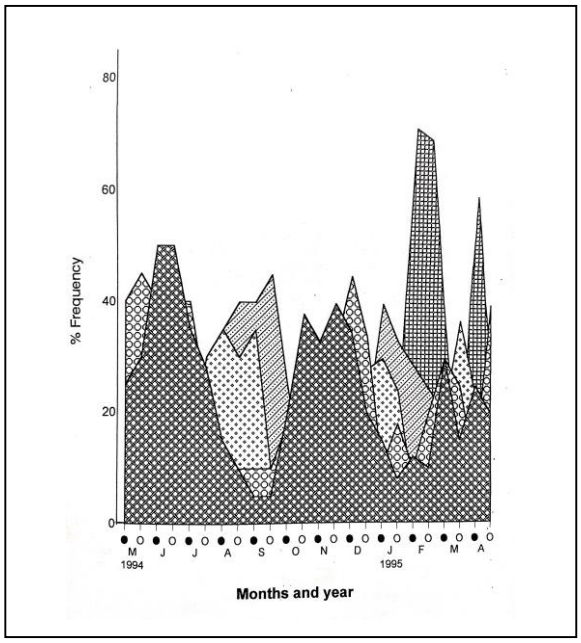

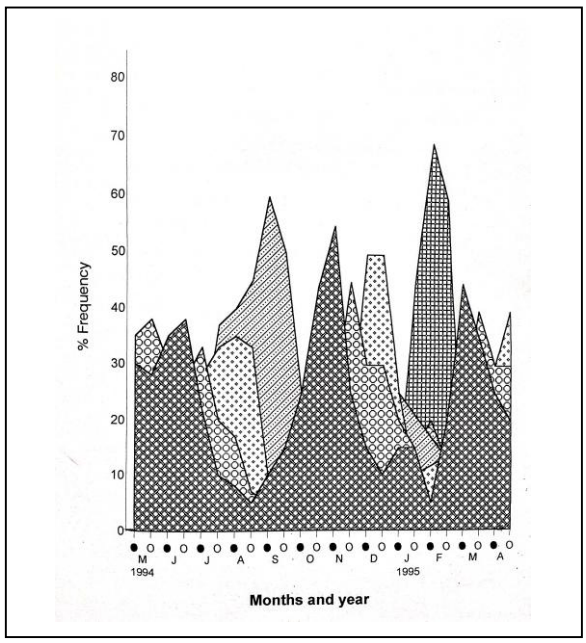

Fig. 7 and 8: Frequency polygon of male and female gonad of S. cucullata from the estuary at Deogad

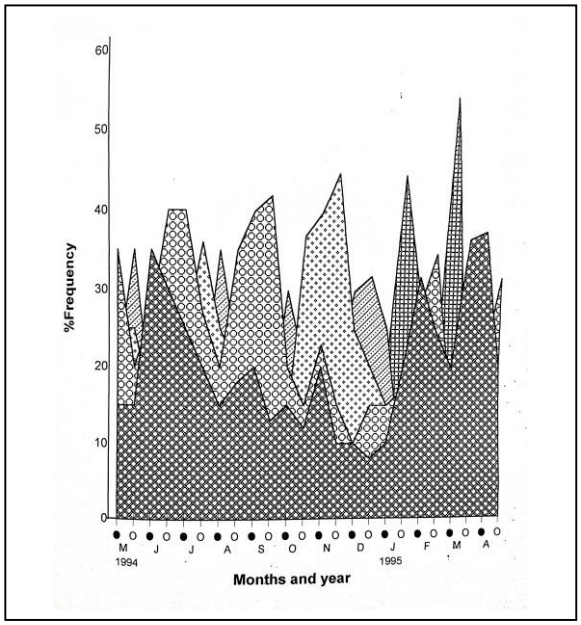

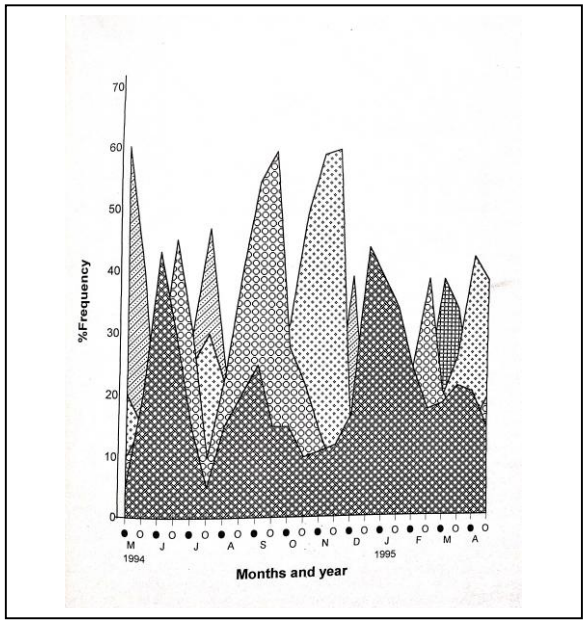

Fig. 9 and 10: Frequency polygon of male and female gonad of S. cucullata from the estuary at Achra

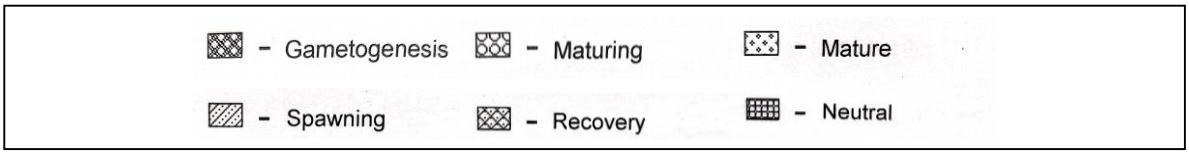

The microscopic details of the gonad tissue processed on every NM and FM days of each month revealed following stages ; (i) Gametogenesis ; (ii) Maturing ; (iii) Mature; (iv) Partial spawning ; (v) Complete spawning ; (vi) Recovery ;(vii) Neutral (**Figs.11** and **12**).

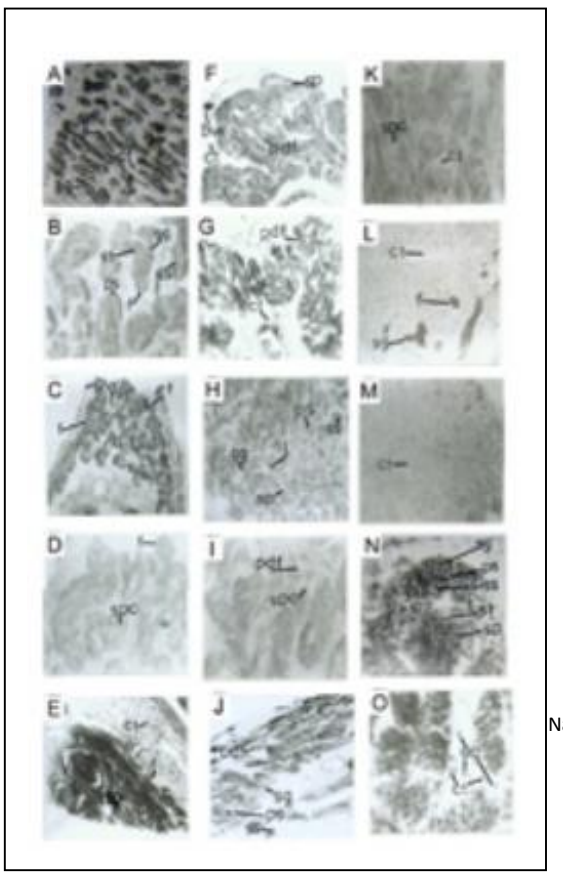

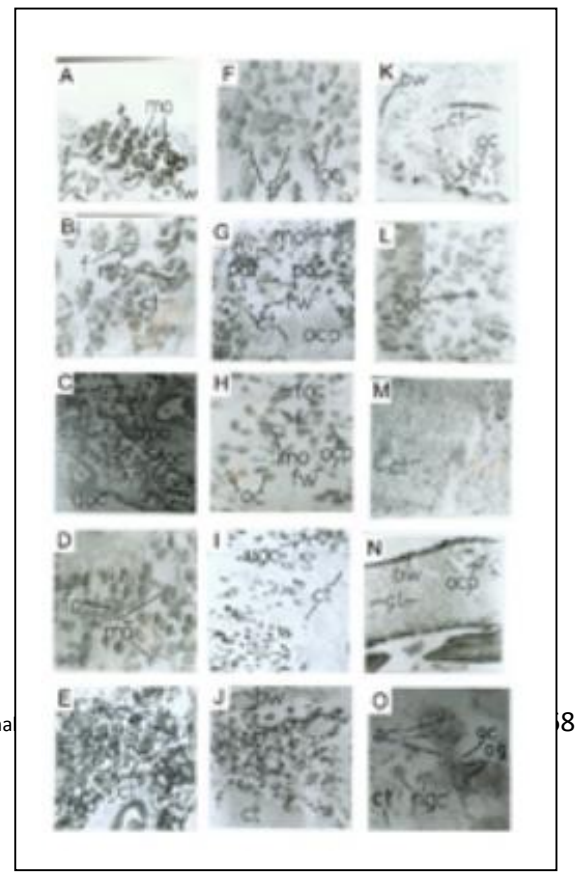

Fig. 11 and 12: Showing sections of gonad of male and female *Saccostrea cucullata* from the estuaries of Deogad and Achra

The study on reproductive cycle in male oysters of *S. cucullata* from Deogad showed that many oysters were in gametogenesis stage in entire June and once again on November NM. Maturing stage was seen on March NM, May FM, July NM and again on November FM and in entire December. Many oysters were in mature stage on March FM, April FM and July FM and again on January NM. Most of oysters were under spent stage on March FM, in entire August and September, and on January FM. Many oysters were under recovery stage on May NM and in entire October. Most of the samples collected in entire February and on April NM showed prominent neutral stage. The female oysters showed that the gametogenesis was dominant on March NM, in entire June and on November NM; maximum on NM of March and on November. The maturing stage was dominant in entire April and May and on July NM and December NM. Oysters under spent condition were dominant on April NM and December FM, and all the gametes were released in entire August, September and on October NM. The recovery stage was recorded in many oysters on October FM and January FM, while the neutral stage was recorded in entire February.

The male oysters from Achra showed gametogenesis stage on March NM, April FM and June NM. The maturing stage was seen in most oysters on April FM, June FM, July NM, September NM and FM. The mature stage was very conspicuous on July FM and November NM. Most oysters were in the spent stage on May FM , August NM ,October NM and December FM. Oysters under recovery stage were in high percentage on December NM , January NM and February FM. The neutral condition was most prominent in many oysters on March NM and January FM. The female oysters at Achra showed that many oysters under the gametogenesis appeared on April NM, June NM and December FM. The maturing condition in oysters was dominant on April FM, June FM, August FM, entire September and on February NM. Many oysters in mature stage occurred on October NM and November NM. The spent stage in oysters was dominant on December NM, in entire May and on July FM. The recovery stage was recorded in December NM, while the neutral stage in oysters was dominant on January FM and March NM.

DISCUSSION:

In the present study it was observed that the gametogenesis in *S. cucullata* from Deogad was at peak in both the sexes with lowering of salinity to 30.75 ppt and temperature to 33^0C in June NM before commencement of monsoon and for the second time in October FM at the time of rise in salinity to 19.25 ppt and temperature to 30^0C and for the third time in March NM at the time of rise in salinity to 34.63 ppt and temperature of 30^0C. Many females on October FM and March NM and many males on June NM showed dominant gametogenic stage compared to those females occurred in sampels during pre-monsoon and males during post-monsoon. On the other hand, the gametogensis stage in *S.cucullata* from Achra was at peak in both the sexes with lowering of salinity to 30.75 ppt and the temperature to 32^0C in June NM before commencement of monsoon and again for the second time in monsoon in August FM further lowering of salinity 21.81ppt and rise in temperature to 32^0C, for the third time in female oysters gametogenesis commenced in December FM at 25.66 ppt and rise in temperature to 31.5^0C. However, in male oysters gametogenesis occurred at peak for the second time in November NM with lowering of salinity to 21.81 ppt and temperature to 30^0C, for the third time in January FM with lowering of salinity to 28.22 ppt and temperature to 27.5^0C and for the fourth in March FM with lowering of salinity to 30.75 ppt and rise temperature to 31^0C. Many females on June

NM and December FM and many males on June NM and March FM showed dominant gametogenic stage compared to those females occurred in samples during peak monsoon and those males occurred in samples during post-monsoon and winter.

The maturaing stage in *S.cucullata* from Deogad was at peak in females with lowering of salinity to 24.37 ppt and temperature to 29^0C in July NM, while in male in October FM with rise in salinity to 17.97 ppt and temperature to 29^0C and again for the second time in November FM in female oysters with rise in salinity to 21.81ppt and temperature to 29.5^0C, while in male oysters in December NM with rise in salinity to 25.66 ppt and tempeature to 30.5^0C, for the third time in female oysters in March FM with lowering of salinity to 32.06 ppt and temperature to 29^0C, while in male oysters in March NM with a rise in salinity to 34.63 ppt and lowering of temperature to 30^0C, and for the fourth time in male oysters in April FM with rise in salinity to 34.63 ppt and temperature to 30^0C. Many females on November FM and March and many males on December NM and April FM showed dominant maturing stage compared to those females occurred in peak monsoon and males during post -monsoon and early summer. On the other hand, the maturing stage in *S. cucullata*_from Achra was at peak in both the sexes with a rise in salinity to 32.06 ppt and lowering of temperature to 29^0C in June FM. Again for the second time many maturing gonads were seen in monsoon, on August FM with further lowering of salinity to 16.69 ppt and temperature to 29.5^0C and for the third time this stage once again appeared with lowering of salinity to 16.69 ppt and rise in temperature to 29.5^0C in September FM. For the fourth time this stage dominated in oysters with rise in salinity to 33.35 ppt and temperature to 29^0C in February FM and for the fifth time in April FM at the time of rise in salinity to 33.35 ppt and lowering of temperature to 30.5^0C. Many females on June FM, August FM, September FM, February NM showed maturing gonad stage than those oysters collected in summer. Many males, on the other hand, on June FM and September FM, i.e. in monsoon showed dominant maturing stage compared to those occurred in samples later part of the year.

The mature stage in female *S.cucullata*_from Deogad was at peak in June NM with lowering of salinity to 30.75 ppt and temperature 33^0C, while in male oysters the peak was in July FM with the lowering in salinity to 25.06 ppt and temperature to 29.9^0C, for the second time in female oysters the peak in this stage was in August NM which coincides with lowering in salinity to 20.53 ppt and rise in temperature to 32.6^0C, while in males in November FM with rise in salinity 21.84 ppt and rise in temperature to 29.5^0C, for the third time many female oysters in this stage December NM with the rise in salinity to 25.66 ppt and temperature to 30.5^0C. In male third peak observed in March FM with the slight lowering in salinity to 32.06 ppt and temperature $29\ ^0$ C, and in male oysters fourth peak in mature gonad was observed in May NM with rise in salinity to 34.63 ppt and temperature to 31^0C . Many females on December NM and many males on March FM and May NM showed dominant mature stage to those females occurred in samples in peak monsoon and summer those males found in peak monsoon and early winter. On the other hand, the mature stage in both males and females *S. cucullata* from Achra was at peak on July FM with slight increase in salinity to 28.22 ppt and temperature to 29.6^0C and on October FM with lowering of salinity to 16.69 ppt and temperature to 29^0C and for the second time in females on April NM at the time of rise in salinity to 32.06 ppt and temperature to 31^0C. Many females on October FM and April NM and many males on July FM and October FM showed dominant mature stage compared to those females occurred in samples in monsoon and winter and those males occurred in winter and summer.

In the present study on *S.cucullata* from two different geographical locations viz. Deogad and Achra on the coast of Sindhudurg district it was observed that the spawning period as determined on the basis of occurrence of spent gonads of oysters was extended

and differed during post-monsoon. There were differences in spawning of females and males in these estuaries. The spent stage on both the sexes of oysters from Deogad commenced from June FM and the percentage of oysters in this stage increased till September FM and later decreased. Once again a part of the population in this stage occurred on January NM and March FM. Extended period in the male oysters in this stage was seen than in females. Many males spawned than females in winter season and many females spawned in monsoon and beginning of post-monsoon than males .A small population of female oysters spawned in May but no male appeared in this stage during this period. The spawning period in both the sexes from July NM to October NM coincided with low salinity range 16.69 to 25.61 ppt and lowering of temperature to 28.5-29.5 ^{0}C. On the other hand , the spent condition in female oysters from Achra was found from October to February and again from April to August while , in male this period was from March to December. The spent gonads of males occurred for a longer period than females, the salinity ranged from 15.4 to 33.35 ppt and temperature between 27.5 and 21.5^{0}C during October to February and from April to August the salinity ranged from 16.69 to 33.35 ppt and temperature between 29 and 33.5^{0}C. Female and male oysters in spent conditions occurred almost round the year. It was found that at the estuaries of Deogad and Achra, *S.cucullata* spawned due to the drop in salinity, in the monsoon season. During July to October the salinity of the estuary at Deogad was 22.66 ppt but lowered to 19.25 ppt during the peak of spawning, while in the estuary at Achra during the peak of spawning in July the salinity was 22.55 ppt and it lowered 12.8 ppt in August. At Deogad for the second time peak of spawning was observed during December and January during which the salinity increased from 28.22 to 30.75 ppt and at Achra for the second time peak of spawning was observed in December during which the salinity was 22.66 ppt. The temperature at Deogad on oyster bed varied before 27 to 32^{0}C and at Achra on oyster bed it was from 29 to 33 ^{0}C.

The recovery stage in female oysters from Deogad occurred from September NM to March FM, while in males this stage was seen June NM, on August NM from September FM to November NM, on January NM, on March FM and April NM. The recovery stage was extended in females than males, wherein it was interrupted. The recovery stage in female oysters from Achra occurred from July FM to August FM, November FM to February FM and May NM to June NM , while in males it was seen from June NM to July NM and September FM to January FM. In males there was extended of this stage from post-monsoon to middle winter.

The neutral stages in female oysters from Deogad was observed August FM to November NM, December FM to March NM and in entire April, the peak was observed in entire February. This stage was observed in male from August FM to November NM, from January FM to February FM, and from March FM to April FM. Many oysters from both the localities were in this stage in February and males in April also. On the other hand , this stage in female oysters from Achra was noticed from December NM to April FM, the peak was recorded in March ,while in male oysters the neutral stage was found in August NM to May FM ,and many oysters were in this stage were found in January FM and again on March NM . The number of oysters under neutral condition was more from winter to mid-summer which exceeded the number of oysters under recovery stage.

The intrafollicular tissue in resorption of residual gametes was noticed in present study on *S. cucullata*. Large number of amoebocytes were observed around the follicles in certain periods of reproductive cycle, especially during post spawning periods. Extensive studies were carried out b Takatsuki (1934) on O. edulis and Tranter (1958a) on the amoebocytes in the former report and the phagocytes in the latter. Various types of amoebocytes and their role in gonad verginion in *S.cucullata* have been described by Yennawar (1997). In the present study, it was found that generally the amoebocytes of type

A(as shown by Yennwar,1997) were in the size range 0.223 to 0.39 μm in their largest area in oysters from Deogad, while those in the oysters from Achra were in the largest size range of 0.223 to 0.376 μm. Much variation in the size range was observed in the gonads of oysters from Deogad than Achra, the largest sized amoebocytes in oysters from Deogad were 0.974 μm, while those from Achra reached 0.557 μm. The largest sized amoebocytes were found in the gonads of oysters form Deogad on February NM and FM at the time many neutral oysters appeared in the samples and some female oysters showed recovering of the gonad. Appearance of large sized amoebocytes was again observed on October NM during which time the spawning in females and males was terminated and few oysters were in the recovery and neutral stages. On the other hand, the amoebocytes occurred frequently in the gonad at various stages of spawning, recovery and neutral during different seasons. The maximum sized amoebocytes occurred in July FM during which time many female oysters were spent and few were under recovery, while a few males were spent. From April FM to September NM and from January NM to February NM generally large sized amoebocytes appeared when compared to those found during rest of the period. During April to September there were frequent appearance of gonads of males and females, either under recovery or neutral and spent gonads occurred throughout this period. Again for the second time these large sized amoebocytes appeared when the gonads of many oysters were neutral and both spent and recovering gonads of oysters also occurred. However, it is probable that because of this redevelopment of gametes the number of oysters in gametogenic and maturing stages occurred round the year. Fully mature gametes were produced by large number of individuals only during certain period of the seasons, probably revealing that oysters could have spawned almost round the year with peaks differing in the estuaries at Deogad and Achra. Many oysters after partial release of gametes showed redevelopment of fresh gametes and only a small population showed recovering of gonad, the unspawned gametes were lysed.

In the present study it has been noted that *S.cucullata* in the estuary at Deogad gets exposed to atmospheric air during each low tide due to its intertidal habitat. This makes the oysters to feed only during the high tides. On the other hand, the oysters from Achra remain submerged during the low tide; however they get exposed to atmospheric air only during the neaptide. It is most possible that these oysters get more chance to feed when compared with those from the estuary at Deogad. These differences in habitat are likely to create differences in the nutrient supply for the gonad development and maturation. It was further noticed that mangrove vegetation persists near the oyster bed in the estuary at Deogad but in the estuary at Achra such vegetation persists away from the oyster bed. It is likely that this vegetation can create impact on the nutrients richness in seawater at both the estuaries , nutrient rich seawater at Deogad than at Achra Since oysters at Deogad are exposed to each low tide, there appears to be energy demand for maintenance , metabolism and during the period of gonad growth it is possible that less energy is supplied for the gametes development and therefore, there is an extended period of post spawning to recommencement of gametogenesis when compared to those from the estuary at Achra. In oysters from Deogad this period was led down in males during entire October and again in February April NM and May NM, while in females during October FM and from January FM to February FM. On the other hand, in oysters from Achra similar period was observed in males during December NM, entire January. February FM and March NM while that in females was during December NM, January FM and March NM. This indicated that oysters from Deogad passed through a comparatively longer period of recovery and neutral condition before commencement of gametogenesis. Though the quantitative data on gametes produced by individual oyster was not obtained, the observations on histological preparations and scanning as television markedly showed less numbers of gametes being

produced in oysters from Achra and Deogad. The afore mentioned longer preparatory period for oysters from Deogad probably show the buildup of body reserves and metabolic status before commencement of new gametogenic cycle. It is possible that the oysters from Deogad are more opportunists to allocate energy for reproductive efforts during a short period of favorable conditions received during high tide and exhibited a direct dependence of nutrient availability with the change in the environment.

In Kelwa back waters, Bombay (Mumbai) the south- west monsoon diluted the salinity from 28.59 to 13.51 ppt in July and stimulated spawning in *C. gryphoides* (Durve, 1965).This spawning continued till September. The spawning in a number of oysters has been reported as a protracted phenomenon. One or two peaks within a breeding seasons lead to an extended breeding season (Mane, 1997).

Conclusion:

In the present study sorting of the oyster gonad tissue into different reproductive stages revealed that *S. cucullata* from both the localities showed simultaneous maturation of gametes as the gametogenesis was advanced. Oysters under under gametogenesis and maturation occurred round the year, however, dominance of each reproductive stage differed from one season to another. Once the matured gametes are produced spawning commenced and advanced with the response to stimuli received exogenously and endogenously from monsoon to post-monsoon period (Salunkhe, 1999). The period of spawning in males from both the localities was longer as compared to females. Many female oysters under gave neutral stage after spawning than males and period of occurrence of oysters in this condition was longer in males from Achra. It was further observed that not all the mature gametes were released by the oysters from both the localities and unspawned gametes were cytolysed in the recovery state which was longer in females than males, especially in the oyters from Deogad. However, successive events in the reproductive cycles in oysters may be affected directly by various factors, and a detailed analysis requires a separate evaluation of each phase. Our knowledge of the environmental interactions and mechanism controlling the pattern of reproductive activity in oyster population is still fragmentary. With the control of reproductive activity and stimulation of gametogenesis in oyters maintained under controlled conditions, it should be possible to determine the effect of various environmental factors singly and in combinations, and to elucidate the mechanisms coordinating the reproductive response at the whole organism level. More data on the influence of various exogenous and endogenous factors controlling the beginning of gametes growth and mechanism, coordinating maturation and spawning in oysters are essential to effectively analyse the reproductive strategy in oyster populations from the given locality.

REFERENCES :

1. Dwiwedi, S.N.1973 Some biological problems of the West coast of India. Mahasagar. Bull. Nat. Inst. Oceanogr., **6**(2): 112-119
2. Gomez, E.D. 1980 The present state of Mangroove ecosystems in South – East Asia and the impact of pollution. Philippines. Working Pap. SCS/ 80/ wp/ 94c /, South China sea, Fisheries Development and Co-ordinating Programme.
3. Mane, U.H. 1997 Mussels and Oysters. In: Fouling organisms of the Indian ocean – biology and control technology, Eds.R.Nagabhushanam and M. Thompson, Oxford and IBH. Publ. Pvt. Ltd. New Delhi, Calculatta: 441 -506.
4. Mitra, G.N. 1970 Development of inland fisheries in India. Resource of Papers: National food congress, Freedom from Hunger Campaign and Ministry of Food, Agriculture and C.D. and Coop. Govt. of India. 20: 8.

5. Nagabhushanam, R. and Mane, U.H. 1991 Oysters in India. In "Estuarine and Marine Bivalve Molluscs" Editor W.Menzel, CRC Press INC, Boca Ratol, Ann. Arbar .Boston USA: 202 - 209.
6. Parson, T.R., Maita, Y. and Lalli, C.M. 1984 A manual of chemical and biological methods for sea water analysis. Pergaman Press, U.K.
7. Takatsuki, S. 1934 On the nature and functions of the amoebocytes of *Ostrea edulis.* Quart. J.Micr. Sci., 76: 379.
8. Salunkhe, R.V.1999 Study on the reproduction of edible bivalve mollusks from Sindhudurg district, Maharashtra state. Ph.D. Thesis, Dr. Babasaheb Ambedkar Marathwada Uni., Aurangabad, M.S., 1-330.
9. Sastry, A.N.1979 Pelecypoda (excluding Ostreidae). In "Reproduction of Marine Invertebrates, Molluscs: Pelecypods and Lesser classes". (A.C.Giese and J.S.Pearse eds.).Academic Press, New York: 113 - 292.
10. Tranter, D.J.1958 A Reproduction in Australian Pearl Oyster (Lamellibranchia) I-*Pinctada albina* (Lamark): Primary gonad development. Aust. J.Mar. Freshwater Res., 9: 135 - 143.
11. Yennawar, P.L.1997 some aspects of reproductive biology of West coast bivalve molluscs from Maharashtra state. Ph.D.Thesis, Dr. Babasaheb Ambedkar Marathwada University, Aurangabad, M.S.India: 1 – 394.

Paper 70

Synthesis, Characterization and Antimicrobial activity of Sm^{3+} doped TiO_2 Nanoparticles

Sheema Kauser* and Venkatesha Babu K R**

*Department of Microbiology, Nrupathunga University, Bangalore-560 001, India
** Department of Physics, Nrupathunga Universtiy, Bangalore-560 001, India
*Corresponding author: Email: sheematmk@gmail.com

ABSTRACT: Pure and Sm^{3+} ions doped TiO_2 nanoparticles were prepared by low temperature solution combustion method, with Glycine and Ammonium acetate as fuels. The nanoparticles obtained were subjected to PXRD studies for purity and shape. The antimicrobial activity of the nanoparticles on *E.coli* a Gram negative bacterium was investigated by using pure and doped TiO_2 by Disc and Kirby-Bauer method. The studies revealed increased and elevated bactericidal activity of doped TiO_2 in comparison to the pure. The observation was confirmed by the Colony forming units on LB agar, Growth measurement curve by turbidity technique LB broth.

Keywords: XRD, *E.coli, Gram –bacilli,* LB broth, Bactericidal activity, Colony forming units.

INTRODUCTION

The synthesis of nano sized particles of TiO_2 doped Sm^{3+} ions with antibacterial properties is of great interest for the development of new biomedical applications. The adaptation of bacteria and resistance to wide range of antibiotics has led to the emergence of some different infectious diseases. The treatment towards these diseases is becoming a difficult task. Hence an effort was made to study. The aim of this study was to evaluate TiO_2: Sm^{3+} nanoparticles for their antimicrobial activity against E.coli, a Gram –ve Bacteria. The fuels used were Glycine and Ammonium acetate for combustion.

2. MATERIALS AND METHODS

2.1 Materials

LB broth, LB agar, Petri plates, Pipettes, Micropipettes, Vials, Double distilled water, *E.coli* culture, *Bacillus* culture, Samarium, Titanium dioxide, UV trans illuminator, Conical flask, Alcohol, Beaker, Streptomycin, Sterilized discs, Sterilized swabs, Cork borer, Incubator[37°C], EMB agar, Nutrient agar, Sonicator, Laminar air flow, Water bath, Oven, Muffle furnace, Methanol, Sulphuric acid, Hydrochloric acid, Autoclave, Glycine, Ammonium acetate, Nitric acid (Chemicals used were of analytical grade). Luria bertani broth, Luria bertani agar, Muller Hinton agar, Nutrient agar, Eosin Methylene Blue Agar were used.

2.2 Method of Preparation TiO_2: Sm^{3+} (0.25-0.75 mol %)

The pure and Sm^{3+} ions doped TiO_2 NPs were prepared from Titanium IV butoxide and samarium nitrate using glycine and ammonium acetate as fuels for low temperature solution combustion method using the stoichiometric calculations. The pre heated muffle furnace at 500^0C was used for combustion of the uniformly mixed solutions using magnetic stirrer. Flakes obtained are ground to form powder and the same is calcinated at 8000C for 2 hours to remove the impurities present in the same. The same procedure was repeated to get the Sm^{3+} doped TiO_2. The antimicrobial activity was done by serially diluting the sample in distilled water and filling into the wells made in the LB agar media. The results are observed after 24H of duration.

2.3 Preparation of stock solution

Stock solution of TiO_2 NPs (both pure and doped) with concentration of 1 mg/ml was prepared and suspended in distilled water. The solution was sonicated for 5 minutes to get a homogenous suspension. The suspension was exposed to UV rays for 30 minutes for the nanoparticles activation.

Table 1: preparation of stock solution

Stock (mg/ml)	0.2	0.4	0.6	0.8	1.0
Distilled water(mg/ml)	0.8	0.6	0.4	0.2	0.0

2.4 Disc method

E.coli inoculated by lawn culture on LB agar. The sterilized whatman paper discs were dipped in pure TiO_2 nanoparticles of concentration 0.2, 0.4, 0.6, 0.8 and 1.0 mg/ml and doped TiO_2 nanoparticles of different mole percentage (1%, 3%, 5%, 7%, 9%) of concentration 0.2, 0.4, 0.6, 0.8 and 1.0 mg/ml were placed on the agar surface and it was labeled. Two plates were kept as control using streptomycin, the discs were dipped with streptomycin of concentration 0.2, 0.4, 0.6, 0.8 and 1.0 mg/ml for *E.coli*. These plates were allowed to dry and then kept for incubation at 37^0c for 24 hours. The zone of inhibition was observed.

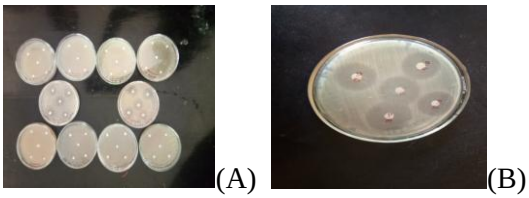
(A) (B)

Fig 1: Results of Disc method
(A) Doped TiO_2
(B) Pure TiO_2

Disc method results shown revealed that maximum zone of inhibition was found to be in the range 0.6-0.8 cm with a varying concentrations of doped TiO_2.

2.5 Kirby Bauer test

It is an agar diffusion test used for studying sensitivity of bacteria using antibiotic discs, to test the extent to which bacteria are affected by those antibiotics. The antibacterial effect of TiO_2 NPs were performed for comparing the inhibition on *E.coli* by Sm^{3+} doped TiO_2 and pure TiO_2 NPs. Seeded agar was prepared by using 24H culture of *E.coli*, poured to the sterile petriplates and allowed to set. Using sterile cork borer 5 wells of 10 mm diameter were prepared. The wells were filled with pure TiO_2 NPs of concentration 0.2, 0.4, 0.6, 0.8 and 1.0 mg/ml and doped TiO_2 nanoparticles of different mole percentage (1%, 3%, 5%, 7%, 9%) of concentration 0.2, 0.4, 0.6, 0.8 and 1.0 mg/ml. Also, two plates with streptomycin of 0.2, 0.4, 0.6, 0.8 and 1.0 mg/ml served as the control. These plates were allowed to dry and then kept for incubation at 37^0c for 24 hours. The zone of inhibition was observed after 24H.

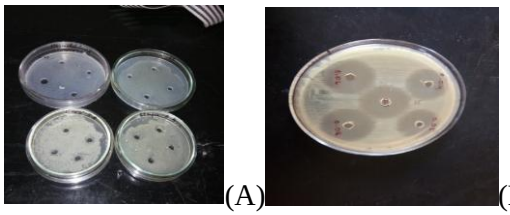
(A) (B)

Fig 2: Results of Kirby-Bauer method
(A) Doped TiO_2
(B) Pure TiO_2

The results by Kirby-Bauer test, zone of inhibition in undoped and Sm^{3+} doped TiO_2 was found to be in the range 0.5-1.6cm with the concentration of 1 mg/ml and Streptomycin taken as control.

2.6 Colony forming unit [CFU]

1ml of *E.coli* was aseptically transferred to the petriplates to which LB agar having varying doped TiO_2 concentrations of 0.2, 0.4, 0.6, 0.8, 1.0 mg/ml with Sm^{3+} of 1%, 3%, 5%, 7%, 9% mole % was added. The petriplate without TiO_2 NPs as control. The five petriplates with different concentrations of 20, 40, 60, 80 and 100 µl/ml of pure TiO_2 nanoparticles of LB agar were poured and the plates were incubated at 37^0c for 24 hours. Growth was observed and colonies were counted. CFU's counted in petriplates with varying concentrations of doped and pure TiO_2.

Conc of TiO_2 in mg/ml	Sm^{3+} doped TiO_2	Pure TiO_2
0.2	250	343
0.4	244	321
0.6	143	297
0.8	95	217
1.0	76	170
Control	283	370

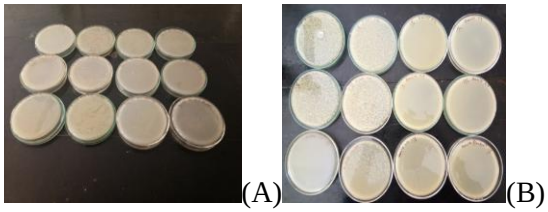
(A) (B)

Fig 3: Colony forming Units in

(A) Doped TiO_2

(B) Pure TiO_2

Results indicate that with the rise in concentration of dopant, the growth of colony decreased considerably. The number of colonies formed decides the inhibitory activity of the metal oxide. The more number of colonies indicates low antimicrobial activity. The high number of colonies indicates the high responding antimicrobial activity of the metal oxide.

2.7 Growth curve

Sterile Luria broth was taken in different conical flask 100 µl of duration 24H culture of *E.coli* was inoculated. 20, 40, 60, 80, 100 mg/ml concentrations of Sm^{3+} doped with TiO_2 was added. The flask without TiO_2 serves as control. Flasks were incubated in a shaker incubator at 37ºC and Optical density at 600 nm taken every hour for about 6H of duration.

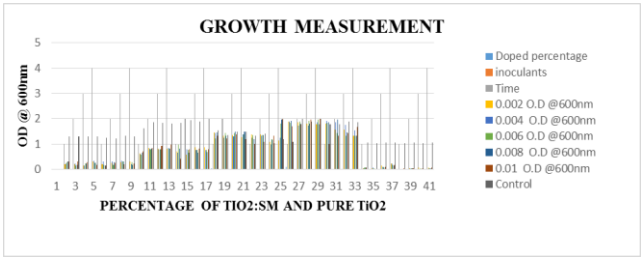

2.8 Effect of TiO_2 in Liquid Media

The concentration namely 20, 40, 60, 80, 100 µg/ml of TiO_2 was added to prepared and autoclaved 60 ml of Luria broth. 100µl of *E.coli* was aseptically transferred. The flasks were incubated in a shaker incubator at 37^0 C for 18 hours. One flask without TiO_2 served as control. The optical density is noted for every hour for 6H.


(A)

(B)

Fig 4: Results of growth measurement
(A) Doped TiO_2
(B)Pure TiO_2

Fig 4 indicates the growth which was directly proportional to the turbidity of broth medium. It was found that the doped TiO_2 nanoparticles showed decreased turbidity with increasing concentration and hence more bactericidal activity.

Fig. 5 depicts that there was a consistent decrease in the bacterial growth rate in the doped TiO_2 in comparison to the pure TiO_2.

2.9 PXRD Analysis

X-ray diffraction is a non-destructive technique used for the qualitative and quantitative analysis of crystalline compounds. It provides information on phase identification, unit cell dimensions, crystal structure and other structural parameters, such as crystallite size, crystallinity, and phase composition and so on. Nano materials exhibit strong inhibiting effect towards a broadened spectrum of bacterial strains. The inhibitory activity of TiO_2 is due to the photocatalytic generation of the strong oxidizing power when illuminated with UV light at wavelength of less than 385nm for 30mins. TiO_2 particles catalyze the –cidal action of bacteria on illuminator in UV light.

Generation of active free hydroxyl radicals by photo exited TiO_2 particles is responsible for the antibacterial activity. Doped TiO_2 nanoparticles are more inhibitory when compared to pure TiO_2 NPs. The process of doping increases the activity, since the empty sites are filled with Sm^{3+} ions.

Results, Graphical presentation and Discussion XRD analysis

Fig 6 shows the PXRD peaks which indicate crystallinity, phase and purity. The JCPDS card numbers are verified. The pure TiO2 exists in the rutile phase and with addition of Sm3+, it changes to anatase phase. The particle size was calculated from Debye Scherrer formula and was found to be about 50nm.

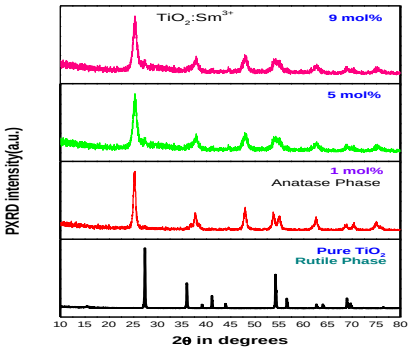

Fig 6: PXRD $_2$ pure and Sm^{3+} doped TiO_2

CONCLUSION

The Comparative study of Sm^{3+} doped TiO_2 NPs by different methods have shown to have bactericidal activity against the bacteria. The effectiveness of these nanoparticles can be enhanced by combining it with the relevant antibiotics minimizing the antibiotic resistance amongst the bacteria. Thus, providing a better scope in future days for combating and treating various diseases.

References

1. Carmen Steluta Ciobanu et al (2003). The synthesis of nanosized particles of Ag-doped hydroxypatite with antibacterial properties is for great interest for the development of new biomedical applications. In this paper Ag: Hap-NPs are evaluated for their antimicrobial activity against Gram positive and Gram negative bacteria and some fungal strains.
2. Dodd AC, McKinley AJ, Saunders M, Tsuzuki T. Effect of particle size on the photocatalytic activity of Nano particulate zinc oxide. J Nano part Res. 2006;8(1):43–51.
3. Elsevier B.V et al (2017) studied the synthesis, characteristics and antibacterial activity of rare-earth metal Samarium/Silver/Titanium dioxide inorganic nano materials.
4. Jose Ruben Morones et al (2005) and co-workers studied nanotechnology is expected to open new route to fight and prevent disease using atomic scale tailoring of materials. The bactericidal effect of silver nanoparticles.
5. M.N. Moore, "Do nanoparticles present Eco toxicological risks for the health on the aquatic environment?" Environment International, vol.32, no.8, pp. 967-976, 2006.